ADVANCED MATERIALS TECHNOLOGIES
www.advmattechnol.de

A Review on Materials and Technologies for Organic Large-Area Electronics

*Cláudia S. Buga and Júlio C. Viana**

New and innovative applications in the field of electronics are rapidly emerging. Such applications often require flexible or stretchable substrates, lightweight and transparent materials, and design freedom. This paper offers a complete overview concerning flexible electronics manufacturing, focusing on the materials and technologies that have been recently developed. This combination of materials and technologies aims to fuel a fast, economical, and environmentally sustainable transition from the conventional to the novel and highly customizable electronics. Organic conductors, semiconductors, and dielectrics have recently gathered lots of attention since they are compatible with printing technologies, and can be easily spread over large and flexible substrates. These printing technologies are usually simple and fast procedures, which rely on low-cost and recycle-friendly materials, intended for large-scale fabrication. Overall, even though organic large-area electronics manufacturing is still in its early stages of development, it is a field with tremendous potential that holds promise to revolutionize the way products are designed, developed, and processed from the factory premises to the consumers' hands. Besides, this technology is highly versatile and can be applied to a large array of sectors such as automotive, medical, home design, industrial, agricultural, among others.

1. Background

Printed electronics (PE) emerged as a concept at the beginning of the XX century, with the invention of the first circuit board, by Hanson.[1,2] Remarkably, the patent written by Hanson, in 1903, was so close to the modern printed circuit board (PCB) that he even managed to describe the possibility of creating conductive circuitry, either by electrodeposition or by controlled dispensing of a metallic powder, dispersed in a suitable medium, which we now recurrently call a conductive ink.[2] Moreover, Hanson also detailed the possibility of drilling the board to create double-sided through-hole circuitry, which is massively used to achieve conductivity on both sides of a PCB, and useful in multilayer and complex PCB development.[3] Even though at the time this invention was envisioned to simplify the telephone system, it would end up serving as a solid precursor to the invention and implementation of the first electroplated printed circuit board (PCB), which was conceived by Paul Eisler during World War II. In an autobiographic book, Eisler elaborates on how decisive the introduction of his discoveries was to improve the allies' aircraft shells, and how impactful the large-scale production of his PCB was in the outcome of the war.[4] Nonetheless, even after his invention was proved invaluable, he still endured a great deal of bureaucracy and had to handle constant rivalry between large corporations, which made it very challenging to officialize and put his ideas into practice.[4] In between these two historical technology landmarks, Charles Ducas introduced the stencil printing of electronics and developed large-area electrical circuits and inductors, that were first applied in the area of radio communications.[5] The proposed apparatus allowed for the imprinting of a conductive paste on top of a supporting surface and was not intended to be restricted to applications in the radio field.[5]

During the seventies, efforts started being made toward adding flexibility to electronics, while simultaneously reducing its costs. As a result, in 1973, George Smith patented a "double-sided flexible circuit assembly" method.[6] This aimed to promote the mass production of printed or etched electronics over thin and nonconductive flexible substrates, in a "continuous in-line processing." Since then, many additive manufacturing technologies, conventionally used with nonconductive inks, have been used in combination with electrically conductive materials and applied in the development of low-cost flexible electronics. Using screen-printing, inkjet, gravure, flexography, offset, transfer printing, amongst other techniques, lightweight, bendable, conformal, and wearable sensor and actuating devices can already be obtained.[7]

Nearly one century after Hanson's discoveries regarding the PCB, a group of investigators was awarded the Nobel Prize in Chemistry 2000 for the development of organic conducting polymers.[8,9] This groundbreaking achievement, combined with developments in the area of synthesis and stabilization of conjugated polymers, led to the development of stable formulations

C. S. Buga
DTx – Digital Transformation CoLAB
University of Minho
Campus Azurém, Building 1, Guimarães 4800-058, Portugal
Prof. J. C. Viana
IPC/i3N – Institute for Polymers and Composites
University of Minho
Campus de Azurém, Guimarães 4800-058, Portugal
E-mail: jcv@dep.uminho.pt
The ORCID identification number(s) for the author(s) of this article can be found under https://doi.org/10.1002/admt.202001016.

DOI: 10.1002/admt.202001016

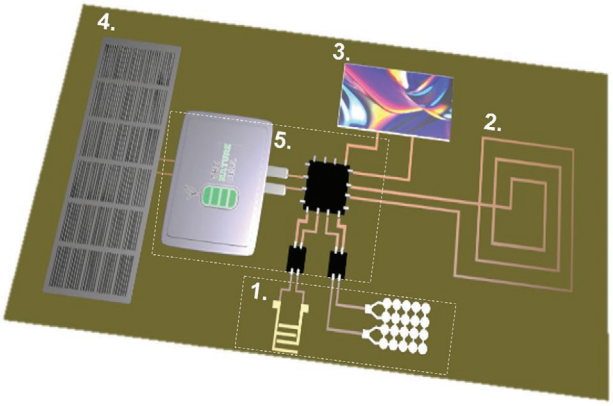

Figure 1. Scheme of a PCB with 1) printed spread sensors, 2) antenna, 3) OLED display, 4) solar-harvester cells, and 5) nonprinted traditional components.

of organic conductive pastes and inks. The interest in this disruptive field developed fast and, in 2005, the first organic transistor obtained from an organic conductive ink was developed and patented.[10] By manipulating their physical properties (p.e., surface tension, viscosity, curing temperature, etc.) with the aid of additives, these inks can be specifically formulated to be compatible with each one of the abovementioned printing technologies.[11,12] Thanks to their versatility, organic materials (small molecules and polymers) can be used as conductors, semiconductors, electroluminescent, and photovoltaic materials and thus, can successfully replace inorganic materials as functional elements in complex sensors and electromechanical devices.[13–15]

Since their discovery, the use of organic materials in the area of consumer electronics has been increasingly popular, and its related field of technology has received the denomination of organic large-area electronics (OLAE).[16] OLAE relies on developments in the areas of printing technologies, electronics, chemistry, and materials science and, with the combined efforts of researchers from these multidisciplinary areas, has become a fundamental approach to achieve mechanically flexible, low-cost, sustainable, scalable, on-demand, and lightweight devices. With the current fast growth of the Internet of Things (IoT), the demand for such devices is greater than ever before, and OLAE is expected to be attributed with a key role in this much-anticipated transition.[17–19] When connected to the IoT, integrated sensors and actuators are called cyber-physical systems (CPS) and, resorting to OLAE technologies, their development is expected to become faster, more economical, and more sustainable.[20,21]

Nowadays OLAE is widely reported in the literature for two different paradigms of production. For instance, it is frequently employed in the fabrication of printed circuit boards (PCB) (**Figure 1**), large surfaces with deliberately spread electronics, such as large OLED displays,[22] large solar panels, and large-area sensing devices with sizes that can reach the square meters.[23,24] On the other hand, it is also vastly used to produce repeated modular components or circuit interconnects of very small sizes in a fast and economical manner.[25,26]

Fully organic printed devices, however, are not yet a reality. One reason for this is that current printing technologies still present some technical constraints, which limit the output resolution and electrical properties of the resulting flexible devices.[27] Besides, inorganic materials such as silicon, metals, metal oxides, and carbon allotropes not only provide greater conductivity, robustness, and longer-term function reliability, but are also already well established in the traditional markets. Thus, although the preferred materials for OLAE are built from carbon-based organic molecules, to achieve acceptable performance, organic electronic elements are still usually integrated with inorganic materials and traditional electronic components, such as IC chips and communication modules. Since organic and inorganic materials are bound to coexist symbiotically for years to come and will feature as complementary segments in the approaching digital transition, both must be present in this review. The approach to these materials should be done in the optic of their compatibility, and a symbiotic relationship should be developed between them, as a way to obtain devices with the best possible cost/performance ratio, that benefit from the advantageous features of both organic and inorganic materials.

This review aims, not only to gather information regarding the materials and printing technologies for OLAE but also to present a complete overview of the current applications. We give special emphasis to the organic functional materials, as they are generally more recyclable-friendly and their exploration is less environmentally damaging. Nonetheless, inorganic materials and their applications are also discussed. Throughout this text, several comparative tables that present the full scope of the contents, and highlight their main characteristics, advantages, disadvantages, and other critical features, are presented. While the term OLAE has been present in the literature for around a decade, the research on this topic has registered an intensified growth for the past five years. With the spreading of the IoT and the emergence of the 4.0 Industry, it is undeniable that the world is on the verge of a global digital transition that will affect every economical sector. In this sense, the growing interest in the field of OLAE is certainly prone to be maintained or even intensified. Ultimately, this comprehensive review aims to serve as a solid and convenient guideline for everyone interested in understanding the materials and processes that stand behind the implementation of ubiquitous flexible sensors and connected systems, which are vital to the implementation of the IoT paradigm.

2. OLAE Related Definitions

Research in printed electronics (PE) has powered the development of ultrathin, lightweight, flexible, robust, and cheap alternatives to complex, energy-demanding, and expensive procedures such as photolithography, vacuum deposition, and baking and etching of the materials. This has enabled the development of new valuable applications. The International Electronics Manufacturing Initiative (iNEMI) uses different definitions to label printed, flexible or organic electronics, and, even though they can sometimes be seen as synonyms, it is important to understand their subtle differences to accurately use them.[28] Some definitions are schematized in **Figure 2**.

OLAE relates to both PE and FHE and, through printing and patterning techniques, allows for large-area and high-volume

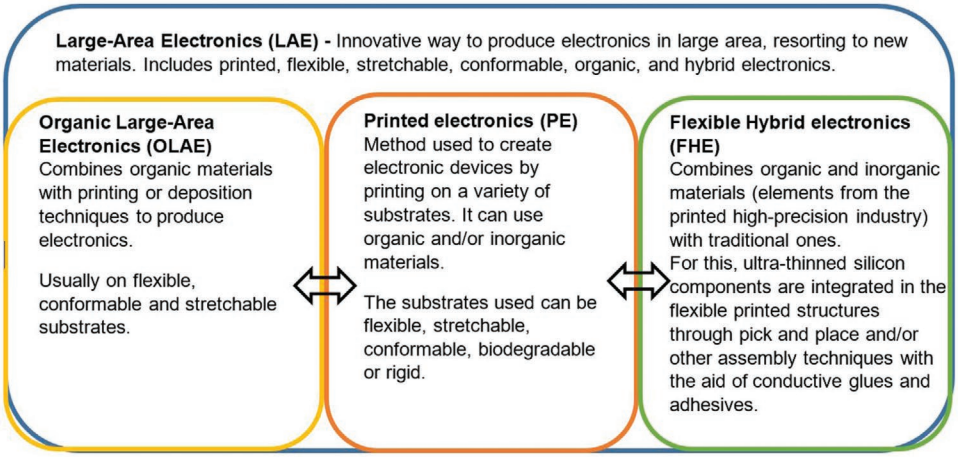

Figure 2. Definitions related to large-area electronics (LAE). The arrows represent points of convergence that exist between the central definitions.[29]

deposition of materials. Although the definition of OLAE highlights the organic nature of the flexible components obtained through this technology, it should be taken into account that it is not yet possible to fully eliminate inorganic materials from CPS devices. Thus, when the envisioned applications are more demanding in terms of performance and output response, OLAE is combined with traditional electronic components, through FHE. For instance, inorganic integrated circuits (IC) are being thinned-down (<50 μm), which conveys mechanical flexibility and allows them to be integrated into flexible circuits.[28,30,31] Thus, the purpose of large-area electronics is to create electronic devices that can be spread across a large substrate, where the dense and highly integrated IC devices can be monolithically integrated and assembled on that substrate, in a hybrid approach.[32]

Other definitions that relate to the above-mentioned ones include flexible, conformable, and stretchable electronics. Flexible electronics (FE) relates to the act of assembling electronic circuits over flexible substrates. It appeared as soon as the rigid PCB started to be replaced by flexible alternatives and its development over the years has been fundamental for LAE applications.[33] FE can be fully flexible, which means it can adapt to virtually any shape (including twisting and rollable applications), or can it can, in some cases be limited to a certain bending angle or a maximum compressive or tensile force. When the substrate and the printed circuitry are able to withstand elastic deformations and return to their original shape, we enter the field of stretchable electronics (SE).[34] This is particularly important in the development of soft-robots and in the wearable and skin-like fields of electronics.[35–39] An emerging feature that is desirable for FE and SE is the possibility of integrating healable materials since the frequent mechanical strains and displacements usually end up damaging and impairing the electrical conductivity of the device. Without healing materials, the damage repair may not be feasible nor cost-effective and therefore hinder the widespread implementation of these materials.[40]

Another branch of large-area electronics is known as conformable electronics (CE). These are particularly important for in-mold electronics (IME) and are known for their compatibility with thermoforming and injection molding technologies. Hence, the materials used in CE should not only be stretchable (to avoid cracks after thermoforming) but also maintain their adhesion to the substrate, even after they are subjected to both high temperatures and mechanical stresses. DuPont inks and substrates, for example, are widely known for their applications in CE.[41]

OLAE technology is compatible with low-temperature processing (<200 °C) and favors tailorable dimensions, that can reach several square meters.[42] OLAE is achievable by new manufacturing processes such as printing and digital fabrication, enabling a wide range of electrical components to be produced and directly integrated through low-cost processes. This empowers the production of free design electronic devices (e.g., photovoltaic solar cells, transistors molecular devices, and sensors, and actuators) that are employed in the development of +new applications.[12] In **Figure 3**, the fundamental elements of OLAE are schematized.

3. Enabling Technologies for OLAE

Nowadays, OLAE still relies on an array of different technologies that complement each other and grant the successful manufacture of multifunctional systems. These systems must combine sensors with power generation, storage, signal processing, communication, and display/actuation elements. Even though some of these functional physical elements are already printable, as evidenced in **Figure 4**, traditional deposition technologies still prevail because they assure better output performance. As an example, active thin elements such as thin film transistors (TFT), organic electrochemical transistors (OECT), metal oxide semiconductor field-effect transistors (MOSFET), and organic field-effect transistors (OFET) are mostly obtained through physical vapor deposition (PVD) and chemical vapor deposition (CVD).[28] However, since PVD and CVD require high-end clean-room spaces that demand high maintenance costs and high-temperature processing (incompatible with the nature of most flexible substrates), current research is mainly focused on the printing technologies.[43]

The growing interest in the development of organic inks for flexible large-area electronics lies in the fact that they can

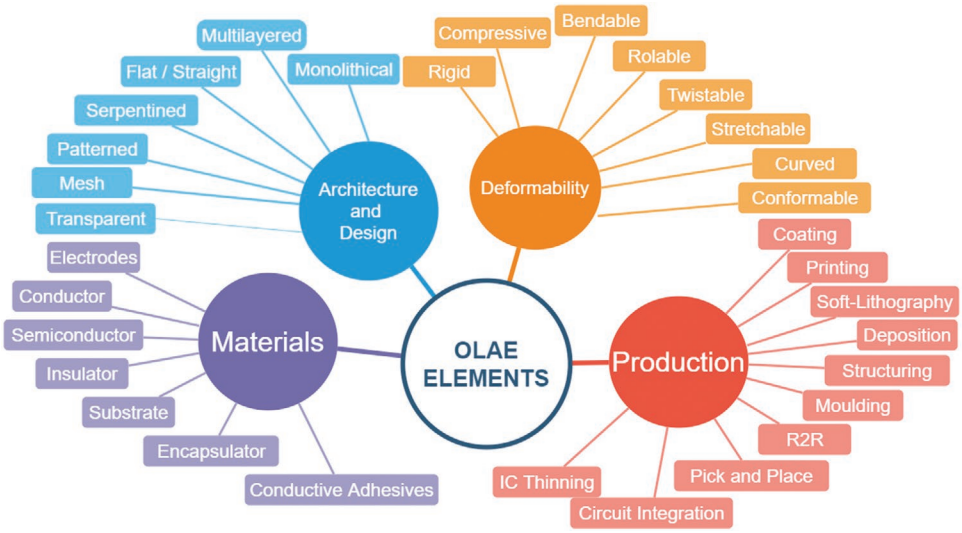

Figure 3. Schematic diagram of the four essential elements in the design and development of OLAE.

naturally be made into ink forms that are easily deposited through printing, bulk coating, or drop-casting techniques.[43] This enables fast and inexpensive coverage over large areas.[43] Once this technology is optimized and applied to each electronic component, low-cost, fully printed, massive production of complex and flexible devices will be a reality. Figure 4 depicts the key elements and technologies needed for the implementation of CPS, highlighting the sectors that will be, or already are, empowered by the OLAE standards and can be processed through printing technologies.

For scalable and sustainable, industrial fabrication of OLAE, the most adequate method is the vacuum-free roll-to-roll (R2R) production. R2R englobes contact and noncontact printing techniques that can be applied to large-scale full-layer deposition of thin films and, in the near future, should allow for the development of fully printable electronic devices.[44]

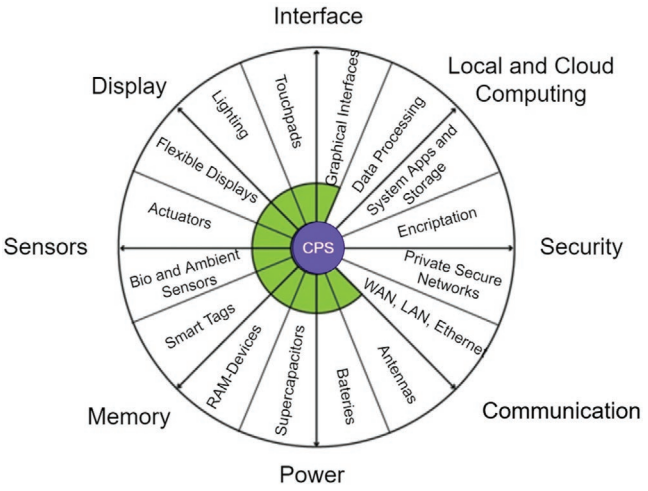

Figure 4. Diagram depiction of elements integrated into the production of CPS. Highlighted in green are the elements already achievable through OLAE technology.

Although this is a promising and attractive idealization, challenges still lie ahead. One limitation relates to the higher production complexity (addition of surfactants, stabilizers, and capping agents) of printable solution based inks and their lower inherent electrical conductivity. Moreover, this will often imply a post-treatment to eliminate organic or toxic additives (these too must be replaced soon by new materials able to sustain processing under normal environmental conditions). Another difficulty concerns the full integration of these technologies, which are still in their early stages of development. Furthermore, some parameters in R2R processes, such as the alignment of consecutive deposited layers and demonstrated ultraprecise repeatability still lack optimization.[45]

To produce TFT with the highest possible electron mobility (key property of semiconductor materials and determinant for the switch performance of transistors), the most effective method is still the PVD process, in detriment of printed alternatives. Moreover, semiconductor organic materials present far lower electron mobility than inorganic ones.[33] To support the understanding of the comparative efficiency of different materials, mobility (μ) values will sometimes be reported in this review. Mobility quantifies the velocity of electrons in response to an applied electric field across a specific material and presents different ranges for conducting, semiconducting and dielectric materials.[43]

Figure 5 depicts the growth of publications that use organic large-area electronics as a keyword, in the last ten years.[46] This figure illustrates the increasing interest in this field of electronics manufacturing, which has faced a linear growth. In the near future, promising developments are expected to happen, as well as a gradual transition to the ubiquitous use of connected devices based on OLAE and envisioned to support the IoT.

3.1. Functional Materials for OLAE

The key elements of printed electronics are electrically conductive, semiconductive or dielectric inks, pastes, or coatings. The

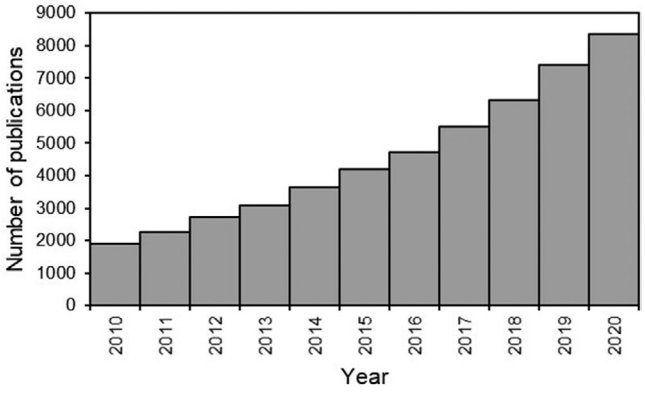

Figure 5. Number of publications on organic large-area electronics, according to Scopus on 25/12/2020.

scale of typical electrical conductivity values of these materials is depicted in **Figure 6**. Given the importance that inorganic materials still have in the current electronics market, and the indisputable advantages they hold in comparison with the organic ones, they feature in the topics discussed below. Furthermore, some materials present a hybrid nature, exhibiting insulator, ferroelectric, piezoelectric, piezoresistive, and photosensitive properties.[47] These hybrid materials combine both organic and inorganic motifs, which leads to their versatile and compelling characteristics. Even though we expect that someday fully-organic and recycle-friendly devices will be a reality, OLAE is still expected to be integrated with inorganic electronics until its related technologies and protocols reach full maturity, which includes worldwide-scale manufacturing, homologation, and marketability.

Conducting materials are central to the production of conductive layers and interconnects of circuits, making up the fundamental components of any electronic device, such as batteries, electromagnetic shields, capacitors, resistors, inductors, and sensors.[12] There is a wide range of conducting materials available for applications in printed electronics.[49] Indisputably, the majority of printable conductive inks are metal-based solutions and pastes. However, the metals that present the best performance are usually expensive (e.g., Au and Ag) and, the more affordable ones (e.g., Cu, Ni), tend to be prone to oxidation.[47] In this sense, other materials such as carbon allotropes, liquid metals, and crystalline organic conducting materials have recently been on the rise as tailorable, flexible, easy processing, and sustainable alternatives.[50–53]

Semiconductor materials, on the other hand, serve as active layers of active devices, such as organic photodiodes (OPD), organic light-emitting diodes (OLED), organic field-effect transistors (OFET), organic thin-film transistors (OTFT), and

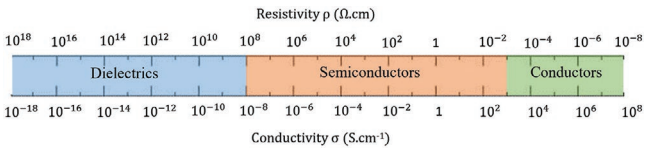

Figure 6. Typical range of resistivity and conductivity for insulators, semiconductors, and conductors.[48]

organic solar cells (OSC).[12,22,47] The most frequently used semiconductor materials are silicon (Si) and metal oxides and, even though these materials can be processed into solutions for printing, they require high annealing temperatures (300–750 °C). This makes these materials incompatible with the majority of flexible polymeric and organic substrates. Therefore, organic semiconductors, fullerenes, and carbon nanotubes (CNT) have emerged as strong competitors to the traditionally employed materials.[40,54,55] The semiconductor-dielectric interface plays a crucial role in the above-mentioned electronic components, as it consists of the active area where the charge carriers accumulate and transport.[56] Adding to these demonstrated applications as insulating layers for TFT, OFT, and OFET, dielectrics also serve as thin layers to encapsulate and prevent the leakage of current in electronic circuits.[26] The most common dielectric is amorphous silicon (a-Si) but it is usually not printable and is consequently unsuitable for flexible applications. This has powered the research on the development of low cost organic dielectric materials, mainly electrolyte solutions, and single and crosslinkable polymers.[57] The printability and organic nature of these dielectrics also favor the compatibility and stability of the semiconductor–dielectric interface, which improves the performance of the above-mentioned components.[47]

As stated before, these materials can be divided into two core categories: organic and inorganic, as resumed in **Table 1**.[12,52]

These materials can be economically printed or coated/deposited on large-area foils, such as polymers, paper, textiles, wood, and even cork substrates. In addition, it is noteworthy that some of the abovementioned materials exhibit hybrid behavior, which means they incorporate both inorganic and organic constituents.[58] Hybrid materials differ from composite materials since they coexist in one single-phase and are integrated at the nanoscale.[59] Contrarily, composites exhibit a multiphase nature, where one phase, known as the filler, is dispersed in the other, called matrix.[60]

Another way of classifying materials respects their dimension. When organic and inorganic materials present at least one dimension in the nanoscale range (<100 nm) they can be classified into 0D, 1D, or 2D.[61] This classification takes into account the number of dimensions above the nanoscale that the particles occupy in space. 0D materials amount to nanoparticles with dimensions no larger than 100 nm, such as quantum dots. 1D refers to materials like nanotubes, nanorods, and

Table 1. Classification of the nature of the materials employed in OLAE.

Inorganic	Organic
Materials	- Organic crystalline materials
- Metallic nano/microparticles	- Polymers
- Metal oxides	
- Metal–organic precursors	
- Low-temperature polycrystalline silicon (LTPS)	
- Carbon allotropes	
- MXenes	
- Quantum dots	
- Perovskite	
- Quartz	
- Transition metal dichalcogenides (TMD)	

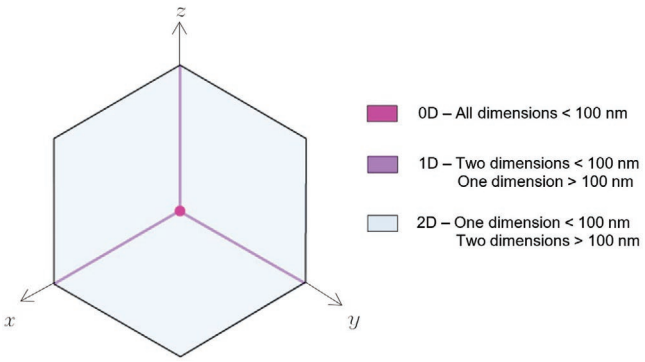

Figure 7. Classification of materials with nanoscale dimensions.

nanowires that exhibit one dimension above the nanoscale. 2D nanomaterials present two dimensions outside the nanoscale and include film-like shapes like graphene, nanolayers, nanofilms, and nanocoatings.[62] When none of the dimensions is in the nanoscale, the materials are considered 3D. **Figure 7** schematizes the classification of nanomaterials.

The inks/pastes should be processable at low temperatures and compatible with printing, deposition, and coating processes.[12,47] Depending on the selected printing method, parameters like viscosity, surface tension, conductivity, as well as compatibility of solvents between layers of different materials, must be taken into account.[63] To improve the final characteristics of the inks sometimes researchers mix several different materials from Table 1 and obtain complex materials, known as composites. To ensure the sustainability of this emerging technology a lot of research is also focused on developing green and biodegradable alternatives.[64]

3.1.1. Conductors

Metallic Particles: Metallic materials such as gold (Au), silver (Ag), copper (Cu), and aluminum (Al) present high conductivity at ambient conditions, mechanical stability, and relatively low Young's modulus. This renders them popular for applications in stretchable and large-area electronics.[65] Metals can be deposited as thin films over flexible substrates by electroplating, sputtering, thermal/e-beam evaporation, and solution methods.[66] Metallic particle solutions of metal nanowires (e.g., CuNW, AuNW, and AgNW) are usually integrated into flexile substrates through printing, or spray coating and present characteristics such as flexibility, stretchability, and transparency.[66] For instance, Wang et al. developed a pressure sensor array by using polydimethylsiloxane (PDMS) thin films embedded with AgNW as stretchable interconnects and sensing electrodes.[67] In a composite approach, Lee and co-workers prepared AgNW/CNT nanocomposites to produce flexible conductors with improved performance.[68] Even though metallic particles are already extensively used for applications in the electronic field, they are usually used as composite reinforcements (to improve electrical conductivity and mechanical stability) and are hardly find independently.

Metallic nanoparticle dispersions, on the other hand, can be inkjet or 3D printed, but they demand the use of organic stabilizers. After printing, the organic layer must be decomposed so that conductivity is guaranteed. This is achieved via a post-processing sintering step, in which the additives and surfactants are decomposed, the solvent evaporated, and the metallic nanoparticles coalesce.[69] Usually, sintering requires temperatures above 100 °C, which may degrade polymeric substrates and therefore limit the use of metallic nanoparticles in flexible electronics. To circumvent this, Agarwala et al. resorted to a fiber-based laser source to sinter aerosol jet printed AgNP.[69] They used Opsite Flexigrid as a substrate (a polyurethane material) and developed wearable strain sensors for home healthcare monitoring. The resulting sensors were able to monitor movements (bending radius), without loss of functionality, in response to detected changes in the system's electrical resistance. Recently, Fernandes et al. synthesized AgNP conductive inks and were able to inkjet-print flexible electrodes. The synthesis involved the chemical reduction of silver nitrate ($AgNO_3$) and the resulting inks presented an adequate viscosity (3.7–7.4 cP). After printing the electrodes on different substrates, sintering temperatures between 150 and 300 °C were tested. It was found that using 150 °C as sintering temperature and photo paper as substrate outstandingly low resistivity (in the order of 10^{-5} Ω cm) could be achieved.[70]

Self-healing properties have also been reported for conductive silver inks by resorting to localized solvent deposition.[71] For this, solvent-filled microcapsules were prepared by dispersing hexyl acetate in water with the aid of a surfactant and using Desmodur L75 as an emulsifier. To test the efficiency of the proposed solution, a silver ink line was printed over an acrylic substrate and, after purposely scratching the surface of the material and adding the prepared microcapsules, autonomous self-repair was observed and the conductivity was reestablished.

Metal Oxides: Metal oxides (MO), or amorphous oxide conductors are not only the most abundant materials on the planet, but also exhibit unique and attractive features, such as optical transparency and outstanding electron transport properties.[72] To modulate their electrical, optical, and structural properties, elemental materials are added in a process called doping. Depending on the degree of doping the metal oxides can act as conductors, semiconductors, or even dielectrics.[73] While MO semiconductors are doped with donors (n-type) and acceptors (p-type) to improve their electrical conductivity, the MO conductors are considered highly degenerate n-type semiconductors.[74]

Transparent conductive oxides (TCO) are recurrently used to produce devices such as photovoltaic cells, transparent electronics, "smart" windows, and touch screens.[74] Indium tin oxide (ITO), the most used TCO, can be deposited through sputtering technologies, which makes it compatible with polymeric substrates. Besides, even though it is not as conductive as the conventional metallic materials, it can be used as a replacement when optical transparency is required.[33] Using MO micro- and nanowires (MOW) is also an emerging solution for the production of electronic components, which grants higher carrier mobility than MO thin films and allows for enhanced flexibility of the devices.[75] ITO coated polyethylene terephthalate (PET) film sheets are commercially available, semitransparent, and flexible, and have been used to produce flexible conductive thin films, with thicknesses ranging from 10 to 200 µm, that are employed in various types of sensors.[76–78] In an innovative approach, Kim et al. resorted to the direct-printing of nanoscale MOW made from conducting indium oxide (In_2O_3) onto a

highly doped silicon wafer to produce field-effect transistors (FET).[75] Since the production of these devices involves the combination of conducting materials with semiconducting ones, semiconducting indium zinc oxide (IZO) wires were also deposited. Carrier mobility of 17.67 $cm^2\ V^{-1}\ s^{-1}$ was reported, which is adequate for the use in transparent FET devices and one of the highest ever reported in the literature for MO materials. Shi and co-workers produced thin and transparent thermocouple sensors by sputtering In_2O_3 and ITO over PI substrates.[79] ITO films presented a slightly lower optical transparency but both were deemed feasible for integration in thermocouples.

However, since In is a costly and scarce material, there is interest in developing In-free alternatives. Thus, antimony-tin-oxide (ATO), aluminum-cadmium-oxide (ACO), and aluminum-zinc-oxide (AZO) have been used as substitute materials for TCO.[66,73] Zhou et al have demonstrated AZO potential after they were able to develop a high-quality transparent flexible electrode, by designing an AZO/Au/AZO multiple layer structure on a mica substrate.[80] This thin film (126 nm) exhibited high transmittance percentage (81.7%) and low resistivity.

These materials are frequently deposited by PVD (sputtering, pulsed-laser deposition, or atomic layer deposition) but can also be spin-coated, spray-coated or printed. Solution-processed printable inks can be obtained through the nanoparticle synthesis route or sol–gel/precursor route.[73] Both routes require an aqueous or organic solvent, stabilizers, and high-temperature postprocessing treatment to coalesce the printed particles. Although there are obvious advantages in printing MO, it is still a challenge to obtain high mobility conductor layers at low temperatures through this approach.[81]

Despite the continuous advancements reported, there are still limitations when it comes to the implementation of MO on flexible electronics applications since they are not fully compatible with flexible and wearable electronic devices.[82] Moreover, alternatives to ITO are needed since it is a scarce resource, has a brittle nature, and requires PVD in clean rooms. As a result, research is focused on alternatives to MO electrodes that may offer higher electrical conductivity, optical transparency, mechanical robustness, and cost-competitiveness. Some of those alternatives include liquid metals, carbon allotropes, and conductive polymers.

Metal–Organic Precursors: Another route for formulating metallic-based inks is through metal–organic decomposition (MOD).[83] This route differs from the previously mentioned particle ink suspensions because the obtained ink consists of a homogenous dispersion of metals in their ionic state. MOD allows for long shelf life, low-temperature processing, and stability of inks. Besides, since their production only requires a metal precursor and a complexing agent, they are very fast to optimize and compatible with large scale production, whereas, a nanoparticle ink demands many optimization steps, and is susceptible to agglomeration, which ultimately leads to variability of results and clogged print head nozzles (in the case of inkjet printing).

Back in 1987, Teng et al. produced one of the first studies describing the use of inkjet technology to print hybrid circuits resorting to silver and MOD inks.[84] In this particular case, however, the ink made from lead titanate, presented a low-k dielectric value and was used to produce the insulating layer. The potential use of this material in the production of TFT for solar cells was also discussed. Nowadays, there is a wide array of MOD inks available and the majority presents very low resistivity. Most MOD inks are made from silver (lowest resistivity value of $1.59 \times 10^{-8}\ \Omega$ m), copper (lowest resistivity value of $1.72 \times 10^{-8}\ \Omega$ m), and metal oxides.[85–88] Even though MOD inks can also be obtained from gold their higher cost and lower conductivity deem them less attractive.[83]

Silver MOD precursors include silver neodecanoate, silver oxalate, silver acetate, and silver tartrate, while some of the most frequently used copper precursors are copper acetate, copper formate, copper acetate, copper acetate, and copper hydroxide. Some of the complexing agents used in combination with these precursors are ethylamine, isopropanolamine, and other different amines. Solvents include xylene, ethylene glycol, isopropanol alcohol (IPA), ethanol, and water.[83] MOD inks have been demonstrated for uses in printed interconnects and circuits, as well as electronic devices. As an example, Vaseem and co-workers use a silver MOD ink to produce radio frequency (RF) inductors.[88] Another very useful application for these inks respects smart packaging.[89] Thanks to their stability, easy processing, and large-scale manufacturing compatibility they pose as adequate materials to be massively printed as cost-efficient radio frequency identification (RFID) chips and near-field communication (NFC) tags.[83,89]

As a result, despite some limitations regarding the large-scale implementation of these materials, MOD inks are very promising in what concerns the future of printed electronics, and innovations respecting their use are expected as the OLAE industry continues to grow.[90]

Liquid Metals: Liquid metals (LM) are rapidly emerging thanks to their interesting and promising electrical, rheological, and thermophysical properties.[53] There are three kinds of pure room temperature liquid metals in nature: mercury (Hg, m_p: −38.87 °C), gallium (Ga, m_p: 29.78 °C), and cesium (Cs, m_p: 28.65 °C) (m_p—melting point).[91] The most widely used are the gallium alloys that, not only present negligible vapor pressure, but also low toxicity.[53,91] **Table 2** summarizes the main characteristics of the two most popular LM alloys.

Like most metals (except for the noble ones), these alloys tend to be rapidly oxidized when their surface is exposed to air, water, or acids.[53] The oxide layer that forms around the liquid metal nanoparticles (LMNP) contributes to most of their rheological properties, resulting in higher mechanical integrity and increased interfacial tension and viscosity. This results in the nonspherical shape of liquid metals (despite their high surface tension) and allows the processing and patterning of LMNP onto the target substrates.[53] Despite being helpful for the deposition step, the oxide layer hinders the conductive nature of LMNP and, therefore, a postprinting treatment (thermal, microwave, photonic, and plasma sintering) is usually required.[94]

Table 2. Gallium based alloys used in OLAE.

Gallium based alloy	Weight ratio	Electrical conductivity [$S\ m^{-1}$]	Ref.
eGaIn (eutectic indium gallium)	Ga:In = 75.5:24.5	3.4×10^6	[92]
Galinstan	Ga:In:Sn = 68.5:21.5:10	3.1×10^6	[93]

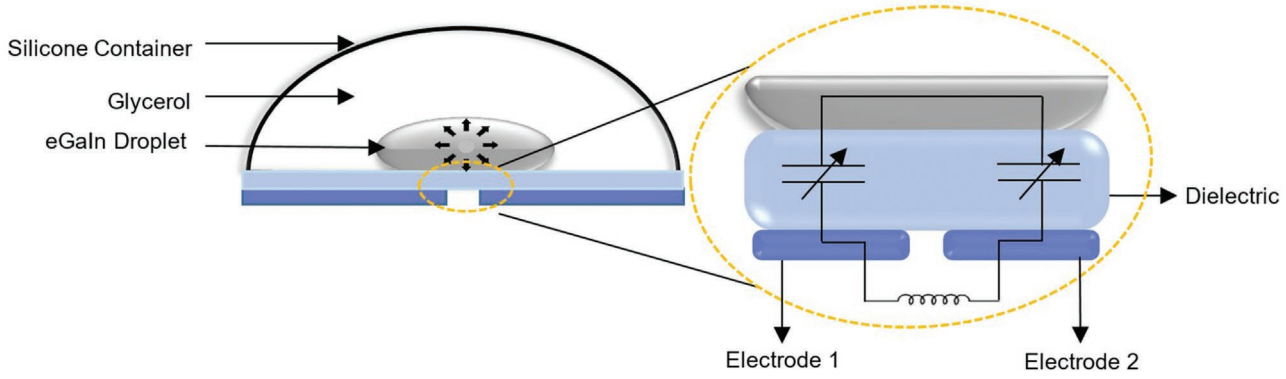

Figure 8. Representation of the LC circuit enlightening its constituents.

LMNP can be produced through complex and cost demanding techniques such as CVD, PVD and lithography-assisted patterning (demanding cleanroom techniques), or through sonication of the bulk liquid metal resorting to a solvent (organic or aqueous), surfactants, and stabilizers.[95] Commercial liquid metal inks are also widely available. These materials are attractive as they can be easily deposited through additive manufacturing (inkjet printing, 3D printing, selective wetting, spin, and spray coating).[53] Since they can be electrically conductive while simultaneously sustaining stretching, bending, and twisting, they are mostly used for sensing devices and applications as resistive and capacitive sensors. LM can also serve as feedstock material to create conductive and compliant interconnects between sensors and solid-state electronic parts, for flexible hybrid electronics manufacturing.[53,96]

To explore the potential of LM in capacitive sensing, Varga et al. produced a wireless inertial on-skin sensor based on the variation of the capacitance of a bulk eGaIn droplet, located between two electrodes and connected to a planar coil, which formed a resonant circuit, also known as an inductor-capacitor (LC) circuit (**Figure 8**).[97] The substrate used was a silicone material (Elastosil P7670), supported by a polyvinyl alcohol (PVA) coating. This sensor could be used in a bracelet, where movements from the user's arm resulted in inductor–capacitor resonant frequencies, which correlated to the movements of the eGaIn droplet, and could be analyzed wirelessly.[97]

Mohammed et al. used two different printing technologies, combined in an automated additive manufacturing process, to fully develop flexible and stretchable tactile sensors.[98] The sensors were produced by extrusion printing of PDMS (Sylgard 184), to create a flexible substrate. Subsequently, eGaIn was spray printed on top of the PDMS and, following contact with the surrounding atmosphere, it was observed that oxide shells formed around the deposited particles. This was overcome by a selective activation procedure, developed by the authors, in which the oxide shells were ruptured and merged by applying pressure directly with the nozzle tip of the extrusion equipment, creating highly conductive and complex geometric patterns at low temperature. This work presented a step forward in terms of fully printed, low temperature, and flexible/stretchable production of devices. What is more, liquid metals can be molded and reshaped without causing mechanical damage, which allows the exploitation of these materials for self-healing applications.[99] Hence, Markvicka et al. developed stretchable and healable circuit interconnects by embedding droplets of eGaIn in a soft PDMS (Sylgard 184) matrix.[99] When damaged, the droplets ruptured and reconfigured themselves around the damaged area, allowing the circuit to operate continuously without interruption of the electrical signal (**Figure 9**).

As far as metallic conductive materials are concerned, liquid metals have the highest conformability factor, with eGaIn being the most popular alloy for flexible and stretchable electronic components. Moreover, eGaIn is biocompatible, presents good rheological and self-healing properties, low-viscosity, and can be integrated into solution systems for printing.[65,66]

Carbon Conductors: Carbon-based materials are electroactive, conducting compounds that share sp^2 bond hybridization. They can be 0D (fullerenes), 1D (carbon nanotubes, CNT), or single-wall carbon nanotubes, SWNT), 2D (graphene and graphene derivatives such as graphene oxide, GO) (**Figure 10**).[100,101]

These materials are solution-processable, exhibit high thermal and electrical conductivity, low resistivity, high specific surface area, exceptional mechanical strength, and flexibility. Such characteristics brand them adequate to fulfill the demand for electronic devices with superior performance.[100] Thus, a lot of research is focused on the synthesis (modification and functionalization) of these materials, since their direct use often causes them to become indissoluble and aggregate, which limits their industrial applications. As a result, they are frequently used as hybrid carbon/polymer or carbon/oxide materials, such as GO and reduced GO (rGO).[50]

Graphene, in particular, is a 2D layered material with extended π-conjugation and unique electronic properties, and is extensively used to create hybrid materials and electronic devices (TFT, battery electrodes, and sensors).[50,66] Although graphene was already obtainable through CVD, the interest in this material increased dramatically after the introduction of mechanical exfoliation of graphene and ultrasonication as methods for obtaining very thin and exceptionally conductive graphene layers (carrier mobility up to 20 000 $cm^2\ V^{-1}\ s^{-1}$).[66,101–103] Henceforth, for simpler and lower-cost applications these technologies are preferred over CVD since they can be used to efficiently obtain liquid-phase ink solutions of graphene fillers (**Figure 11**).[104]

Since these solutions must be stable against precipitation they imply the use of adequate solvents, surfactants, and sometimes other additives such as polymer binders (**Table 3**).[103,104]

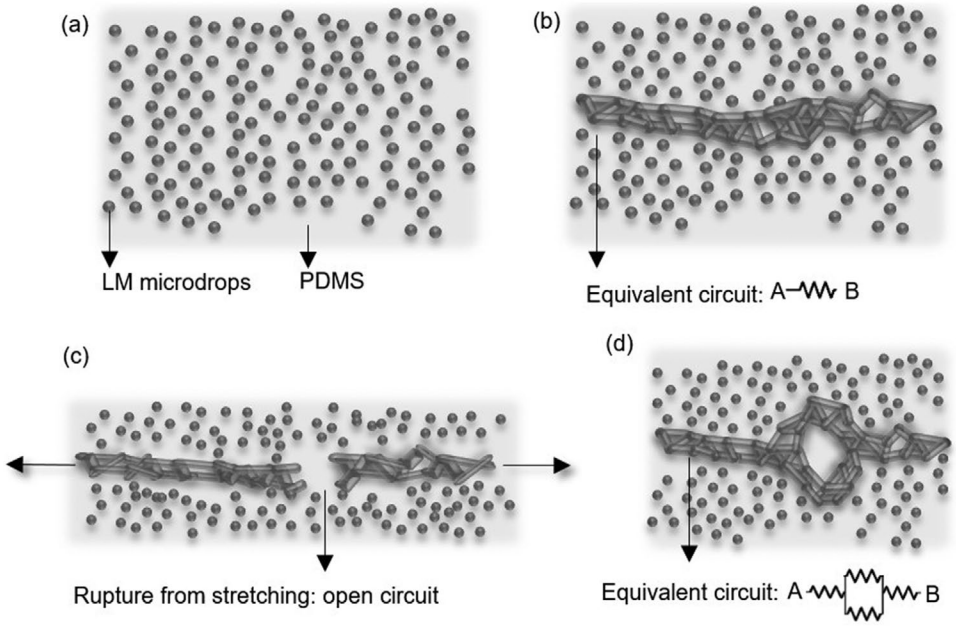

Figure 9. a) Illustration of the LM-PDMS composite; b) image depicting the selective conductive pathways created through compression and respective equivalent circuit; c) representation of the damage to the conductive pathway as a consequence of stretching. Conductivity between the terminals of that section is lost as a result; d) depiction of the same section after the LM segments reconfigure autonomously and reestablish electrical conductivity to the segment.

Although effective, these widely used methods present some drawbacks. Because of the use of organic solvents with high boiling points and the addition of binders, a high-temperature postannealing step is required.[105] Moreover, graphene, by itself, has limited stretchability (7%) and usually needs to be combined with polymers or CNT to form composites.[104,106]

Casiraghi et al. were able to avoid these steps by formulating a graphene ink via ultrasonic-assisted liquid phase exfoliation in water, using 1-pyrenesulfonic acid sodium salt as the surfactant.[107] After this, the aqueous dispersion was centrifuged, and the sediment graphene redispersed in a printing solvent.[108] This ink was inkjet printed over a paper sheet and was successfully used as a strain sensor, attached to a LED. No pretreatment of the paper substrate was carried out and the entire printing process was performed under ambient conditions. Water-based dispersions of graphene and CNT are particularly interesting because they are inherently more sustainable. Nonetheless, they rely on the use of surfactants and other additives so that stability and proper viscosity and surface tension are achieved and thus, their formulation tends to be more complex.[109] Despite this, many successful and detailed examples of devices produced using such inks exist and have been proved in the literature.[110–113]

Graphene-polymer composite inks are also extensively reported and grant a compromise between high conductivity and compatibility amidst the ink and substrate.[114,115] Classic examples have been advanced by Boland et al., who embedded liquid-phase-exfoliated graphene (using *N*-methyl-2-pyrrolidone, NMP) into a lightly crosslinked silicone polymer.[114] This resulted in highly flexible composites with unprecedented electromechanical characteristics, which were compatible with the development of extremely sensitive electromechanical strain sensors. Another composite form of graphene, with great conductive and flexible properties, is achieved by preparing graphene–poly(3, 4-ethylenedioxythiophene)-poly(styrenesulfonate) (PEDOT:PSS) composite solutions.[116] Fourier transform infrared (FTIR) analysis suggested the establishment of π–π electron donor–accepter interaction between graphene and PEDOT:PSS. As an example, these composite solutions can be inkjet printed on top of an interdigitated electrode to produce highly selective response sensors to gases.[116] The graphene-PEDOT:PSS compatibility is widely studied and composite inks can be obtained either by using organic solvents or by simply using water as a dispersion medium.[110,117] For large-area applications, He and

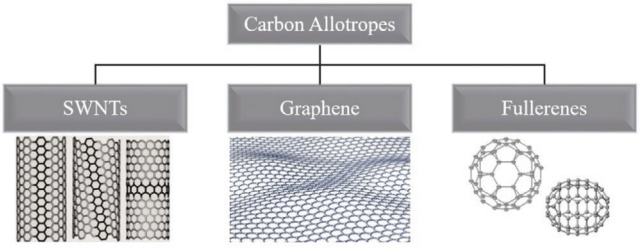

Figure 10. Different types of carbon allotropes used in printed electronics.

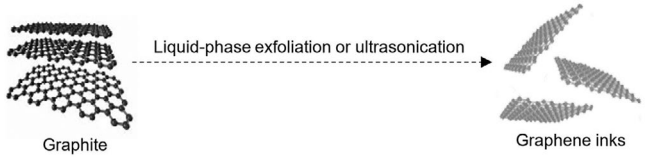

Figure 11. Representation of the processes used to integrate graphite into graphene dispersions. Adapted from with permission.[103] Copyright 2018, Elsevier.

Table 3. Some commonly used solvents, surfactants, and polymers used to aid the processing of graphite into graphene dispersions. Adapted with permission.[103] Copyright 2018, Elsevier.

Solvents	Surfactants	Polymers binders
N-Methyl-2-pyrrolidone (NMP)	Sodium cholate (SC)	Polymethyl methacrylate (PMMA)
N,*N*-Dimethylformamide (DMF)	Sodium dodecylsulfate (SDS)	Polyvinyl alcohol (PVA)
1,2-Dichlorobenzene	Sodium dodecylbenzenesulfonate (SDBS)	Polyvinyl pyrrolidone (PVP)
Cyclohexanol	Pluronic F-127	Ethylcellulose (EC)
Chlorobenzene	Triton X-100	
Toluene	Poly(sodium-4-styrene sulfonate) (PSS)	
Acetone	Flavin mononucleotide sodium salt (FMNS)	

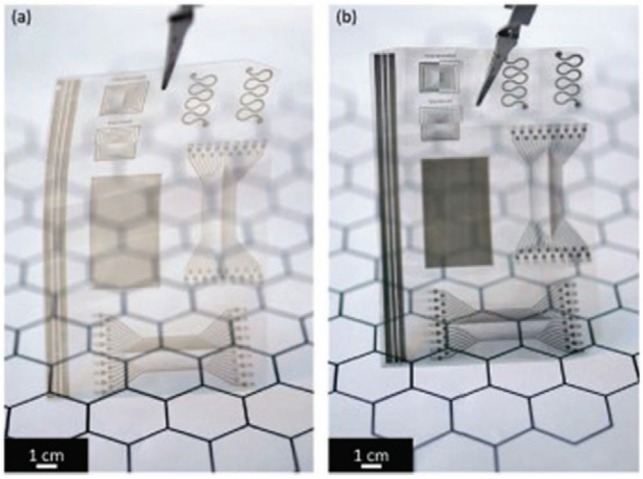

Figure 12. a) Photograph of screen-printed GO and b) rGO showing the printed conductive circuits after chemical reduction. Reproduced with permission.[105] Copyright 2017, Wiley-VCH.

co-workers were able to design a highly sensitive and fast-response capacitive pressure sensor.[118] For this purpose, they engineered a sandwich-like structure over a PDMS substrate. CVD was used to deposit the graphene electrodes, which were subsequently transferred to the substrate resorting to a PMMA film (this was later removed with acetone). Afterward, a polyimide (PI) netting was deposited over the graphene electrode (via scotch-tape method), and covered with another layer of graphene and PDMS.[118]

Graphene/AgNP composites and graphene/AgNW are also reported in literature.[119] In an innovative approach, Chen et al. produced highly stretchable strain sensors integrating graphene, thermoplastic polyurethane, and AgNP into one composite material.[119] This was used to produce a sandwich structure on a PDMS film.

When graphene is chemically modified with functional oxygen groups it is called graphene oxide (GO). As a way of avoiding the use of materials like the ones appointed in Table 3, researchers found a way of synthesizing GO ink in a simple and scalable way, by using water as the solvent.[105] After being deposited onto a polyethylene terephthalate (PET) substrate through screen-printing, the GO layer was reduced to conductive rGO resorting to industrial chemicals (commercial trifluoroacetic acid (TFA/HI)) at moderate temperature (**Figure 12**).

Besides being used in combination with graphene, CNT are also frequently merged with π-conjugated polymers.[50] Polymers such as poly(p-phenylenevinylene) (PPV), poly(*p*-/*m*-phenylene ethynylene) (PPE), poly(9,9-dialkylfluorene), polyvinylpyrrolidone (PVP), and poly (3-alkylthiophene) have been reported to form self-assembled hybrids with CNT.[50,120] Poly(9,9-di-*n*-dodecylfluorene) (PFDD), for instance, was combined with SWCNT to fabricate an ink, which was used in the production of a transistor on a test chip.[26] Multiple layers of the SWCNT-functionalized ink were printed through a procedure that combined roll-to-roll (R2R) gravure and inkjet printing. The resulting TFT, which were printed on SiO_2 wafers, were reported to present mobility values of ≈25 $cm^2\ V^{-1}\ s^{-1}$, while the TFT printed over PET substrates reported lower mobility values, but still higher than 5 $cm^2\ V^{-1}\ s^{-1}$.[26] SWCNT and MWCNT can also be combined with PEDOT:PSS to enhance its conductivity and mechanical resistance.[121,122]

Fullerenes, like C_{60} or C_{70}, are known for their potential applications as semiconductors in the field of organic photovoltaics (OPV) and organic solar cells (OSC).[123] They are sometimes used as a blend of C_{70}:C_{60} as a way of compromising between the higher performance of C_{70} and the lower costs of C_{60}.[123] Nonetheless, the most efficient OPV and OSC are still produced resorting to environmentally harmful organic solvents and additives (such as chloroform, chlorobenzene, and halogen-containing processing additives). To avoid this, Novikov and co-workers have recently developed a printable, environment-friendly aqueous solution of C_{60} to be applied to the production of OFET as gas sensors for ammonia detection.[54] For this, they took advantage of previous knowledge that sulfur-containing fullerene derivatives undergo easy thermal decomposition, reforming pristine C_{60}, and releasing some nontoxic byproducts, such as thiols and disulfides. Aqueous solutions of sulfur-containing fullerene derivatives were spin-coated over glass substrates and the obtained films were annealed in a nitrogen glove box for 30 minutes at temperatures varied from 100 to 300 °C.[54] Through this approach, they were able to achieve electron mobility of $5.1 \times 10^{-2}\ cm^2\ V^{-1}\ s^{-1}$, which represents a great step toward the development of environment-friendly organic electronics.

MXenes: Materials known as MXenes belong to the family of transition metal carbides, nitrides, and carbonitrides, and were only discovered in 2011.[124] They are emerging, highly conductive 2D materials and are obtained through chemical functionalization via a solution-etching process.[125] Thanks to their solution processability they can be used in the formulation of highly conductive inks and have recently, therefore, been rising in popularity for the printed electronics field. MXene-based inks are compatible with inkjet printing, screen printing, and spray coating. Their characteristics make them suitable for energy storage (batteries and supercapacitors), optoelectronics,

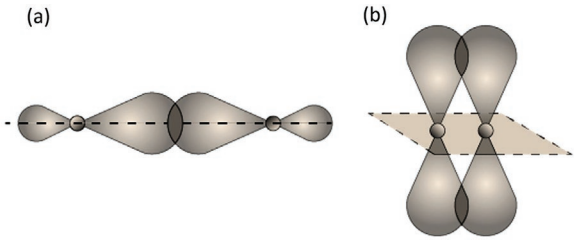

Figure 13. Illustration of a) a sigma (σ) bond and b) a π) bond.

and sensing applications.[125–128] Zhang et al. manufactured flexible and coplanar micro-supercapacitors by using 3D printed stamps to imprint water-based MXene dispersions on paper.[128] Zhao and co-workers recently developed a polyaniline/MXene nanocomposite to produce flexible gas sensing devices on PET films.[127] These devices presented not only high ethanol sensitivity but also a remarkably fast response/recovery time at room temperature. This study established MXene nanocomposites as the next-generation sensing materials for the detection of volatile organic compound (VOC) gases.

Organic Conductors: As previously stated, organic materials can compete with inorganic ones as feedstock for flexible large-area electronic functional elements. Moreover, they present low-temperature processability, flexibility, biocompatibility, and even biodegradability in some cases.[129]

Organic materials are mainly composed of hydrogen, oxygen, and carbon atoms (which constitute their backbone chain). These materials are unique since the carbon atom can have many different configurations. For instance, its electron configuration is $1s^2$–$2s^2$–$2p^2$, meaning that there are four valence electrons available for bonding at the 2s orbital and the 2p orbitals.[130] Carbon forms four bonds in most compounds through single CH_3–CH_3 bonds, double CH_2=CH_2 bonds, or triple CH≡CH bonds. When two *p* orbitals are perpendicular to each other and overlap, a pi (π) bond is established.[130] When the two sp^2 orbitals overlap in a "head-on" overlap way it is known as a sigma (σ) bond (**Figure 13**a). The later ones establish saturated bonds and are denser than the unsaturated π bonds (Figure 13b).

Many conductive polymers present intrinsic conductive properties and have been synthesized as functional materials for their electrical, magnetic, and optical properties.[66,131] The macromolecules are often based on polypyrrole (PPy),[132] polythiophenes (PT) (and various other polythiophenes, e.g., based on poly(3,4-ethylene dioxythiophene), PEDOT, and on poly(3-hexylthiophene-2,5-diyl), P3HT),[133] polyphenylene vinylene (PPV), and polyaniline (PANI).[131] While bulky crystals are fragile, low-dimensional crystals exhibit better flexibility and elasticity.[52] The most frequently used method for the fabrication of organic crystalline semiconductor-based flexible devices is PVD, however, solution-processing techniques (drop-casting, solvent exchange, and solvent–vapor diffusion methods) are also widely used.

Poly(3,4-ethylene dioxythiophene) (PEDOT), in particular, can form a stable particle suspension in water with polystyrene sulfonate (PSS) as a counter-ion, originating PEDOT:PSS, a conducting polymer compatible with various open-air deposition methods and inkjet printing.[133] PEDOT:PSS is vastly employed in the fabrication of sensors and can be prepared in addition to carbon materials and other polymers to form composites with enhanced electrocatalytic performance and sensitivity.[116,134] Guo et al. concluded that the conductivity of PEDOT:PSS was increased when printed onto a nonwoven PET fabric substrate.[133]

This was a result of enhanced phase segregation between the polymer and the surface chemistry of the textile. Recently, Tseghai and co-workers screen-printed PEDOT:PSS/PDMS composites over the textile fabric to produce large-area flexible and stretchable sensors.[135] By varying the ratio of PEDOT:PSS to PDMS it was possible to tune the electrical properties of the resulting material depending on the envisioned application (sensors, interconnections, antenna, and storages). For instance, highly conductive fabrics can be used to produce humidity sensors, the average ones to produce strain sensors and the ones with lower conductivity can be used as ECG, EMG, and EEG electrodes. In another study, researchers successfully printed PEDOT:PSS-based sensors for wireless real-time monitoring of human skin and other objects' temperature (**Figure 14**).[136]

The sensor was printed over a PEN substrate and an Ag electrode and the addition of a top layer of fluorinated polymer passivation (CYTOP) helped increase its humidity stability and temperature sensitivity.

PEDOT:PSS is not only electrochemically active but it also exhibits electrochromic attributes.[137] To take advantage of this particularity, PEDOT:PSS is often combined with metal oxides and other monomers or polymers to explore the color-switch (electrochromic effect) that derives from the following general electrochemical reaction, where the acid (PEDOT) and sodium salt (PSS) go through a redox reaction (Equation (1))

$$\text{PEDOT}^+\text{: } \text{PSS}^- + \text{M}^+ + \text{e}^- \leftrightarrow \text{PEDOT}^0 + \text{PSS}^-\text{M}^+ \quad (1)$$

A common design of an electrode for electrochromic displays is depicted in **Figure 15**. The layered structure includes a flexible substrate, on top of which PEDOT:PSS and a conductive line are deposited (through printing or coating techniques). The electrolyte, which allows for the ionic change to happen, is deposited on both electrodes (pixel and counter electrode). When in the oxidized state, the PEDOT:PSS goes from a dark bluish color to a semitransparent appearance. This color change can be tuned by varying the thickness of the two electrodes.[137]

This effect is widely explored in applications such as smart windows and smart displays.[138,139] Nemani et al. created electrochromic devices using PEDOT:PSS as the functional electroactive material, an ionic liquid as the ionic medium, and graphene as the counter electrode.[140] In this work, they were able to obtain interchanging color devices with fast response time and antiwetting properties, which represented a significant step forward in the development of low-cost and robust optoelectronic devices. Kololuoma and co-workers used PEDOT:PSS from Ynvisible Interactive Inc. to create an activity meter demonstrator with a flexible electrochromic display.[138] This display was embedded in a device through in-mold electronics, a process that allows to integrate printed and hybrid electronics in a device structure through injection molding.

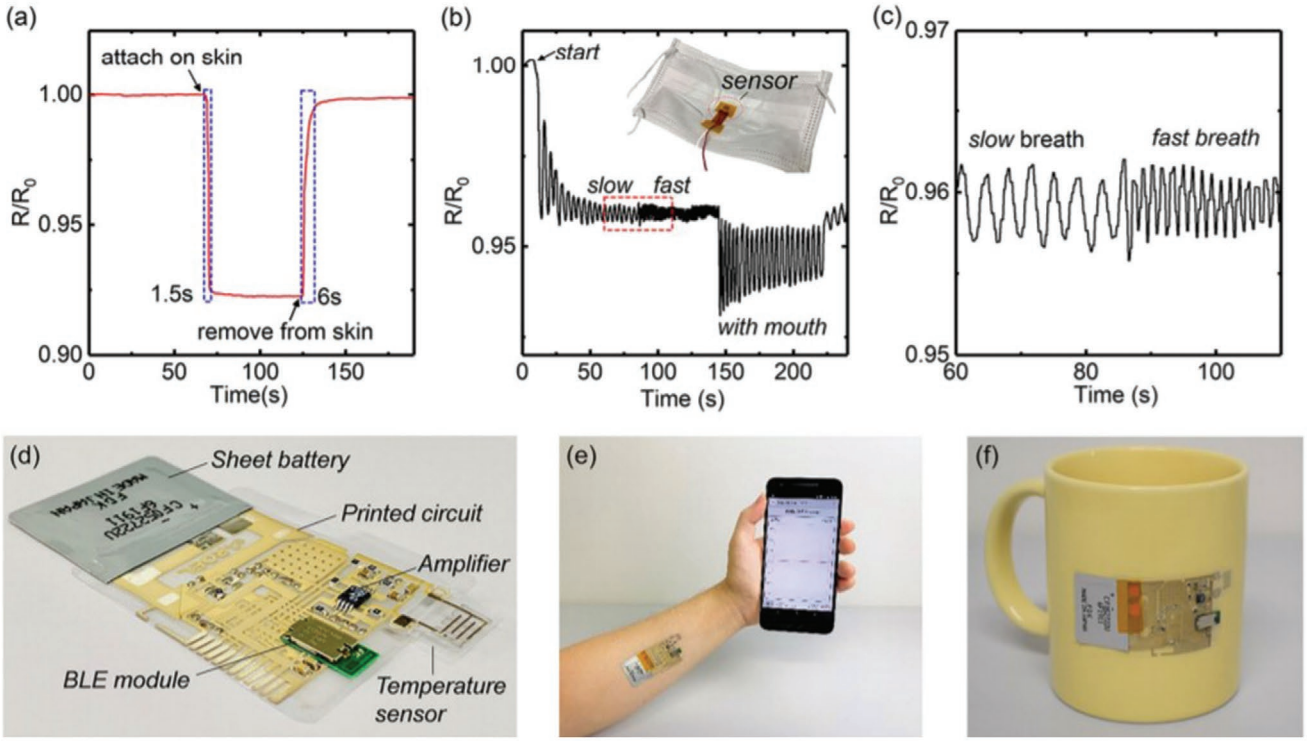

Figure 14. a) Time-dependent resistance response of a printed temperature sensor to human skin. b) Sensor integration in a facemask for rate and breathing type monitoring. c) Enlarged image of date in red box region of (b). d) Wireless temperature-sensing platform with a printed temperature sensor. e) Schematic diagram of wireless sensing platform mounted on an arm for real-time body temperature monitoring. f) The sensing platform adapted to a coffee cup for real-time object temperature monitoring. Reproduced under the terms of a Creative Commons Attribution 4.0 International License.[136] Copyright 2020, The Authors, published by Springer Nature.

PEDOT:PSS is also a classic example of an organic material whose conductive properties are greatly enhanced by combination with carbon allotropes, particularly graphene, SWCNT, and MWCNT. As a result, numerous case studies can be found across the literature regarding the use of these composite inks in printed temperature, humidity, pressure, and strain sensors.[117,121,141–146] Last but not least, thanks to its great stability when in contact with air and its capability to endure strain, PEDOT:PSS has been successfully used in the printing of stretchable interconnects and circuits.[147]

Another functional electrochemically active polymer is PANI. The conductivity of PANI is higher when oxidized or doped, and can be applied to the manufacture of sensors, inks for printable electronics, photovoltaics, and actuators.[148] The fact that it becomes more conductive after proton doping, and decreases its charge carrier density as gas molecules are absorbed, makes it particularly interesting for integration in chemical and biological sensors.[149] Moreover, its conductivity is increased by integration in composites with carbon materials. For example, Seo et al. studied the use of graphite, rGO, and graphene nanoplatelets in combination with PANI to produce flexible sensors to detect hazardous chemicals.[149] Similar to PEDOT, PANI can be doped with PSS to enhance its properties.[150] This was proved by Cho and co-workers, who developed a hydrogen sulfide sensor (H_2S) by preparing PSS-doped PANI/graphene solutions and spin coating them over PET substrates, making them suitable for flexible sensor electrodes.[150] PSS-doped PANI/graphene composites with 30 wt% graphene displayed the highest conductivity and detection of H_2S gas was successful for concentrations as low as 1 ppm. This formulation enhanced the intermolecular interactions between PSS-PANI and the graphene sheets, which facilitated charge transport in the electrode materials.

PPy is also widely reported in the literature and is recognized for its mechanical flexibility and solubility. It is usually applied to surfaces through bathing, electrodeposition, or in situ polymerization.[66] Jamalabadi et al. used an electrospinning technique to deposit PPy and a PPy-ZnO hybrid nanocomposite, with different ZnO loading percentages, over a copper thin film to produce a novel 4-element chemiresistive sensor array.[151] The sensor was capable of identifying and quantifying different amine vapors and their respective concentrations.

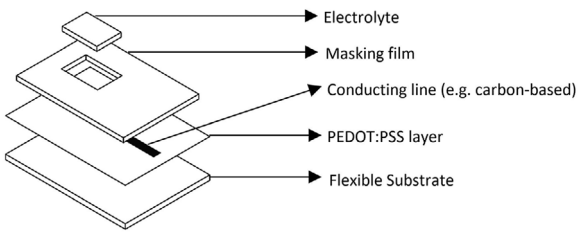

Figure 15. Depiction of one of the electrodes used to create an electrochromic display. Adapted with permission.[137] Copyright 2012, Elsevier.

3.2. Semiconductors

3.2.1. Metal Oxide Semiconductors

As previously stated, MO semiconductors (MOS) are doped with donors (n-type) and acceptors (p-type), which grant them their semiconducting ability.[74,152] Some distinguished MOS are zinc-oxide (ZnO), zinc tin oxide (ZTO), indium-zinc-oxide (IZO), indium (III) oxide (In_2O_3), tin(IV) oxide (SnO_2), tungsten trioxide (WO_3), titanium dioxide (TiO_2), copper(I) oxide (Cu_2O), and copper(II) oxide (CuO).[73]

Amorphous metal-oxide semiconductors (mainly amorphous indium–gallium–zinc-oxide (a-IGZO)) are also perceived as promising candidates for flexible LAE, as they can be manufactured at a low processing temperature, which is compatible with fabrication on polymeric and natural substrates.[152,153]

In 2011 researchers were successful in producing In_2O_3, ZTO, and IZO TFT by a solution process at a temperature as low as 200 °C, resorting to a novel self-energy generating combustion chemistry procedure.[154] In the following year, Hennek et al. printed an IGZO TFT with mobility of 2.45 $cm^2\ V^{-1}\ s^{-1}$, with an annealing temperature of 400 °C.[155] In 2014, Lim et al. were able to print ZnO TFT with an annealing temperature of just 150 °C.[156] The reported mobility was 3 $cm^2\ V^{-1}\ s^{-1}$. More recently, Park et al. developed self-powered ultraflexible organic photovoltaics (OPV) using a solution-processable zinc oxide nanoparticle layer as the electron-transporting layer and an ITO electrode.[157]

MOS are also noteworthy materials for integration into flexible circuits.[66] Pierre and co-workers produced a multiplexing circuit composed of IGZO TFT with an integrated array of sensors composed of ion-selective organic electrochemical transistors (IS-OECT).[158] This resulted in a low-cost electronic device that allowed for high-resolution mapping of the environmental concentration of ions. Münzenrieder et al. applied IGZO TFT to a large-area magnetosensory system.[159] The system integrated a differential giant magnetoresistive (GMR) sensing element and an operational amplifier with differential high impedance, composed of 16 IGZO TFT, sputtered on a flexible 50 µm PI film. This system was envisioned for applications ranging from proximity sensors for on-skin or wear-able electronics to acoustic virtual reality for visually impaired people.

Recently, MOS have been used in self-healable applications. To achieve this, Wu et al. produced titanium dioxide/polyurethane (TiO_2/PU) nanocomposites.[160] The TiO_2 and the PU motifs were reversibly covalently bonded by in-situ polymerization, through the Diels–Alder reaction. When a crack or a rupture occurred in the composite polymeric matrix, the materials were able to self-heal upon heating at 150 °C, combined with applied pressure. After healing, the electrical and thermal conductivity of the nanocomposites was recovered.

Quantum Dots: Quantum dots (QD) are semiconductor particles with sizes approaching the Bohr radius of excitons (nanoscale) and are usually referred to as 0D materials. They present attractive characteristics, such as size-tunable bandgap, small exciton binding energy, high photoluminescence quantum yields (when irradiated with UV light), and high available surface area.[33] Usually, wet chemical techniques are employed to produce QD with a high degree of crystallinity and homogenous size distribution.[161] To stabilize the inorganic nanoparticles, ligands are often added to solution-processed colloidal semiconductor QD. Their small size, monodispersity, distinctive properties, and low cost renders them valuable for future applications in commercial electronic components, information storage, and sensing.[161] They can be used as active layers in field-effect transistors (FET) and present higher mobility than 30 $cm^2\ V^{-1}\ s^{-1}$. QD have also been examined as potential candidates for photovoltaic cells.[162]

Some examples of QD used in large-area electronics are cadmium sulfide (CdS) and Cadmium selenide (CdSe). In a recent publication, researchers were able to integrate CdSe and CdS quantum dots into quantum rods (QRs) and encapsulated them resorting to surface crosslinking of ZnS (avoiding the oxidation of the QR).[163] In this work, by Chen et al., CdSe/CdS/ZnS QR were used to produce white light-emitting diodes (WLED) with higher efficiency than those presented by nonencapsulated QD.[163] Que and co-workers presented a flexible solar cell where cobalt sulfide (CoS) quantum-dots sensitized with ZnO were used as the photoanode. The ZnO nanorod arrays (NRAs) were directly fabricated on the flexible ITO/PET substrate by a hydrothermal method, and CdS and CdSe quantum dots were subsequently deposited on the ZnO NW by chemical liquid deposition.[164] The counter electrode was composed of cobalt sulfide (CoS) NRA on graphite paper (GP).

Other types of highly efficient specimens, that have already been used in the development of WLED, are graphene quantum dots (GQD).[165] Luo et al. produced them through a microwave-assisted hydrothermal method and were able to obtain high current density and luminance.[165] Another field of application of flexible quantum dot light-emitting devices (QLED) is the medical industry, more specifically in the production of devices for photodynamic therapy against Gram-positive bacteria.[166] As a proof-of-concept, Chen et al. successfully synthesized QLEDs and deposited them onto a PEN flexible substrate. They presented high efficiency, narrow spectra, and specific wavelengths of interest to photomedicine.

Another type of increasingly popular material are the perovskite quantum dots (PQD). Recently, Shi et al. used a strategy called in-situ inkjet printing (ISIP) to generate displays with anticounterfeiting and enhanced photoluminescence properties.[167] This strategy encompasses the use of an inkjet ink made from perovskite precursors dissolved in DMF. After printing drops of this ink in a controlled manner onto a heated polymeric substrate, the printed dots were allowed to spread, partially dissolve on the solvent matrix, and were finally left to dry and crystalize as PQD thanks to slow solvent evaporation. The patterned crystalized PQD dots emerge as pixelated images upon UV lighting.

Low-Temperature Polycrystalline Silicon (LTPS): LTPS (p-Si), as the name hints, are synthesized at low temperatures and are very attractive for flexible electronics, particularly in the production of TFT for displays.[168] The most attractive methods to deposit LTPS over polymeric substrates are plasma-enhanced chemical vapor deposition (PECVD), excimer laser annealing (ELA), and solution processes. Contrarily to a-Si, which usually cracks when subjected to bending tests, even with low tensile strains of 0.5%, LTPS can be implemented in flexible sensors with improved results.[66,169] They also present good electrical

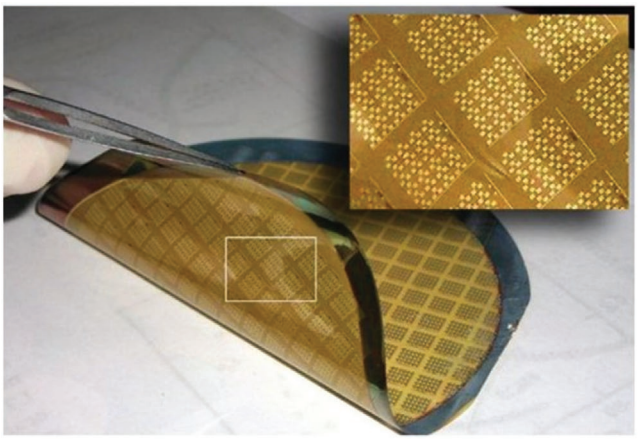

Figure 16. Depiction of the LTPS TFT deposited onto the substrate with evidence of its flexible nature. Reproduced with permission.[171] Copyright 2008, Elsevier.

characteristics with carrier mobility up to ten times higher than the one presented by MO semiconductors (50–100 $cm^2 V^{-1} s^{-1}$). Hence, to provide the same current supply, a-Si and metal-oxide TFT require a larger device-width. This means a higher resolution of OLED can be achieved using LTPS TFT (a pixel must contain space for TFT and OLED, and therefore, the less space the TFT occupies the larger the OLED component can be, leading to increased brightness).[170] Another advantage of LTPS over MO semiconductors seems to be their higher stability, reliability, and lower reported thermal degradation.[94] These advantages, altogether, appoint LTPS as the most promising semiconductor for TFT in the scope of the currently used organic and inorganic materials for large-area and flexible electronics.

The preferred substrates for bendable and twistable displays are thin glass, metal foils, and polymers. While glass and metal foils can sustain high process temperatures and present great compatibility with LTPS, they have limitations regarding their brittleness and fragility.[170] Polymers, on the other hand, are ideal substrates for malleable applications, but often suffer damage or expansion during the deposition of the LTPS film layer, as a result of temperature shock. This was observed by Pecora et al. that, as a preventive measure, suggested the deposition of a SiO_2 layer as a thermal buffer layer between the substrate and the amorphous-Si film, which suppressed the conduction of heat to the substrate.[171] During the selective wet-etching patterning of the doped Si-layer, the maximum registered temperature was 350 °C, which was endurable by the used PI substrate (**Figure 16**).

Gao et al. also demonstrated the production of an active-matrix organic light-emitting diode (AMOLED) by using amorphous silica as barrier layers between the PI substrate and the LTPS TFT.[172] The deposition was conducted through PECVD followed by a 450 °C dehydrogenation oven annealing process. Although LTPS are, indeed, materials with tremendous potential for OLAE applications, they are usually only compatible with substrates that can withstand relatively high temperatures, with PI being the go-to polymeric substrate for manufacturing flexible LTPS based TFT. Nonetheless, Trifunovic et al., were able to successfully produce a solution-processed LTPS from a Si-based ink, named cyclopentasiloxane, and deposited it over a paper substrate.[173] This was carried out in a contained environment and at low oxygen presence, resorting to a blade. Subsequently, ELA was performed at a maximum temperature of 150 °C. This work allowed for the direct integration of Si on inexpensive substrates.

Organic Semiconductors: Organic semiconductors include molecules and polymers that present aligned and patterned structures such as rubrene, pentacene, poly(3-hexylthiophene) (P3HT), poly(diketopyrrolopyrrole-terthiophene) (PDPP3T), diphenylanthracene (DPA), amongst others. Their crystalline conformation grants device uniformity and reproducibility, representing a step toward large-scale, simple, and low-cost fabrication of organic crystalline material (OCM) flexible devices.[52,66]

For electronic applications, pentacene is usually used as 6,13-bis(triisopropylsilylethynyl)pentacene (TIPS-pentacene). TIPS-pentacene exhibits much higher molecular packing than pentacene alone, thus granting higher conductivity properties to the envisioned applications (**Figure 17**).[174] In a 2008 study, OFET were produced by evaporation of an inkjet printable formulation of TIPS-pentacene, which was printed over a PEN substrate.[175] In a recent study, Kim et al. spin-coated a TIPS-pentacene solution at various spin rates (1200, 1500, and 2000 rpm) and studied the consequent formation of a 2D crystalline film (through the formation of spontaneous π–π interaction).[176]

In 2016, Park et al. conducted a study regarding the inkjet-assisted nanotransfer printing (inkjet-NTP) of TIPS-PEN, C_{60}, and P3HT to produce photodetectors and strain sensors.[177] Inkjet-NTP allows the printing of large-area devices with monolithic integration of distinct and patterned organic functional materials. Thus, it was possible to integrate 12 sets of circuit arrays with FET, inverters, and heterojunction diodes into one single substrate. Each one of the active components consisted of nanopatterns composed of TIPS-PEN, C_{60}, and P3HT (**Figure 18**).[177]

This synergistic combination of inkjet printing and nanotransfer printing represented a breakthrough in the large-scale fabrication of multimaterial and multifunctional devices.[177]

Rubrene organic single crystals have also been extensively used to produce low-cost flexible FET. Briseno et al. produced OFET growing rubrene crystals through physical vapor transport in a flowing stream of argon. ITO/PET substrates were used as bottom-contact flexible substrates and a mobility as high as 4.6 $cm^2 V^{-1} s^{-1}$ was reported.[178]

In the case of diphenylanthracene (DPA) crystals, strong intermolecular C—H…π interactions are established between the neighboring DPA molecules to form 1D stacked arrangements.[52] This OCM allows for excellent electrical properties. High electrical mobility (34 $cm^2 V^{-1} s^{-1}$) has been reported by Liu et al. in a report where OLED based on 2,6-DPA organic semiconductor were developed.[179]

Hybrid Semiconductors: Some materials incorporate both organic, inorganic, or chalcogenide motifs, presenting versatile and compelling properties that arise from their complementary nature.[180] Perovskites,[162] Rochelle salts,[180] and transition metal dichalcogenides (TMD) have been reported for their potential as hybrid materials for electronics manufacture.[181,182]

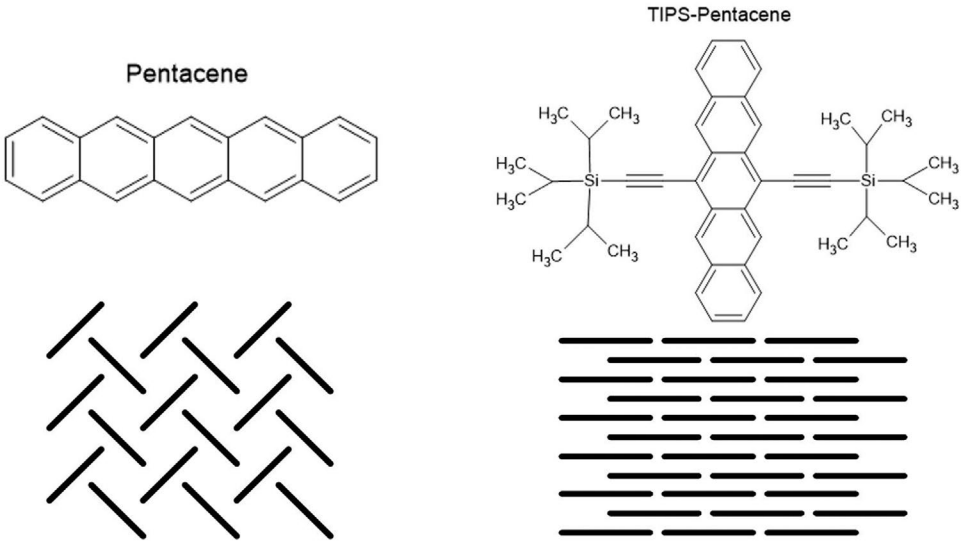

Figure 17. Molecular packing motifs in organic crystals, with examples of pentacene in herringbone packing (face-to-edge) without π–π overlap (face-to-face) between adjacent molecules and TIPS-pentacene in lamellar motif, 2D π-stacking.

Ever since 2009, perovskite has been extensively employed in the manufacture of organic solar cells (OSC).[162] They are widely studied for their optical and electrical properties and their solution and deposition processability at low temperatures.[66] For instance, perovskite solar cells have been fabricated using a low-temperature solution in a one-step process or a two-step sequential process.[183,184] For these applications, the preferred compounds are organic–inorganic hybrid perovskites (methylammonium lead halides of bromide, iodide, or chloride).[66] Kojima et al. studied the potential of lead halide perovskite compounds such as $CH_3NH_3PbBr_3$ and $CH_3NH_3PbI_3$ as visible-light sensitizers in photoelectrochemical cells.[162] These nanocrystal particles were successfully used to coat a TiO_2 film (as n-type semiconductors) and used to produce photoelectrodes with power conversion efficiency (PCE) around 3–4%. Although at the time the resulting PCE was considerably low, this was a pioneer work and resulted in the upsurge of a new type of solar cell technology. In 2014, researchers reported a groundbreaking PCE of 19.3% using a lead halide perovskite deposited through an enhanced reconstruction process conducted in controlled humidity and low-temperature environment (<150 °C).[185] One year later, Yang et al. achieved the highest PCE reported for a perovskite solar cell.[186] Resorting to formamidinium lead iodide ($FAPbI_3$) perovskites fabricated from PbI_2(DMSO), through an intramolecular exchange process (IEP), they obtained higher efficiency solar cells (PCE > 20%) with a great degree of reproducibility. Hu et al. were able to produce a printable perovskite module that exceeded 10% PCE.[187] This work proved the scalability of the production process of perovskite solar modules by fully printing 10 serially connected cell modules (10×10 cm^2). **Figure 19** depicts the production line proposed by Hu and co-workers to continuously print the solar multilayer modules. First, the conductive glass layers are etched with parallel laser rays. Then successive layers of TiO_2, zirconium dioxide (ZrO_2), carbon, and perovskite solution are deposited. Finally, the surface of printed modules is etched with a laser to create the electrode patterns.

Other large-area approaches for scalable fabrication through roll-to-roll (R2R) printing appear in the literature. For instance, Hu et al. used organic–inorganic hybrid halide perovskite nanowires (PNW) of methylammonium lead iodide to produce photovoltaic devices at ambient conditions of 45% humidity and 28 °C.[188] Both silicon oxide (SiO_2) and flexible polyethylene terephthalate (PET) were successfully used as substrates. Besides being inherently hybrid, they can form composites with MO,[189] CNT,[190] and organic conductors, such as PEDOT:PSS.[191,192] Composite halide perovskites present increased electrical and mechanical properties. As an example, Xie and co-workers

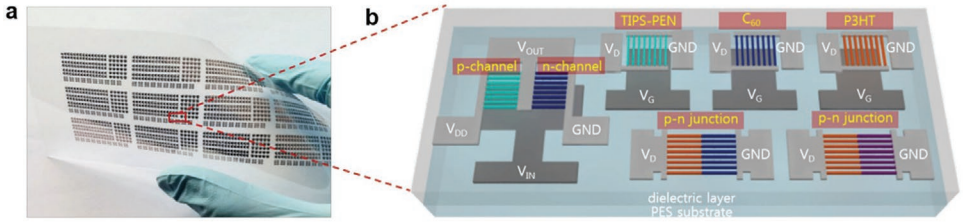

Figure 18. a) Large-scale integrated circuits of functional organic nanopatterns on a plastic substrate (Photograph). b) Schematic diagram of a representative area of the integrated electronic devices. The FET were produced with TIPS-PEN (green), C60 (blue), and P3HT (orange), the inverters with TIPS-PEN and C_{60}, and the p–n diode arrays each used P3HT with C 60 and P3HT with *N*,*N*′-dioctyl3,4,9,10-perylenedicarboximide (PTCDI-C8). Reproduced with permission.[177] Copyright 2016, Wiley-VCH.

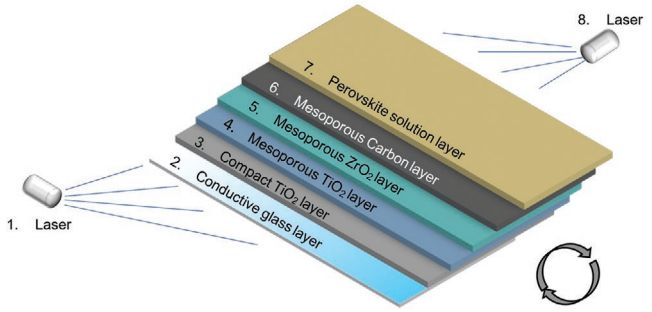

Figure 19. Schematic illustration of the successive printed layers during the production line of the solar modules.

produced perovskite/organic–semiconductor phototransistors for ultrasensitive broadband photodetection, based on methylammonium chloride/PEDOT:PSS.[192] For this purpose, a $CH_3NH_3PbI_{3-x}Cl_x$ perovskite film was spin-coated over a previously deposited PEDOT:PSS layer and subsequently subjected to thermal annealing at 100 °C. The devices produced through this process showed higher gain and higher responsivity than what was previously reported for perovskite-based photodetectors.

Quartz and Rochelle salts are natural materials that exhibit piezoelectric sensing potential, which arises from variation in their conductivity upon deformation of their crystalline structure when pressured.[180] Although they have a lot of potential in sustainable electronic manufacturing, reports of applications are yet to be developed. Quartz, however, is already widely employed as a substrate material.

TMD are 2D layered materials usually obtained by CVD or by the previously described liquid-phase exfoliation process (resorting to hydrofluoric acid or other etchants, in this case).[125] They can be organic when incorporated with conjugated polymers or carbonaceous materials, or inorganic-based, when incorporated with noble metals or metal oxides. Besides, they can be produced through low-cost and scalable procedures.[193] Applications in photovoltaic cell development, chemical sensors, and energy conversion and generation have been reported for TMD. Semiconducting TMD include MoS_2, WS_2, and $MoSe_2$. Discovered in 1963, MoS_2 rose to prominence in 2011 after it was first used to produce a transistor with an excellent current ratio.[194] MoS_2 is unarguably the most popular TMD for large-area applications and has been used to produce printable inks resorting to solvents such as water, IPA, ethanol, among others.[125] It has applications in gas sensors and photodetectors. To demonstrate this, Yao et al. produced inkjet printable NH_3 gas sensors using a high concentration aqueous dispersion of MoS_2.[195] Ethanol and glycerol were also added to the solution to improve its viscosity and assure its printability. In another work, layers of graphene/MoS_2 and MoS_2 were deposited through CVD over a PI substrate to produce photodetectors and transistors.[196] In a different approach, Kim and co-workers synthesized MoS_2 phototransistor arrays on flexible polymer substrates using CVD.[197] The resulting material had great transparency and tolerance, which was maintained even under tensile strains.

3.3. Dielectrics

Dielectrics are a fundamental integrating part of several electronic devices for applications that demand high capacitance and insulation.[47] The dielectric layers should be uniform and smooth to promote adequate integration between components and efficient activation of the medium caused by the electric field actuation. In the field of printed electronics, this is no exception, and they are an essential part of printed FET and capacitive sensors.[66] In commercial devices, the gate dielectric is usually composed of thermally oxidized SiO_2.[57] Si-based dielectrics, such as PECVD silicon nitride (SiN_x) and silicon oxide (SiO_x) thin films, have been used in the electronics industry for years and are widely reported.[43,198]

More recently, to achieve scalable and low-cost production of various electronics, solution-processable MO, polymers, and hybrid dielectrics have risen in popularity.[57] As previously discussed, MO (such as aluminum oxide (Al_2O_3), zirconium oxide (ZrO_2), hafnium oxide (HfO_2), and yttrium oxide (YO_2)) are printable materials and, for dielectric applications, the most popular one is Al_2O_3. By inkjet printing, it is possible to achieve high-quality thin films from Al_2O_3 inks, however, some disadvantages such as nozzle clogging and grain boundary formation have been reported.[199] McKerricher and co-workers used Al_2O_3 to develop a sol–gel dielectric, which was employed in the manufacture of printable metal–insulator–metal (MIM) capacitors.[199] Researchers were able to suppress coffee ring staining by optimizing the solution and the resulting capacitors showed good dielectric properties for currents under 20 V. Nonetheless, some improvements should be made to reduce the variation in the performance of the printed devices and to lower the required processing temperature.

Polymers are also widely employed as dielectric inks thanks to their easy processing. PMMA, PVA, PVP, poly(4-vinylphenol) (PVPh), poly(acrylic acid) (PAA), poly(perfluorobutenylvinylether), polystyrene (PS), polylactide acid (PLA), poly(vinylidene fluoride) (PVdF), and PVdF-Trifluoroethylene (PVdF-TrFE) are some of the most reported ones.[66] Polyesters, polyurethanes, epoxy resins, and epoxy-based UV curable materials are also reported in the literature.[27,200,201]

PVP, PVA, PS, and PMMA can be used as single polymers or manufactured into crosslinkable inks.[202–204] Mohapatra et al. produced inkjet printable parallel plate capacitors using a PVP ink that demanded curing at 180 °C to crosslink and solidify the polymer.[205] Silver ink was also printed to produce the metal plates. To avoid high-temperature processing, Jeon and co-workers demonstrated the use of ultraviolet (UV) crosslinkable PVA solution as a dielectric.[206] They developed a transistor and a capacitor to produce high-gain logic circuits over a polymeric substrate. To achieve this, semiconducting pentacene was deposited over the PVA dielectric through vacuum deposition. Li et al. copolymerized PMMA and PS with propargyl and azido groups and were able to crosslink it resorting to low temperatures (100 °C).[207] SU8 is another material with interesting dielectric properties.[208] Since it is widely commercially available and UV crosslinkable, it appears as an affordable alternative that demands low-temperature processing. Zea et al. inkjet printed SU-8 over paper to create a hydrophobic layer, which was cured with UV radiation for 30 s.[209] After treating the surface of the

paper, a three-electrode array, made of gold and silver layers, was inkjet printed, sintered, and treated with oxygen plasma. The process was finalized by the inkjet printing of another UV curable SU-8 layer, which served as the passivation layer. Other UV curable polymers such as acrylic conductive inks and electromagnetic inks allow for fast and low-temperature curing and have been used in the development of microelectronic devices for several years.[210,211]

In a recent work by Ashtiani, the dielectric properties of PVP, PMMA, and barium titanate ($BaTiO_3$) were combined by developing a low-temperature processing $BaTiO_3$/PMMA/PVP nanocomposite solution.[212] This organic–inorganic nanocomposite was used as a dielectric gate and revealed promising capabilities for optoelectronic applications.[212] Nanocomposites obtained by dispersing $Ca_2Nb_3O_{10}$/PMMA in acetone have also been used to produce thin dielectric films with higher dielectric constants than PMMA alone.[213] Hybrids between MO and polymers are also studied for their combined properties as insulators.[214–216]

PVPh is also a very useful polymer to create printable dielectric material. It is used in its crosslinked state, as cPVPh, and is frequently employed as an organic gate dielectric layer in the production of OTFT.[217] In 2014, Eloi Garcia drew inspiration from previous literature and optimized a formulation to create a printable ink, based on the cross-polymerization of PVPh.[218,219] To achieve this he used poly(melamine-*co*-formaldehyde) methylated (PFMF) as the crosslinker, and propylene glycol monomethyl ether acetate (PGMEAE) as a solvent. Ever since, several examples using inkjet-printed cPVPh, obtained through this methodology, have been published to create printed electronic components.[13,220–223] cPVPh is also frequently used in combination with rapheme and SWCNT to create gate dielectric layers with low operating voltage and higher environmental stability and flexibility.[224,225]

The ferroelectric PVdF is a hybrid piezoelectric material known for its flexibility and easy processing. It is known as a metal–insulator–ferroelectric–insulator–semiconductor (MIFIS) and its copolymer, poly-(vinlidenefluoride-trifluoroethylene) (PVdF-TrFE), is extensively used in the preparation of thin films for electronics.[226] In 2016, Kheradmand-Boroujeni et al. fully-printed polymeric amplifiers using piezoelectric loudspeakers.[227] For this, they created a layered structure with a top and bottom layer electrodes made from PEDOT:PSS and a middle piezoelectric layer made from PVdF-TrFE.

An example of a wearable device made from PVdF-TrFE films has been advanced by Hu's research group.[228] In this work, they took advantage of the piezoelectric characteristics of PVdF-TrFE and enhanced its performance via conjugation with rGO. This improved the crystallinity of PVdF-TrFE and empowered its use as an energy-harvesting nanogenerator. The preparation method of the composite films was in situ-polarization followed by sputtering deposition. Cu wires were then attached with silver ink to form the electrodes.[228] This method was compatible with the scalable development of devices for human motion energy harvesting for powering wearable or portable electronic devices. PVdF has a huge potential for future IoT applications, particularly for object and/or skin-integrated sensors for monitoring of mechanical, thermal, and vital parameters.[229] Besides, they can be used as energy harvesting materials which will be a key element in this technology. Moreover, PVdF-TrFE also presents a higher dielectric constant when processed at 140 °C by spin-coating than the one presented by Al_2O_3.[230]

Some of the above polymeric and polymer-based inks, as well as other literature examples, are listed in **Table 4**.

Table 4. Polymeric and polymer-based materials for the production of printable dielectrics. Adapted with permission.[57] Copyright 2018, Elsevier.

	Dielectric	d [nm][a)]	Semiconductors[b)]	μ [$cm^2 V^{-1} s^{-1}$][c)]	Ref.
Single polymer	PVA	9	Pentacene	1.100	[202]
	PVP	922	Pentacene	0.150	[203]
	PMMA	300	Pentacene	0.241	[204]
Polymer blend	PAA+PI	300	$F_{16}CuPc$	0.006	[231]
	PMMA+PS	–	CuPc	0.010	[232]
	PVdF+TrFE	325	CP-DIPS pentacene	–	[226]
Crosslinked and photo- crosslinked polymers	PVP with thiolene functionalized	50	TIPS-pentacene	0.117	[233]
	PMMA with azide/alkyne functionalized	410	TIPS-pentacene	0.590	[207]
	PVP with TMPTE	560	Pentacene	0.500	[234]
	PVA with ammonium dichromate	150	Pentacene	0.480	[206]
	SU8 (self-crosslinked)	1160	TIPS-pentacene	0.400	[208]
Hybrid bilayered dielectrics	TiO_2/PVP	317/317	P3HT	0.026	[214]
	Y_2O_3/PMMA	–	C8-BTBT	3.110	[215]
	TiO_2/PS	4.7/21.1	Pentacene	0.310	[216]
Polymer nanocomposites	$BaTiO_3$/PMMA/PVP	≈750	ZnO	–	[212]
	$Ca_2Nb_3O_{10}$/PMMA	50	IGZO	2.400	[213]

[a)]d refers to layer thickness; [b)]Semiconductors refer to the functional material used in combination with the dielectric; [c)]μ refers to the electron mobility–velocity of the electrons on the dielectric.

Table 5. Typical substrates used in LAE.

Substrates	UWT range [°C]	Temperature
Most polymers, paper, wood, cork, cotton	<150	Low
High temperature polymers	150–350	Medium
Thin glass and metals	150–400	Medium
Ceramics, quartz	>350	High

These polymer-based dielectrics have shown great potential in applications such as flexible, wearable, and foldable electronics, presenting processing and interface compatibility with polymeric substrates.

3.4. Substrate Materials for OLAE

The abovementioned functional materials should be deposited over flexible, stretchable, or twistable substrates, depending on the envisioned application and, therefore, some key substrate materials for OLAE have already been mention thorough this work.

This section presents an overview of the different substrates available, their nature, characteristics, and some preprocessing techniques are discussed. These techniques may be applied to the substrates before the deposition or printing steps. Substrate materials should be selected taking into account the envisaged application and temperature needed for deposition/printing and annealing (when required). In **Table 5**, some substrates are presented, complemented with the upper working temperature (UWT) range they can withstand for the sake of comparison.

The ideal high-performance flexible substrate presents a low coefficient of thermal expansion (CTE), good solvent and thermal resistance, thermal stability, and optical transparency.[235] Since this review focuses on organic materials, we will discuss in detail the use of polymeric and natural substrates.

3.4.1. Polymeric Substrates

When flexible, stretchable, and/or twisting properties are required, the preferred substrates are usually polymer films or foils. Most polymers, however, are not compliant with high temperatures and, as a result, their use in traditional printed electronics is limited. Most recently, and with the development of alternative low-temperature printing and coating processes for OLAE manufacturing, there has been an increase in the use of polymeric substrates such as PDMS,[236] poly(ethylene terephthalate) (PET),[133,164,178,188] poly(ethylene naphthalate) (PEN),[136,166,175] polyurethane (PU),[117] and polycarbonate (PC).[237] Other classes of polymers that are on the rise as substrates for electronic devices include epoxy rubbers, commercially available silicones such as Ecoflex and Dragon Skin, and thermoplastic polyurethanes (TPU), such as NinjaFlex and TangoBlack.[238]

Recently, research in thermal endurable substrates is gaining traction, and polymeric substrates that exhibit high thermal endurance have been reported. Highlighted in the literature are polyimide (PI),[171] heat stabilized polyether ether ketone (PEEK),[43,238] polyarylates (PAR),[239] polyethersulfone (PES), and liquid crystal polymers (LCP).[30]

Polymeric materials are relatively low-cost, present low density, and are appropriate for industrial high-speed roll-to-roll printing processes.[43] Despite all these advantages, there are still some difficulties associated with high permeability, low dimensional and thermal stability, low adhesion, and reduced temperature tolerance of these materials. Moreover, the fact that most polymers are permeable to water and oxygen may cause the degradation of organic devices.[43] Most polymers also have a high CTE, which may result in distortions to the substrate.[240] Besides, the majority of them are nonpolar and present low surface energy, which challenges the wettability and adhesion of inks.[241]

PDMS, a thermal or UV curable elastomer, has been a key material in the development of lab-on-a-chip systems.[242,243] It is not only optically transparent and mechanically flexible but also biocompatible and chemically stable.[242] It has, therefore, been established as the go-to polymer for stretchable devices and is widely employed in the medical industry.[30] Since PDMS exhibits a high CTE, its structure deforms considerably when exposed to temperatures above its working range.[236] As a result, its use as a substrate is limited to low-temperature fabrication procedures, such as low-temperature printing and coating. Printing inks, however, do not seem to adhere well on PDMS without surface pretreatments, due to its nonpolar and hydrophobic nature. To circumvent this, some tactics have been developed that allow the enhancement of the bond strength between conductive inks and elastomer surfaces.[236] Such ways include spray coating of the substrate with a primer, printing a glue layer, functionalizing the PDMS substituting methyl groups, adding binders to the functional inks, and/or surface modification of the substrates.[236,244,245] As an example, Chiolerio et al. were able to inkjet print piezoresistive PEDOT:PSS electrodes onto PDMS, only after it was subjected to a plasma treatment.[246] Metal nanowires and CNT have also been embedded in elastomeric substrates of sensors to improve their stretchability and electrical conductivity.[247,248]

Substrates such as Ecoflex and Dragon Skin (PDMS) are highly stretchable (elongation at break > 600%) curable materials that are commercially available and, therefore vastly reported for large-area flexible electronics.[249,250] These materials are permeable to air and are preferred for large on-skin applications for their soft, stretchable, and biocompatible properties. Tian et al. developed innovative devices for epidermal electronic interfaces resorting to bilayer substrates.[249] For this, they deposited large-area sensors over Ecoflex (curable biodegradable silicone rubber) and resorted to a PET release substrate to aid the deposition of the layered system over the skin. The PET substrate was removable and its function was to ease the manipulation and deployment of such large-area devices over curved surfaces of the body. The skin interface was encapsulated with an outer layer of PI.[249] The resulting device was magnetic resonance imaging (MRI)-compatible and was able to offer reliable and robust body-scale electrophysiological recordings.

NinjaFlex and TangoBlack are both thermoplastic rubber-like materials that are envisioned for 3D printing applications. With

the rise of printed electronics, the use of 3D printers for rapid fabrication of devices is also becoming recurrent.[238] Thus, flexible filaments are being selected to 3D print substrate materials. As an example, Rizwan et al. produced wearable antennas using NinjaFlex, a strong, lightweight, and flexible material. The substrate was printed using a nozzle temperature of 230–235 °C and a bed temperature of 60 °C.[251] Afterward, a stretchable silver conductive paste was brush painted on top of the substrate and the device was cured at 110 °C. The bending performance was evaluated and it was concluded that this fully-printed antenna was compliant with wearable applications. Other authors have used similar approaches to 3D print NinajFlex as the substrate for antennas and flexible RFID tags. This substrate material is often combined with silver or PEDOT:PSS, as the conductive component.[252,253] In 2015, Vaithilingam et al. conducted a study in which they evaluated the use of TangoBlack (TB) as a flexible substrate for printed electronics.[254] In this study, they extensively characterized the surface adhesion and flexibility of an AgNP ink and a PEDOT:PSS ink on top of the substrate. They concluded that, while the AgNP ink had potential in flexible electronics, it failed to pass the requirements to be used in stretchable electronics, since the topography of the ink suffered extensive cracking when stretched. On the other hand, the PEDOT:PSS ink was deemed compatible with both flexible and stretchable electronics when printed over a TB substrate. TB has also recently been used as a substrate material in the production of 3D printed self-powered triboelectric sensors.[255] TB exhibited triboelectric properties similar to those of PU materials and was paired with PDMS to develop the triboelectric touch sensor. The sensing spring structure was made of polyamide and 3D printed between the TB and PDMS layers (**Figure 20**).[255]

This was the first time a 3D printed soft material (TB) was employed in the development of a triboelectric flexible sensor. Recently, the use of TB has been extended to soft actuators. Pece et al. envisioned a flexible and wearable haptic feedback actuator (named MagTics) in which TB was used to print all the flexible components.[256]

PET and PEN are the most commonly used polymers in the field of OLAE and, for this reason, have already been referenced above several times.[30] They are both low-cost, transparent, and compatible with low-temperature development processes. Besides, their CTE is relatively low. However, for IC chips integration (in hybrid electronics), the soldering processes can demand temperatures that surpass their glass transition temperature (T_g). Thus, to enlarge their temperature endurance they are sometimes heat stabilized, which augments their T_g and prevents shrinkage of the substrates during processing.[47]

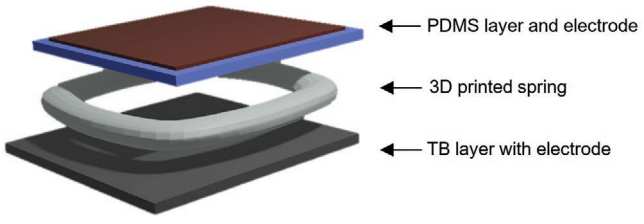

Figure 20. Trilayer printed structure to produce self-powered triboelectric sensors.

Although PET and PEN are related polymers, PEN allows for higher upper operating temperatures, has better dimensional stability, improved strength and modulus, and has better ultraviolet (UV) light resistance.[257] Other polyesters used in FE are PAR and polyhydroxyalkanoates (PHA). PAR is a high performance and transparent thermoplastic material.[239] Yang et al. used it as a flexible substrate for a hybrid TFT device.[239] Although annealing temperatures of 300 °C were required, the PAR substrate exhibited high thermal stability and was not damaged during this procedure.

Thin epoxy films have also been used as flexible substrates for printed electronics. In a recent study, Ohsawa and co-workers studied the bending reliability of transparent electrodes (made from Ag-grid/PEDOT:PSS) that were gravure printed over 50 µm thick epoxy film substrates and PEN film substrates, for performance comparison.[258] The flexible printed electrodes were then subjected to 20 000 outer bending cycles and their performance evaluated. It was observed that while the Ag-grid layer deposited over the PEN substrate suffered evident cracking, the grid deposited on top of the epoxy layer was able to endure the deformation tests without any damage. This was a result of a stronger adhesion between the epoxy film and the Ag-grid electrode and PEDOT:PSS. Another widely used epoxy-based substrate material is the fire-resistant FR-4. As a composite material, it uses epoxy to bind fiberglass and has been used as a substrate for printed electronics for several years. However, this material is very heavy and stiff and, therefore, not compatible with flexible electronics applications.[259,260] To produce an epoxy material with better mechanical characteristics and assure flexibility, Zeng et al. fabricated a fibrous epoxy substrate. To achieve this, they resorted to the electrospinning of a liquid crystal epoxy resin prepolymer.[261] The obtained films were subsequently dried and thermally cured (150–220 °C). After curing, electrically conductive silver ink circuits were screen printed on top of the fibrous epoxy films.

PC is a polymer characterized by an outstanding impact strength, optical transparency, high dimensional stability, and moderate thermal properties.[262] It is usually used as a substrate material for TFT production. Hsu et al. developed IGZO TFT with improved performance using PC as a substrate. For this purpose, they resorted to deposition techniques (electron beam evaporation and radiofrequency sputtering) at room temperature.[262] Chang and co-workers developed an affordable fully-additive printing process and used PC as a substrate.[263] No pretreatment was necessary and the maximum temperature to which the PC film was exposed during the processing of the inks was 120 °C.

Still, while most of the above-mentioned polymers cannot sustain temperatures above 150 °C, new materials ("super heat-resistant" polymers) with higher mechanical and temperature tolerances have been developed. These materials exhibit lower CTE combined with ductile properties and have been used to develop OLED displays.[264] Some examples are commercial PI, such as Kapton and Uniplex. Limitations, however, arise from their use. For instance, they account for higher associated manufacturing costs and are usually less optically transparent than other polymers.[30,264,265] The need to combine the great thermal endurance of PI with optical transparency led to the upsurge of colorless and optically transparent polyimide (CPI)

films.[266] These colorless films can be obtained through alternative synthesis methods, which were first proposed by Ha and co-workers.[267–269] Recently, simpler production methods that rely on soluble PI resins, purified by filtration, have been advanced.[270] By combining flexibility, physical and thermal endurance, and transparency these materials are particularly interesting to be applied in the field of flexible displays and as flexible solar cells.[266]

Another substrate alternative is the use of PEEK, which is a fire-resistant polymer that can be employed in applications that demand nonflammable materials.[30] Corea et al. studied the use of several substrates for printing receive coils.[271] The produced devices were to be applied to magnetic resonance-guided focused ultrasound (MRgFUS) therapy. From the six tested substrates, PEEK was selected as the most appropriate material for screen-printing the conductive silver ink coil. PEEK showed the best performance stability in and out of the water (since the submersion of the device was required for acoustic coupling).

PES has high optical transparency (>89%), high T_g, and outstanding chemical and mechanical properties.[272] Vo and co-workers published a study in which they used PES as a substrate to produce OLED.[272] For this application, they were forced to find a solution to decrease the CTE value of PES. By adding cetyltrimethylammonium bromide (CTAB) to the PES films as a stabilizer (0.5 wt%), the researchers successfully lowered the CTE of PES from 55 to 50 ppm $°C^{-1}$.

Liquid Crystal Polymers (LCP) are another class of highly thermally and mechanically resistant polymers. These materials share properties with highly ordered solid crystalline solids and amorphous disordered liquids over a defined temperature range.[273] There are two main types of LCP: lyotropic (formed by solution) and thermotropic (formed from the melt).[273] LCP networks can be formed by photoinitiated polymerization of liquid crystal monomers. A liquid crystal monomer must be mixed with a photoinitiator and cured at a specific wavelength. Different molecular alignment of the crystalline structure can be obtained through photopolymerization and it is possible to pattern distinct shapes on LCP depending on their envisioned application.[274] This programmable behavior, along with a low CTE, makes them attractive substrate materials for sensors and actuators. Since they are anisotropic they are also extensively used as functional materials in optic and optoelectronic devices.[275] Jeong et al. used LCP to produce a retinal prosthesis.[276] The LCP material served as the substrate structure (package) and Au electrode arrays and an IC chip were integrated inside the eye conformable shaped structure. Long-term reliability of this structure was evaluated for in vitro and in vivo environments, and a longevity of 2.5 years was estimated. Maeng and co-workers used photolithography to pattern conductive pathways on liquid crystal elastomers (LCE).[277] The LCE substrate was prepared between two glass slides and its shape programmed resorting to photoalignment above the T_g of the LCE. Then, researchers metal deposited thin-film electronics over the LCE substrate, while it was still in a planar configuration and, upon release from the glass slide, the device transitioned into the envisioned programmed 3D shape. This multichannel electrode array was able to withstand stretching and buckling strains of 60% for 10000 cycles.

A similar approach was followed by Kim and coworkers that also used LCE substrates to create 3D "pop-up" electronics.[278] These materials have the potential to be used as responsive devices in wearable or implantable electronics. Taking that into account, Kent and associates developed soft actuators using an eGaIn alloy (previously described as an LM alloy) embedded on an LCE substrate.[279] By spray deposition and UV laser ablation, they were able to deposit the LM alloy (in the shape of a Joule heater device) on top of the LCE substrate. Then, using UV laser patterning photopolymerization, the LCE substrate was programmed to exhibit differential bending and flexing modes of actuation (**Figure 21**).

During heating and cooling cycles (20–80 °C), the soft actuator contracts and expands, depending on the changes in resistance experienced by the LM channels.[279]

Table 6 compares the main thermal characteristics of the most frequently used flexible substrate polymers.

Typically, the ideal polymeric substrate should combine a relatively high upper working temperature with a low CTE, as well as good flexible and stretchable capabilities. This compromise, however, is quite rare and thus, the "ideal" substrate should be selected taking into account the application and the characteristics of the other functional materials. For applications that demand stretchability, PDMS and PDMS-based materials are the most adequate, as long as the manufacturing temperature remains low (<150 °C). TPU are also stretchable and present a lower CTE than PDMS which can be advantageous for applications where better shape stability at higher temperatures is required. High-temperature polymers, on the other hand, are generally characterized by lower CTE values (except for PEEK) and considerably lower elongation at break (**Table 7**), which deems them less stretchable. Nonetheless, they are far more suitable for flexible applications that require high-temperature processing and/or are envisioned to function under extreme environmental conditions.

Natural (Biodegradable) Substrates: The use of biodegradable substrates has been gaining a lot of visibility since there is an increasing concern regarding the sustainability of large-scale production of OLAE devices. Besides, the increasing demand for wearable electronics has powered the research into paper, wood, cork, and cotton substrates.

Paper is a very light, low-cost, abundant, biodegradable, and recycle-friendly substrate.[287] When used in combination with

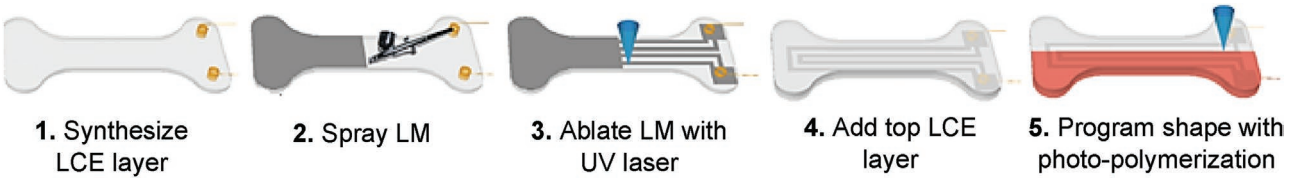

Figure 21. Fabrication of UV laser-ablated LM Joule heaters on LCE substrate. Reproduced under the terms of a Creative Commons Attribution 4.0 International License.[279] Copyright 2020, The Author(s). Published by IOP Publishing.

Table 6. Comparison between the main characteristics of flexible polymeric substrates.[12,235,272,280–286]

Polymer	T_g [°C]	T_m [°C]	UWT	T_{deg} (onset) [°C]	CTE [ppm °C^{-1}]
Low temperature					
PDMS	−123	−54	150	250	310
PU	135	–	150	301	57.6
TPU	−35 to −10	200–216	150	245–380	153
PET	70–110	115–265	150	365	15–59.4
PEN	120–155	270	150	380	20
PC	150	265	130	420	65–75
High temperature					
PI	280–330	–	400	574	8–20
PEEK	143	334	278	575	72–194
PAR	183-206	270-370	–	415	12–14
PES	220	–	180–220	498	55
LCP	120	–	200–240	–	3–70

functional materials its performance can be improved, making it suitable for applications such as electronic components, energy storage devices, generators, antennas, and electronic circuits (**Figure 22**).[287]

The first remarkable steps in the field of paper as substrate were taken by Fortunato and co-workers in 2008, when a transistor was first deposited on top of paper, through radio frequency magnetron sputtering of a gate electrode of In_2O_3-ZnO, at room temperature.[288] On the other side of the paper, the source and drain regions were deposited through e-beam evaporation of aluminum. This discovery rendered Fortunato and her team worldwide acclaim.[288] More recently, Fortunato has been involved in the development of other paper-based platforms for multifunctional IoT applications including RFID tags, printed electrochromic displays, biomarkers for oxidative stress, cholesterol, and glucose.[289,290]

Huang et al. used photo paper as a substrate to develop a flexible ammonia gas sensor.[291] To achieve this, the paper was made electrically conductive by inkjet printing of a silver dispersion on its surface. Subsequently, an NH_3 sensitive composite dispersion of SWNT-poly(*m*-aminobenzene sulfonic acid) (PABS) was inkjet printed onto the paper. Paper has also been used in the development of disposable humidity sensors for medical applications.[292] For this purpose, a silver nanoparticle ink was inkjet printed on paper and its sensitivity to moisture was studied. Nassar et al. used a simple approach to print health monitoring sensors (temperature, humidity, and pressure) on post-it cellulose paper.[293] To design the temperature and humidity sensors they resorted to an Ag ink-filled pen and drew the sensors directly on top of the paper. As for the pressure sensor, they used aluminum foil as electrodes and placed a microfiber wipe (that worked as the pressure sensing dielectric material) and an air gap between them. These sensors were fully recyclable and low cost.

Matias and co-workers were able to grow ZnO and TiO_2 semiconductors on top of different paper substrates (Whatman filter paper, office paper, and commercial hospital paper) through a hydrothermal method combined with microwave irradiation.[290] Multiple applications can be envisioned for these ZnO/TiO_2 heterostructures.

To reduce the environmental footprint of plant-based cellulose exploration, alternative bacterial cellulose substrates have also attracted a lot of research interest. Moreover, bacterial

Table 7. Comparison between the most important physical characteristic of the polymers discussed in this section.

Polymer	UWT	CTE [ppm °C^{-1}]	Thermal conductivity [W m^{-1} K^{-1}]	Dielectric constant	Surf. energy [mN m^{-1}]	Hardness (shore A/D)	Tensile strength [MPa]	Elongation at break [%]
Cellulose	55–95	80–180	0.16–0.36	1.2	–	30A–80D	12–110	3.2–11.3
Paper	90	–	–	2.31–3.6	≈60	–	–	–
Wood	–	2.8 (∥ to grain) 30 (⊥ to grain)	–	1.2–2.1	–	–	1000–3000	1.5–2
Cork	–	–	0.045	1.7	24–28	A	20	15
NinjaFlex	130	153	–	3	–	85–94A	26	660
TangoBlack	130	153	–	2.8	–	61A	0.8–2.4	45–220
PC	130	65–75	0.2	2.9	34.2	80D	55–75	80–150
PU	150	57.6	0.02–0.03	4.7–9.5	51.5	55A–75D	5.4	270–800
PET	150	15–33	0.15	3.0–3.3	44.6	67–70D	61.7	10
PEN	150	20	0.15	3.2	–	79–87D	200	60
PDMS	150	310	0.25	2.32–2.4	19.8	44–45A	2.24	420
Ecoflex	170–275	310	0.16	2.7–2.8	–	20–50A	1.1–1.4	800–1000
PES	180–220	54	0.18–0.24	3.7	46.6	95D	83–85	25–80
LCP	200–240	3–70	0.27–0.32	3–5.9		82–95D	175	1–5.5
DragonSkin	232	310	0.25	–	–	10–30A	3.3–3.4	620
PEEK	278	72–194	0.26	3.1–3.3	42.1	62–89D	70.3–103	45
PAR	340	12–14	0.18	3.13		70D	68	50
PI	400	8–20	0.1	2.8–3.2	56.7	65–92D	139–231	8

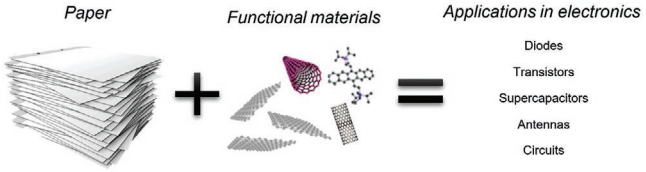

Figure 22. Applications of functionalized paper. Adapted with permission.[287] Copyright 2016, MDPI.

cellulose substrates can exhibit optical transparency, which amounts to another advantageous factor of this technology, with possible applications ranging from electronics to biosensors.[294]

Using nanotechnology it is also possible to create wood films with high transparency, higher flexibility, and strong mechanical properties.[295] Wood nanotechnology processes are used to obtain nanocellulose and 2D cellulose-based materials, such as cellulose nanofibrils (CNF) and transparent wood films (TWF). This process consists of the removal of lignin and hemicellulose from original wood samples and subsequently pressing and drying them into thin transparent films. These materials are abundant, thin, flexible, and have low CTE which, altogether, turns them into a promising technology with applications in the flexible electronics field.[296,297] When compared to PET and copy paper substrates, CNF nanopaper, and transparent wood films (TWF) both revealed better thermal stability for electrical performance.[296]

Rao and co-workers have recently prepared TWF/PVA films to achieve flexible and thin wood composites.[298] For this, they resorted to a "green" method in which PVA was added as a plasticizer. First, the optical transparency of the wood structure was successfully obtained through chemical treatments (that did not damage the wood structure). The treated material exhibited anisotropic microstructure and was subsequently infiltrated with an aqueous dispersion of PVA in propylene glycol (PG).[295] The resulting material was increasingly flexible depending on the increase in PG content of the dispersion. The outcome substrates showed potential for applications in light-transmitting smart buildings and other optoelectronic devices.[298]

Wood has also been used as a substrate in its original macrostructure. This is possible by cutting it into thin layers. In a low-cost and additive deposition approach, Sipilä et al. resorted to a brush-painting and stencil method to manufacture RFID tags on top of large-scale wood and cardboard substrates.[299] The stencil was a 50 µm thick PI film and one single layer of ink was deposited. The wood substrate was 4 mm thick composed of 3 layers, whereas the cardboard was a normal packaging material. Copper and silver inks were used to produce the antennas and demanded sintering, thus, to avoid the use of high temperatures (incompatible with both substrates), photonic sintering at ambient conditions was performed.[299] After sintering, an IC chip was integrated onto the structure, which enabled wireless communication. However, the flexibility of the wood substrate was limited. Rawat and co-workers used a 4.8 mm wood substrate, covered on both sides by 0.25 mm thick copper, to create a patch antenna.[300] This antenna operated in a frequency range of 3.28–3.37 GHz, thus presenting great potential for radiolocation, radio-astronomy, and even aeronautical radio navigation.

Cork is another interesting substrate material that derives from natural resources, namely the oak tree trunk, and is known for its hydrophobic, elastic, and fire-retardant properties.[301] Since it is vastly used to manufacture wine stoppers, one of the first applications of cork as a substrate was in the form of RFID tags on wine stoppers which were connected to the IoT for product identification.[301] Copper tape was used to develop the electrical circuit and directly attached to the substrate. The authors also suggested the future integration of a temperature sensor in the passive antenna sensing device. In a work by Esteves, piezoelectric structures made of PVDF-TrFE membranes were electrospun over 4 and 2 mm thick cork substrates.[302] An epoxy resin was spread over the cork layer and served as a binder. The piezoelectric PVDF-TrFE was able to convert mechanical strain energy into an electrical charge, and vice versa. Thus, the manufactured structures were evaluated regarding their sensing and energy harvesting potential. It was concluded that, when well-calibrated, these membranes were able to show a stable and high output signal that could, in fact, be used for future environmentally friendly applications such as green sensors and energy harvesting devices. In 2019, Figueira et al. were able to fully screen-print UV photodetectors on a cork substrate.[303] They used a low-temperature, ecofriendly, and low-cost procedure to deposit ZnO/ethyl cellulose (EC) composite layers on the substrate. EC acted as a binder and dispersing agent, ensuring the adhesion between the screen-printed layers and the cork sheet. The deposited pattern was dried at 100 °C, which was the maximum temperature reached during the whole process. No previous treatment was needed before deposition and commercial carbon ink was used to print the electrodes.

In recent studies focused on wearable electronics, cotton has also emerged as a key substrate. Tessarolo and co-workers developed novel sensors for body stress monitoring.[304] For this, they drop cast PEDOT:PSS mixed with ethylene glycol (EG) (for enhanced conductivity) onto cotton fabric. For case-study implementation, they incorporated the PEDOT:PSS/EG sensors on a wearable glove prototype. The variations in the thickness of the substrate (caused by the bloodstream) were detectable through changes in the piezoresistivity of the sensing material. In a work, under development at the Institute for Microelectronics and Microsystems (IMM), researchers developed polymeric strain gauge sensors that were printed onto a breathable cotton wristband.[305] The sensors were able to maintain high-reliability monitoring, which was a breakthrough in the field of gestural recognition.

Gesture recognition and human motion detection devices can also be developed to be used directly on the skin, such as described in the previously mentioned work by Varga et al., where a wireless inertial on-skin sensor based on capacitance variation of a bulk eGaIn droplet.[97]

Bihar et al. suggested an innovative manufacturing approach to produce biosensors.[306] For that purpose, they combined skin tattoo electrodes with electronics printed onto a textile substrate ("tattoo/textile electronics") for bio-signals detection. This device has the potential to be applied to the fields of myoelectric prosthesis, and muscle injury prevention/detection. For this, they contact printed PEDOT:PSS onto a conformable textile (satin ribbon) wristband, that served as the transducer, and also

printed PEDOT:PSS on a commercial tattoo sheet, which consisted on the data acquisition system. The tattoo/textile device allowed for accurate electromyogram (EMG) reading, comparable with the performance of the traditional wet Ag/AgCl electrodes.

Substrate Materials Properties: The use of these materials as substrates demands the control of some critical characteristics. To make sure that the printing process is efficient and that the inks/pastes effectively adhere to the substrate their nature must be evaluated and, in some cases adequate pretreatment of the surface is needed. Table 7 resumes the most preeminent physical characteristics that should be considered during the printing process.

3.5. Manufacturing Technologies for OLAE

The manufacturing of electronic applications requires the creation of very thin patterned layers of conductors, semiconductors, and/or dielectric materials on the substrate surface, with high precision and extremely uniform thickness.[47] Traditional large-area electronics applications, like TFT for displays, demand high resolution, patterning, and high performance, relying on plasma, sputtering, and vacuum deposition techniques of amorphous silicon or organic small molecules.[307] On the other hand, OLAE applications with less strict needs for resolution and performance are compatible with simpler and cheaper processing methods, based on printing and coating of water or solution-based pastes or inks.[22] Over the years, several manufacturing techniques have been developed to assemble distinct materials over thin and flexible substrates.[47] In **Table 8**, these techniques are compared and some of their respective advantages and disadvantages are presented.

To select the most effective method the pros and cons of each process must be weighted and the most adequate method should be chosen taking into account, not only the nature of the materials but also the manufacturing costs, the scale of fabrication, the required resolution and the sustainability of the process. The classification of technologies can be done using different grouping approaches. In **Table 9**, the different techniques are classified regarding their dry/wet nature, high/low scalability, contact/noncontact nature, and additive/subtractive processing.

The majority of the wet processes involve the use of liquid inks or pastes and include printing and bulk coating technologies (both additive processes). Although these inks sometimes demand complex formulation steps and can be hard to stabilize into solutions, they allow for fast processing. Besides, they can generally be applied to the large-scale production of large-area electronics that do not require resolution above the micrometer range. Dry processes, on the other hand, use gas phases, powder or light-sensitive inks and encompass, e.g., vacuum deposition, CVD, PVD, e-beam, ion-beam deposition, sputtering photolithography, laser ablation, wet and dry etching, and shadow masking. These processes are associated with the traditional microprocessing of high-performance electronic components and devices and are mature and reliable technologies. Amongst the CVD techniques, spray pyrolysis coating is worthy of further mentioning.[308] This technique is usually used in the deposition of inorganic materials, specially metal-oxides, and allows for higher process flexibility when compared with the remaining deposition techniques.[308,309] Such characteristics are useful in the preparation of thin films and other nanostructures and, as a result, spray pyrolysis is a very well-established technology, whose potential in the production of transparent solar cells has been recognized for over 40 years.[310] Nonetheless, the process is considerably complex, which adds difficulties in what concerns the control of the processing steps.

Moreover, the use of the above-mentioned technologies in OLAE is limited since they are envisioned for high-resolution applications with intricate layered designs. Moreover, their processing often requires complex intermediate steps and involves the use of expensive material, vacuum environments, clean rooms, hazardous reactants, and protective gear. The end-of-life processing of components obtained through these traditional routes is also a problematic factor. Most of these devices integrate several different hazardous materials and their separation from each other is not very efficient. Recycling treatments are, therefore, not only ineffective but also rely on high energy consumption and release emissions to air and water.[311]

All things considered, when it comes to the scale of fabrication, sustainability, and cost-efficiency, the versatility and higher throughput of the printing techniques is evidenced with an emphasis on its potential for larger-scale processes (batch and roll to roll).[22] On the other hand, coating techniques, deposition, and other processes are associated with increased demands in terms of maintenance, processing, and higher feedstock material waste, which makes them less attractive for OLAE.

3.5.1. Printing Technologies for OLAE

As previously discussed, printing technologies are particularly critical in the field of OLAE manufacture. They allow rapid prototyping, large-scale production, multiple layer deposition, deposition over nonplanar surfaces, and good overall performance of the resulting devices. Besides, more than one printing method can be merged to create high-speed roll-to-roll production lines for system-level integration.[47]

As abovementioned, printing technologies can be divided into contact and noncontact printing. While contact printing technologies are still predominant, they generally involve higher material waste. Another drawback concerns contamination and structural damage risks to the device structure, which comes along with the required physical contact between the inked surfaces of the patterned structures and the substrate.[12,47] Contact printing technologies also demand accessory equipment, such as stamps, molds, or masks, which define the printing pattern. These materials are designed for each specific device or application, which increases production and maintenance costs.

Contact Printing Techniques: Screen printing (SP) demands the use of a mask, which can be manufactured by cutting out the desired patterns on a stencil material (usually a metallic frame). The stencil can also be produced through 3D printing or mold casting. SP is the most commonly used printing method and has been employed in the production of electronics for a long time, mostly to create the metallic interconnects on

Table 8. Main differences between flexible electronics manufacturing technologies.

	Printing/Patterning	Coating/Deposition		Structuring
		Bulk Coating	Deposition and growth	
Definition	- Successive application of thin layers of functional ink in a given pattern over a substrate	- Application of a thin film of functional material with controlled thickness over a substrate; usually followed by solvent evaporation	- Thin films deposited through chemical or physical routes, or grown on the surface of substrates through chemical reactions	- Create patterns on a surface in a subtractive or additive manner
Technologies	• Lithography • Soft-lithography • imprinting • Nanoimprint lithography (NIL) • Transfer and direct transfer printing • Gravure and reverse gravure printing • Gravure offset and reverse offset printing • Pad printing • Flexographic printing • Doctor-blade • Screen printing • Direct printing with pen • 3D printing (direct ink writing, DIW and fused deposition modeling, FDM) • Laser printing • Inkjet printing • Electrohydrodynamic printing (EHD) • Aerosol jet printing	• Blade/bar coating • Spray coating • Dip coating • Spin coating • Slot-die • Selective patterning • Solution processing techniques (drop-casting, solvent exchange, and solvent–vapor diffusion methods)	• Chemical vapor deposition, CVD (usually assisted by plasma treatment, APCVD, LPCVD, PECVD) • Spray pyrolysis • Physical vapor deposition, PVD (evaporation techniques – thermal, e-beam, ion-beam, plasma assisted (PECPVC), pulsed-laser, sputtering, ATD) • Sol–gel techniques • Chemical bath deposition • Laser direct writing • Plating (electroplating and electroless deposition) • Electrospinning	• Photolithography • Laser direct writing • Laser ablation • Wet etching • Dry etching • Shadow masking • LDS (laser-direct structuring) • LAD (laser-assisted deposition)
Functional materials	- Organic or inorganic inks or pastes. Can be solvent based, water based, UV or electron beam curable	- Organic or inorganic inks or pastes. Can be solvent based, water based, UV or electron beam curable	- Organic small molecules, metal ions or amorphous silicon in the form of gas phases, powder or light-sensitive inks	- Organic small molecules, metal alloys or amorphous silicon in the form of gas phases, powder or light-sensitive inks
Advantages	• Most of these methods can be applied to R2R manufacturing • Intricate designs	• Most of these methods can be applied to R2R manufacturing • Good thickness control	• Area selective deposition • Intricate designs • High resolution (nm range)	• Intricate designs • High resolution (nm range) • Multimaterial simultaneous processing
Limitations	• Low resolution (μm range) • Some techniques demand curing	• Low resolution • Usually demands curing or additional patterning • High ink waste • Limitations in large-area covering • Lack of film homogeneity	• Usually demands vacuum environments, expensive materials and equipment and clean rooms • Intermediate steps and use of hazardous reactants • Limitations in large-area covering	• Low scalability • Intermediate steps and use of hazardous reactants

printed circuit boards. This process is compatible with both inks or pastes and is fast, repeatable, versatile, affordable, and adaptable to the manufacturing process.[47,312] Screen printing can be executed in a planar (flatbed) or a rotary system and both can be applied to large-scale R2R manufacturing.[44]

In the flatbed system, mostly present in laboratories, a screen mask is used in direct contact with the substrate (**Figure 23**). A squeegee or blade moves and distributes the ink/paste, filling the mask, and imprinting the image from the stencil openings onto the substrate.[12] This process demands optimization of variables, such as solution viscosity (needs relatively high viscosity inks to avoid spreading and bleed out of the material after printing), printing speed, angle, and geometry of the squeegee and mask mesh size. Moreover, for adequate adhesion of the ink/paste to the substrate and consequent high resolution of the printed patterns, it is important to establish a compromise between the surface energies of the substrates and surface energies of the inks/pastes.[47] Shi et al. screen printed an array of 4×7 interconnects for temperature sensor units on a PET film. Discrete components (resistors and diodes) were subsequently assembled with the help of an adhesive and the devices cured at 120 °C.[313]

Large-area flexible pressure sensors have also been produced and deposited through SP over PI. For this purpose, Chang

Table 9. Comparative grouping of some flexible electronics manufacturing technologies.

		Wet	Dry	Large scale	Small scale	Contact	Noncontact	Additive (A) subtractive(S)
Printing/patterning	Soft-lithography	X		X		X		A
	Gravure printing Reverse gravure printing	X		X		X		A
	Gravure-offset printing Reverse offset printing		X[a)]	X	X	X		A
	Flexographic printing	X		X		X		A
	Screen printing	X			X	X		A
	Transfer printing	X		X		X		A
	3D printing	X		X			X	A
	Inkjet printing	X		X			X	A
	EHD inkjet printing	X					X	A
	Aerosol jet printing	X		X			X	A
	Pad printing	X		X		X		A
	Pen printing	X		X		X		A
Bulk coating	Blade/bar coating	X		X		X		A
	Spray coating	X		X			X	A
	Dip coating	X			X	X		A
	Spin coating	X			X	X		A
Deposition coating	CVD		X		X		X	A
	PVD		X		X		X	A
	Sol–gel	X		X			X	A
	Chemical bath	X		X			X	A
	Laser direct writing (does not use mask)		X	X			X	A
	Plating	X	X	X			X	A
Structuring	Laser ablation		X	X			X	S
	Shadow masking		X	X			X	S
	Wet etching	X		X			X	S
	Dry etching		X	X			X	S
	Photolithography		X	X			X	S

[a)]Semidry process.

and co-workers resorted to a thixotropic material with a viscosity of 10^6 cP and a glass transition temperature of 150 °C.[314] In another work, MWCNT were mixed in a PDMS matrix (MWCNT/PDMS) and screen printed over a PET substrate. Different wt% of MWCNT in PDMS were tested and it was found that a 3 wt% solutions of MWCNT/PDMS allowed for the best result viscosity.[315]

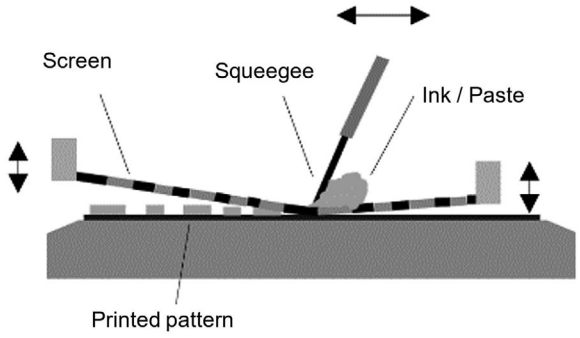

Figure 23. Screen printing illustration.

As a way of testing SP as a method to obtain fully-printed devices, Chang et al. successfully printed differential amplifiers on PC in a "fully-additive" manner.[263] To achieve this, they resorted to SP of a readily available silver paste to produce the TFT gate, the bottom electrodes, and the inductor. They also screen printed the dielectric layers of transistors and capacitors and used the same dielectric ink (Dupont 5018) to isolate the circuit. Resistors were fabricated by SP of a carbon conductor ink (Dupont 7082). Finally, a semiconductive layer was added through the die coating of TIPS-Pentacene. All these steps demanded a thermal (90-120 °C) or UV cure in between them.[263] **Figure 24** schematizes the fully-printed components described above. The gain and performance of the resulting amplifier were competitive with the ones of amplifiers obtained through conventional subtractive processes.

Although this method is established as a mature and dominant technology in OLAE, it still presents some disadvantages, such as large waste of material (inks) and some difficulties

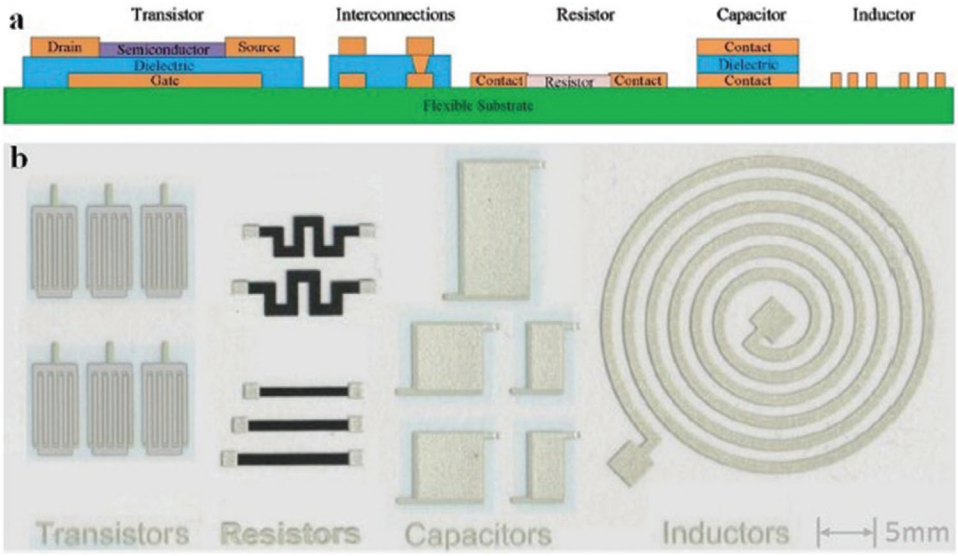

Figure 24. a) Cross-section of the printed transistors, interconnections, resistors, capacitors, and inductor; b) microphotographs of each one of the printed components. Reproduced with permission.[263] Copyright 2014, Elsevier.

linked with a high wet thickness of the film and exposure of the ink to the atmosphere. Besides, SP involves some maintenance costs since the mask must be meticulously cleaned between each use to avoid its deterioration and loss of printing resolution and repeatability.[316]

Flexographic and gravure printing both demand the use of cylinders to pattern conductive arrays for flexible electronic devices.[12] Similar to screen printing, the patterns are specific to one application and frequent maintenance and cleaning of the cylinders are mandatory to assure high resolution and repeatability of the printed materials.

In flexographic printing, the ink transfer occurs through contact between the substrate and the printing plate cylinder that functions as a stamp where the printing pattern is embossed. A fountain roller (which is immersed in an ink bath) supplies the ink through capillary action to an anilox cylinder. A doctor blade then removes the excess of ink from this cylinder and the remaining ink film is transferred onto the printing plate.[44,47] The use of higher viscosity inks is not recommended because they are flow resistant and therefore not compatible with the continuous transfer in between cylinders.

This process is compatible with OLAE technologies and has been used in the manufacture of logic circuits, smart packaging, and printed batteries.[12,317,318] Various characteristics of the process (inks and physical properties of the mechanism itself) must be optimized to achieve the best outcomes. Recently, Zhong and co-workers published a work where they studied the effects of the anilox speed, volume, force, and its embossed patter depth on the resolution of printed lines.[319] Different commercial silver inks (LS-411 and HPS-021LV) were also tested. Although their objective was to achieve a finer line width than the current 45–100 μm range (manageable with flexography), an average width of ≈52 μm was obtained for both inks.

This low-cost and continuous high-speed process offers better resolution than gravure printing yet, some disadvantages are reported. For instance, there is the possibility of occurrence of the Halo effect, which is characterized by patterns that are imprinted with an excessive amount of ink and can decrease the overall quality of the printed patterns.[47] This technology is also susceptible to film instability and de-wetting, which may cause cracks, overlapping, and other defects on the printed lines, which makes the printing of multiple layers impracticable.

Alternatively, the gravure printing process consists of a two-roller system and can be thought of as the reverse process of flexography.[12,174] Although this process also offers high-speed processing and can be used in the R2R deposition of materials, the patterns are engraved in the gravure cylinder, which works as a reverse mold.[174] The functional inks are transferred from the engraved cavities of the gravure cylinder to the substrate on the impression cylinder through capillary action. A doctor blade is placed between the cylinders to remove extra ink from the rotating gravure cylinder, avoiding its accumulation in undesired spaces.

Gravure printing allows for low-cost and high-quality patterning and has been explored in the fields of photovoltaic technology, RFID tags, and logic and memory circuits.[320] Previous tuning and optimization of the ink properties are often required. Also, proper cell spacing, adequate dimensions on the gravure cylinder, and shear force in the printing mechanism are important features to be studied.[12] Kempa et al. printed a complementary ring oscillator resorting to both gravure and flexography methods.[318] For this purpose, they used a water-based dispersion of a commercial PEDOT:PSS, which was reformulated to become compatible with the manufacturing processes (viscosity of 1000 cP). The main disadvantage of this technology is that it demands the costly replacement of the engraved roller to produce new patterns and, therefore, lacks printing versatility.

Other paradigms of gravure printing have also been reported for PE. One of those related technologies is known as reversed

gravure printing. This technic is similar to the classic gravure technique with the exception that, in this case, the gravure roll rotates in the opposite direction of the substrate.[321] Also, as a way of varying the amount of transferred ink, the cylinder moves at a differential speed. Recently, reverse gravure has also been optimized for large-scale manufacturing of OLAE, including organic photovoltaics.[321] As an example, Vak and co-workers blended P3HT with phenyl-C61-butyric acid methyl ester (PCBM), to print OSC, which rendered a PCE of about 2%.[321]

Another analogous process respects gravure-offset printing, which allows ink to be printed over harder or brittle surfaces that cannot be pressed by the gravure cylinder directly.[322,323] In this case, a soft elastomeric cylinder, frequently made from PDMS and called blanket roll, mediates the ink transference by picking up the ink from the grooves of the gravure cylinder and transferring it onto the substrate.[324] The use of this mediating step causes the inks to start solidifying into a dried or semidried state, before being transferred. This process helps to prevent wetting and coffee-ring effect, which are disadvantageous for the quality of the final product and usually associated with wet inks.[325] To adapt gravure-offset printing to large-scale manufacturing, Lee et al. developed an R2R system aimed at printing silver electrodes.[323] Other industrial application of gravure-offset includes the large-scale printing of interconnecting circuit wiring.[326] To improve the resolution of the offset technique, reverse-offset printing (ROP) was developed. Since its invention in the 80s, ROP has become very popular and has registered applications in a large array of sectors from TFT to OLED, displays, sensors, antennas, and solar cells (amongst other applications).[325,327] This process differentiates itself from the gravure-offset printing because the impression cylinder collects the ink from a flat surface, instead of directly from the blanket roll.[325,328] This means the blanket roll is used to deposit the ink over an intermediate substrate, usually made from engraved glass, and then, the roll with the final flexible substrate collects the ink from the embossed surface. The success of this process relies on the differential surface tension of the successive surfaces and on the cohesive force inside the inks that allow for the material to be transferred throughout the steps.[325,328] This process requires inks of lower viscosity that also become semidried before reaching the final substrate and allows for better final resolution and printing quality. In one example, advanced by Fukuda et al., OTFT with sub-micrometer channel lengths were produced resorting to ROP.

Soft-lithography and transfer printing both rely on the use of stamps and on the transfer of inks between the stamp interface and the receiver substrate. Soft-lithography, however, depends on the previous fabrication of a mask or mold to produce the soft stamp (typically in PDMS). Then, the solution-based ink is deposited on a stamp and transferred to the substrate. This includes manufacturing technologies such as microcontact printing (μCP) and nanoimprinting (NI), replica molding (REM), micro transference molding (μTM), micromolding in capillaries (MIMIC), and solvent assisted micromolding (SAMIM).[12] These technologies depend on the use of the components described in **Table 10**.

These processes allow for the production of devices with multimaterial layers and are compatible with the manufacture of flexible sensors, microlens, and supercapacitors.[330,331] However, they involve many manufacturing steps, which inhibits their use for rapid throughput applications. They are also costly and are susceptible to the occurrence of imprinting defects like the presence of air bubbles and ink sticking to the mold instead of being transferred.[329]

Table 10. Functional components for soft-lithography[12,329].

Component	Description
Master or mold	Pattern replication masks that are used to mold the stamps (their structure is the inverse of the desired pattern). They can be produced using photolithography on silicon wafers (resolution > 1 μm), or through e-beam patterning and reactive ion etching of a silicon-on-insulator (SOI) wafer (high resolution < 1 μm).
Elastomer	Thermocurable material poured into the master to create the stamp (usually PDMS).
Stamp	Object obtained from the demolding of the cured elastomer inside the master (with desired topographic pattern). Thermal and chemical shrinking must be taken into account and compensated by designing a slightly larger master.
Ink	Conductive solution-based material that is deposited on the substrate by imprinting with the stamp. It should offer good adhesion to the substrate, low chemical reactivity, good electrical conduction, and be compatible with multiple layer deposition. In some processes resist-forming inks are used.
Substrate	Flexible thin material (e.g., PDMS, Kapton, silicone).

Mannsfeld and co-workers created an "electronic skin" through soft-lithography by imprinting a large array of pressure-sensitive pixels on a flexible and stretchable substrate.[332] To achieve this, they created microstructured PDMS films using a micromolding process (**Figure 25**) and obtained flexible and highly sensitive capacitive sensors.

Tabatabai and co-workers used μCP to print eGaIn and Galistan capacitors.[333] To achieve this, they placed a stencil mask (obtained through photolithography) on top of an elastomer (Ecoflex 0030) and then spread the alloys on top of the stencil mask. After removing the stencil, copper wires were inserted as electrodes, and the resulting capacitor sealed with an additional layer of elastomer. As a conclusion for this work, the researchers concluded that further studies on an oxygen-free environment were needed to prevent the oxidation of the LM alloys.

NI allows for a resolution of about ten times higher than μCP. The higher quality of devices produced with NI relies on the higher resolution of the fabricated stamps.[334] As an example, Maurer et al. produced transparent and conductive metal grids to be applied to the production of electronic devices.[335] For this, they nanoimprinted gold nanowires (AuNW) using a PDMS stamp. The AuNW were able to self-assemble in a conductive nanomesh through solvent evaporation. Afterward, the stamp was removed and the imprinted structure was subjected to plasma treatment.

In the case of transfer printing, the printing system consists of only three layers (stamp/ink/substrate) with two interfaces (stamp/ink and ink/substrate interfaces).[336] In general, a soft elastomeric stamp is used to transfer the ink between a donor substrate or mold and a receiver substrate. For this purpose, the stamp is placed into contact with the donor substrate (where the

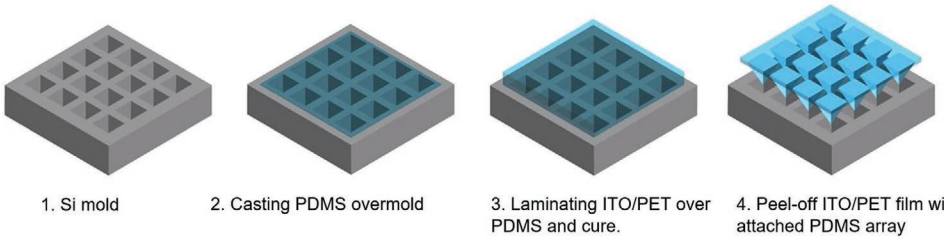

Figure 25. Fabrication of microstructured PDMS features over a flexible film. 1) Si wafer mold; 2) PDMS mixture is drop-casted onto the Si mold. 3) PDMS film is vacuum-degassed, partially cured and an ITO-coated PET substrate is laminated to the mold, followed by thermal cure. Application of even pressure during the curing is crucial to obtain arrays of PDMS features with uniform size across the entire substrate. 4) After curing, the flexible substrate is peeled off the mold.

inks can be previously prepared through wet chemical etching or dry etching). For a successful transfer, conformal contact and adhesion between the stamp and inks must be guaranteed.[336] Moreover, the stamp/ink interface must be stronger than the ink/substrate interface. Then, the inked stamp is pressed against the receiver substrate and, as long as the stamp/ink interface is weaker than the ink/substrate interface, the inks should be easily released from the stamp to their final substrate (**Figure 26**).[336,337]

This technique is frequently used for micro and nanofabrication and allows for the integration of different classes of materials in a heterogeneous manner.[337]

Huang et al. used transfer printing to create their 3D integrated stretchable device for healthcare applications.[338] The device was composed of four different layers of stretchable circuits, which were previously designed through laser ablation on a silicone elastomer. One by one, each one of those layers was then transfer-printed, resorting to a water-soluble tape, to a receiver Ecoflex/PMMA/glass substrate. In a different approach, Park and co-workers combined inkjet printing with transfer printing to heterogeneously integrate different organic materials on a single receiver substrate.[177] In comparison with soft-lithography processes, transfer printing has been deemed more precise and scalable.[338] Another ramification of transfer printing is the direct transfer printing. This appeared as a way of simplifying the process and reducing its iterative steps and associated costs.[339] An example has been recently advanced by Zhao et al., who selectively patterned Cu-eGaIn circuits over a coated paper resorting to laser, and directly transferred them onto a 3D half-sphere shaped surface, made from Ecoflex.[339] In this process, no stamp is required and the circuit passes directly from the donor substrate to the receiver one. Melzer and co-workers also used direct transfer printing to apply magnetoresistive sensors on top of human fingers, which were envisioned to serve as stretchable strain-invariant sensors.[340] In this case, the donor substrate was a Si-wafer coated with PAA, and the receiver was prestretched PDMS.

A similar technique to transfer printing is based on a soft silicone pad and is known as pad printing (or tampography). This process uses a highly deformable stamp, which makes it ideal to print electronic circuits over uneven substrates or finished products. The pad collects the ink from a 2D surface and deposits it over a 3D construct.[341] Merilampi et al. resorted to pad-printing to manufacture ultrahigh frequency (UHF) RFID tags directly onto convex surfaces.[341]

Finally, another technique that allows to rapidly print flexible electronic circuits on top of substrates, is the use of pens filled with conductive inks. Although it involves direct contact between the printing nozzle and the substrate, no additional material is required.[293,342] However, even though pen printing allows for rapid and low-cost prototyping, it is not a scalable technology. Russo and co-workers used a conventional rollerball pen filled with silver ink to directly write conductive text, produce "electronic art" and create interconnects on paper.[342] As a sustainable way of producing low-cost prototypes for health monitoring systems, Nassar and co-workers, also used an Ag ink pen to directly print temperature and humidity sensors over paper substrates.[293]

Noncontact Printing Techniques: Contrarily, noncontact technologies rely on openings or nozzles to dispense the ink solutions or pastes on any kind of substrate (metals, glass, rubbers, polymers, paper, wood, or even cork). The structures are digitally defined, without the need for any further equipment apart from the printer. The nozzles, or the substrate holder, move

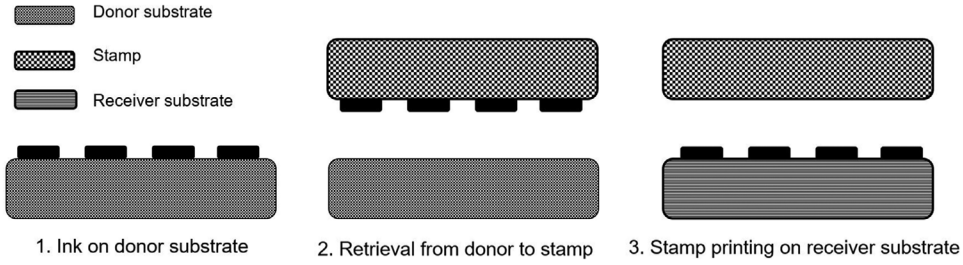

Figure 26. Illustration of the transfer printing process. 1) Inks are prepared on the donor substrate in a releasable manner. 2) Retrieval process: an elastomer stamp is used to retrieve the inks. 3) Printing process: inks are printed onto the receiver substrate.

Table 11. CIJ and DoD printing characteristics.[344]

Printing method	Submethod	Particle size [μm]	Viscosity [cP]	Surface tension [dynes cm^{-1}]	Density [g cm^{-3}]
CIJ	–	<1	1–10	25–70	≈1
DoD	Thermal	<1	5–30	35–70	≈1
	Piezoelectric	<1	1–20	35–70	≈1

accordingly to the preprogrammed pattern which allows the printing of virtually any pattern with accuracy and no additional costs.[12,47]

Inkjet printing is a widespread technology used in personal printers. Despite this, it has recently started to gain traction as a new promising technology for the direct patterning of solution-based materials. Inkjet allows for high-resolution 2D patterning, ink economization, and noncontact deposition via a micrometer-sized inkjet nozzle head.[12,343] To avoid clogging the nozzle the functional inks must be produced taking into account specific properties such as particle size, viscosity, surface tension, and density.[344] The nozzle is designed to be resistant to organic solvents and is therefore compatible with a wide range of solvents for ink formulation.[47]

Inkjet can be divided into two distinct processes—continuous inkjet (CIJ) printing and drop on demand (DoD) printing.[344] As the name suggests, in CIJ droplets are continuously generated and deposited when subjected to an electrostatic field, caused by a charging electrode. DoD, on the other hand, relies on the selective activation of the print-head through impulses that can be acoustic, electrostatic, thermal, and piezoelectric (the latter two are the most reported cases).[344] The characteristics of both methods are synthesized in **Table 11**.

The highest resolution reported, so far, using inkjet printing is around 7 μm and is achievable via graphene-based inks.[25,110] Hyun and co-workers printed arrays of graphene microsupercapacitors (MSC) using for this purpose a modified graphene ink.[25,345] Sensors, antennas, electrodes, and interconnects can also be produced through inkjet printing.[65,343] While the most studied material for inkjet printing is indeed graphene, recently liquid metals have also been attracting a lot of attention. In a study from 2019, Marques et al. developed large-area multilayer circuits and microelectronics to be applied to the development of electromyography (EMG) patches for gesture recognition.[346] They also developed a touchpad for human–machine interaction (**Figure 27**). For this purpose, they used eGaIn ink with low viscosity and toxicity, and inkjet printed the circuits over PDMS.[346] After printing, the eGaIn circuit layers were laser-ablated, and rigid traditional Ics were displayed by direct integration in a top half-cured layer of PDMS.

Seipel et al. combined the potential of digital inkjet printing technology and UV curable photochromic inks to produce cost-efficient UV-sensing textiles.[347] For this purpose, an ink with optimized surface tension (35 mN m^{-1}), viscosity (10–14 cP), particle size (<0.1 μm), and improved stability was developed. The curing step was carried out resorting to UV-LED irradiation and it was found that the intensity of light during this step influenced the yields and kinetics of the coloration reaction of the final sensor when exposed to UV-light.[347]

Another type of inkjet printing that appeared recently is called electrohydrodynamic (EHD) inkjet printing. EHD allows for low-cost printing of samples with higher resolution than the one obtained with the conventional nozzles (**Figure 28**). Moreover, EHD goes around one of the most disadvantageous aspects of the conventional inkjet printing, which is the small range of supported ink viscosities.[348] As a result, EHD is compatible with viscosities that range between 1 and 1000 cP, making it suitable to dispense most inks available in the market. This method depends on the establishment of high voltage between the nozzle and the substrate, which causes fine jets of ink to be expelled from a cone-shaped meniscus that is created at the tip of the nozzle, as a result.[349]

Although these processes have been proven very promising in the field of OLAE, inkjet printing technologies still present

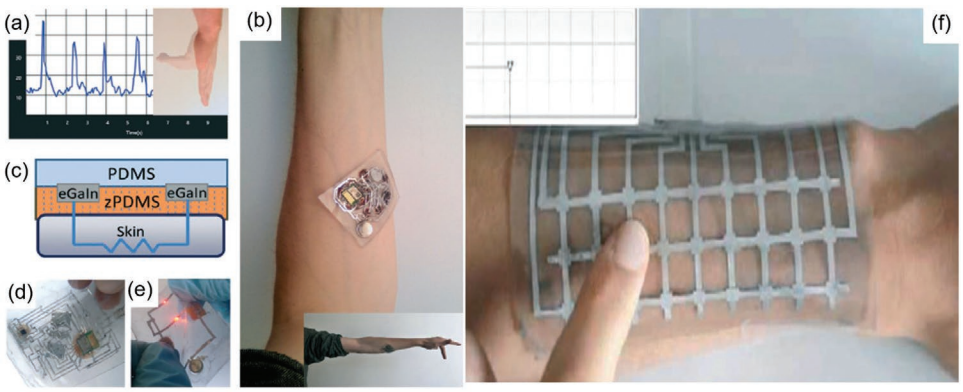

Figure 27. a) EMG signal from a hand gesture is transmitted to a computer application. b) All-integrated EMG patch on the forearm. c) Crossview of a *z*-axis conductive PDMS and schematic of the electrical path. d) EMG patch seen from the bottom; e) double-layer LED circuit with a coin cell battery and button (each LED is on a different circuit layer). f) human–machine interaction with a soft touchpad. Reproduced with permission.[346] Copyright 2019, The Royal Society of Chemistry.

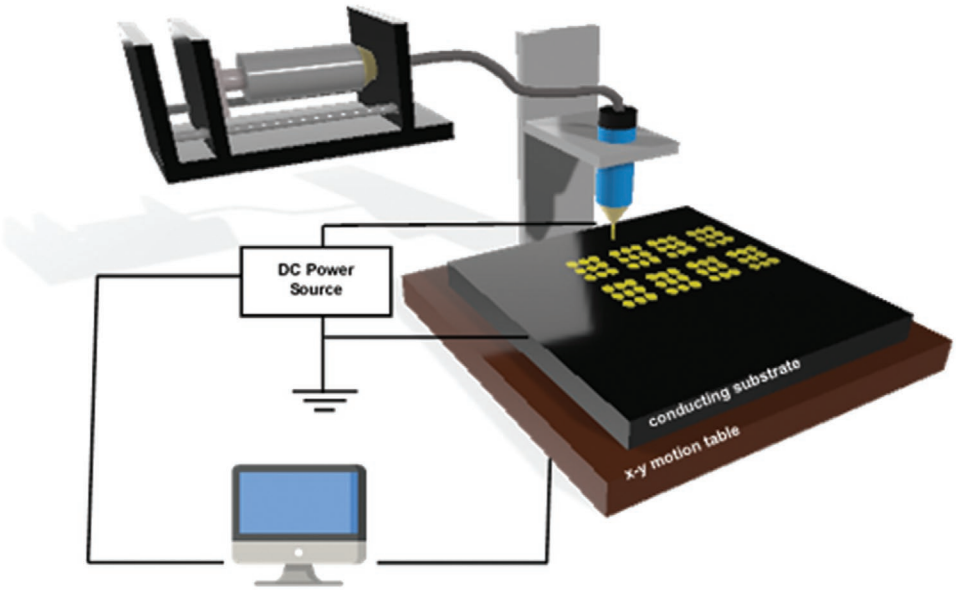

Figure 28. Schematic representation of the EHD printing system. The ink is supplied by a syringe pump and jetted through a controlled system that involves the use of a computer software and the establishment of a current differential between the tip of the dispensing syringe and the substrate.

some disadvantages when compared to contact methods. For instance, in the majority of the cases, the resulting morphologies are less uniform and the low concentration of the inks requires more printing passes (for better conductivity), thus making the inkjet printing time-consuming.[47,110]

3D printing is used to produce flexible conductive devices that demand 3D architectures, unachievable by inkjet printing.[110] It allows for simple additive manufacturing of high complexity constructs in a layer-by-layer manner. These complex shapes are achievable through computer-assisted design (CAD) software modeling and subsequent uploading of the corresponding stereolithography (STL) file into the 3D printer operative system that slices the 3D model into layers of desired thickness. Currently, it is mostly used to produce tactile sensors, since both the flexible substrates and the flexible sensitive electrodes are printable. The mechanical signals (force, pressure, strain, shear, torsion, bend, vibration) are converted into electrical signals by piezoresistive, capacitive, and piezoelectric sensors.[350] It has also empowered the manufacture of integrative devices such as current collectors, electrolytes, and packaging alternatives.[110]

The most popular 3D printing technologies are based on the extrusion of materials through a heated nozzle. These technologies include fused deposition modeling (FDM), which works by extruding filaments of thermoplastic materials, rubbers, and eutectic metals, and direct ink writing (DIW), which is based on the direct deposition of heated viscous inks over the substrates in a noncontact manner.[350] DIW includes dispensing methods such as microdispensing and electrostatic-force-assisted dispensing.[351,352] Another 3D printing technology is the laser powder-bed fusion (PBF).[351,352] Instead of using filaments and viscous inks as feedstock materials, PBF techniques use loose powders and binders, which are fused together through selective laser sintering (SLS), selective laser melting (SLM) or through electron beam melting (EBM). Other processes such as stereolithography (SLA), digital light projection (DLP), Polyjet, and two-photon polymerization (2PP) demand the use of UV curable photopolymers and resins, which are selectively crosslinked through computer-aided irradiation.[351,352]

Both inorganic and organic materials are compatible with these technologies. 3D printable inorganic materials generally include alloys (such as eGaIn) and metals, while organic materials include conductive polymers or nanocomposites. Nanocomposites consist of a polymer matrix and dispersed nanoparticles such as metal NW, metallic nanoparticles, polymer micro/nanostructures, CNT, and graphene, which enhance the conductivity of the printed materials.[353–355] These materials have been applied to the design of piezoresistive and flexible tactile sensors.[55,356,357] To produce piezoelectric pressure sensors the most used materials are piezoelectric ceramics, ceramic/polymer composites, and single crystals.[358,359] As for capacitive sensing applications, SWCNT-PDMS electrodes are effective options.[55,360]

Mousavi et al. produced a highly selective multidirectional tactile sensor to be integrated into a robot.[357] Both the sensing electrodes and the conductive interconnects were 3D printed using carbon nanotube reinforced PLA (PLA/CNT) and the elected substrate was a TPU. The printed sensors demonstrated high sensitivity and selectivity to different mechanical displacement movements, namely tensile and compressive bending. Moreover, the system allowed for bending direction recognition.[357]

DIW can be used to fabricate low-cost and durable flexible electronic devices and PCB through the direct extrusion of ink (of medium to high viscosity) on a substrate.[351] Abas and coworkers used microdispensing DIW to deposit a conductive carbon paste on PET.[351] To tune the rheology of the carbon paste and turn it more suitable for dispense printing the carbon paste was slightly modified resorting to PVA. The electrical conductivity and mechanical resilience of the fabricated device were evaluated and the results proved that this technique was

Figure 29. Drawing depicting the precise deposition of ink on a 3D construct through 5–6 DOF dispensing systems.

adequate to obtain reliable, durable, and stable operative circuits. Electrostatic-force-assisted dispensing is frequently used to produce electrodes resorting to highly viscous inks and pastes. Shin et al. used this process to print electrodes on texturized crystalline silicon solar cell wafers.[352] In this work, the efficiency of the devices obtained through electrostatic-force-assisted dispensing was compared with devices produced by conventional dispense printing. It was found that, while the electrodes obtained through the conventional method peeled off easily from the substrate, the ones dispensed with the aid of electrostatic force remained tightly adhered to the textured wafer surface. Another innovative DIW technology is the 5- or 6-axis degree of freedom (DOF) dispensing system. Thanks to its accuracy and freedom of transitional and rotational movements, this technique allows for the dispensing of organic or inorganic inks over different substrates with 3D conformations. In **Figure 29**, a 3D printed antenna, obtained resorting to this technology is illustrated.[361]

Powder bed-based printing methods use binders, powders, and heat from lasers or electron beams to produce high-resolution shapes.[362] Although they allow for multimaterial integration and rapid prototyping, these methods are not usually employed in the manufacture of flexible electronics.

Gel-type UV curable resins are used with photopolymerization methods such as Polyjet. In this method, jetting heads spray the resin delimiting the object shape in a 2D pattern in a layer-by-layer way.[362] In between each deposition, an integrated UV lamp photopolymerizes each layer, which brings about a smooth and precise object that does not require post-treatment.[362]

Aerosol jet printing (AJP) is another material patterning technology for the fabrication of printed electronics. The ink solutions or nanoparticle suspensions are loaded into an atomizer. The aerosol is then carried with the help of an inert carrier gas stream to a deposition nozzle and sprayed over a substrate (**Figure 30**).[12,363,364] This technique is compatible with a large variety of materials, includes the possibility of printing over nonflat surfaces, and allows for high-resolution prints.[363]

An AJP atomizer is usually used to create an aerosol of ink droplets. Depending on the ink viscosity, the diameter of the droplets varies between 20 nm and 5 µm. Smith et al. studied the printing of silver lines over different large-area substrates.[364] The substrate temperature was varied to study the effects on the adhesion, cracking, and resulting resistivity of the ink. Graphene/silver inks have also been used to print flexible and conductive interconnecting patterns for flexible devices. These inks have been proved to be compatible with AJP to obtain uniform microstructures and crack-free conductive designs.[365] The clogging of the AJP nozzle is also less probable than when using other techniques, such as IJP.[363] Some limitations, however, are related to material waste, since a cloud of powder is created in the surroundings of the print area. Besides, the sheath gas induces localized crystallization/solidification phase at the trace pattern, which ends up reducing the layer quality.[12]

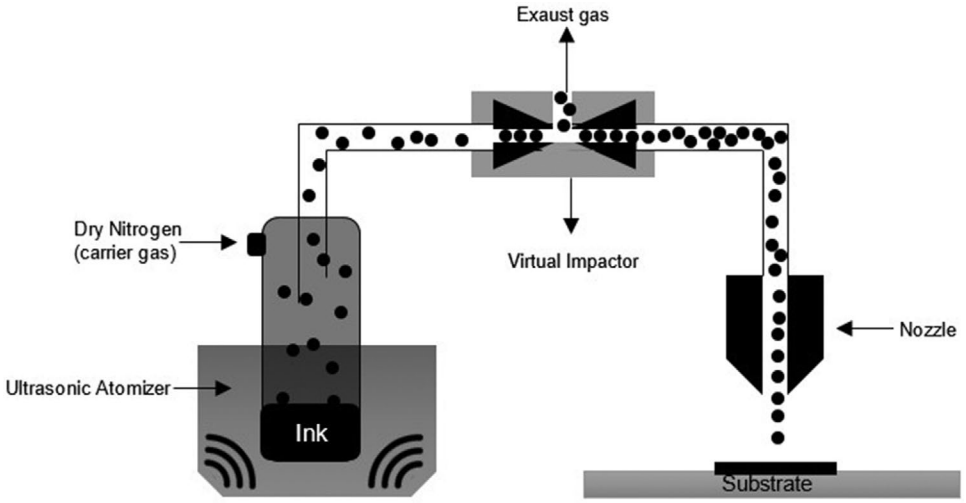

Figure 30. Schematic of the aerosol jet process using an ultrasonic atomizer.

Table 12. Printing characteristics of the previously described technologies.

		Line width resolution [μm]	Ink/paste viscosity [cP]	Ink waste	Mask	Ref.
Screen printing		30–100	500–5000	High	Yes	[366]
Flexography		20–80	10–500	High	No	[366]
Gravure printing		2–200	50–200	High	No	[367–369]
Reverse gravure printing		5–200	10–200	High	No	[321,369,370]
Gravure-offset printing		20–70	10–50	High	No	[323,369]
Reverse offset printing		0.5–1	1–10	High	No	[325,328,371]
Soft-lithography	μCP	0.1	–	Low	Yes	[372]
	NI	0.01	–	Low	Yes	[330]
Transfer printing		≈3	50–500	Low	No	[337]
Inkjet printing		20–100	1–30	Low	No	[376]
EHD Inkjet printing		0.2–1	1–1000	Low	No	[377,378]
3D printing	FDM	10–200	$>10^5$	Low	No	[350,373,374]
	DIW	1–100	10^4–10^5	Low	No	[375]
Aerosol jet printing		10–20	0.5–2000	Medium	No	[364,379]

Comparison Between Printing Techniques: The following **Table 12** compares the most prominent characteristics of the described printing technologies for OLAE.

Main Pre- and Postprocessing Techniques: To optimize the manufacturing procedures, improve the performance and increase the lifespan of the final devices, some treatments can be applied to the functional materials (both inks/pastes and substrates). The available pre and postprocessing techniques serve to improve many factors of the overall device fabrication steps.[363,380]

Pretreatments are generally employed to increase the substrate surface energy, turning it more hydrophilic.[236] To achieve this, the selected methods are usually oxidation reactions, such as oxygen plasma,[381] corona discharge, and UV irradiation.[382,383] This step is particularly critical when the printing inks are aqueous and assures uniformity and adhesion of the printed films. The adhesion between inks/pastes to the substrates and/or other layers of inks/pastes can also be improved by previous cleaning, activation, or surface functionalization, by doping with other materials that compatibilize the active surface for a specific material.[49] Moreover, in the particular case of extrudable nanoparticle inks, to avoid nozzle clogging, help the homogenization of the extruded material and homogenize its conductivity, previous efficient mixing or sonication may be required.[33]

Ultimately, post-treatments are vital to activate the conductivity of the deposited materials. These treatments are predominantly employed as a way of removing organic solvents, surfactants, binders, thickeners, or other additive materials that are necessary to the manufacturing process, but end up hindering the electrical conductivity and functionality of the final products, and ought to be eliminated.[33] For this purpose, sintering mechanisms are the most commonly used. The most frequently applied treatment is heat, which vaporizes the organic additives and sinters the ink/paste, maximizing the electrical conductivity by assuring connectivity between particles.[49,384] Alternative sintering methods include low-temperature sintering (Ostwald ripening), selective laser sintering (SLS), microwave sintering, mechanical sintering,[98] argon ion laser beam sintering,[385,386] UV curing, and photonic curing.[49] Annealing, on the other hand, includes heat treatments that alter the microstructure of a material (causing changes in properties such as strength, hardness, and ductility).[387] Some of the most used annealing treatments are thermal, solvent vapor,[388] and excimer laser annealing (ELA).[384] **Table 13** summarizes the pre and post-treatments that can be applied to both printing inks and substrates to improve and optimize the overall quality of the final product. Major advantages and disadvantages of each process are also displayed.

4. Implementation Examples

While OLAE is still a fairly recent concept, some companies have already managed to develop devices with demonstrated reliability, scalability, and maturity, which are currently competing with traditional electronics and disrupting the precursory market. Some success examples have already been reported in the healthcare,[389] automotive,[390] energy harvesting,[391] industrial,[392] packaging,[393] environmental safety,[394] wearables,[39] and even in the fashion and sports fields.[395,396]

In the medical and healthcare field, these devices help to increase the biometric sensors' compatibility with the human body, increasing both data reliability, comfort, and improving the users' overall experience. As a result, with the aid of the IoT, which connects these devices to the cloud and allows on-time and continuous processing and monitoring, chronic patients can be fully followed and advised by healthcare workers even while recovering at home.[397] The spectrum of applications in this field is extensive and ranges from neonatal to elderly care.[398,399] One application is the development of alternatives to physically wired electrodes for biosensing that limit mobility and are prone to malfunctioning. Hence, alternatives based on wireless sensor networks are being developed and prototypes

Table 13. Pre- and post-treatments used in OLAE manufacturing.

Type	Function	Technique	Advantages	Disadvantages
Pretreatment	1. Cleaning the substrate	Rinsing	√ Easy, inexpensive, and fast procedure; √ Water, detergent, or organic solvent can be used, depending on the substrate; √ Remove dust, grease, or other contaminants;	× Must be followed by a drying step or dehumidification step.
		Dehumidification	√ Easy, inexpensive and fast procedure; √ Serves to treat substrates that present hygroscopic features and absorb moisture from the environment or from the rinsing step.	-
	2. Dry cleaning and improving/ promoting adhesion on substrates	Atmospheric plasma	√ Improves ink adhesion by forming polar groups and increasing surface energy; √ Reduces the degradation of surface morphology over time and improves printing quality; √ Uses single narrow nozzle electrode and high-pressurized air that helps cleaning dirt and hydrocarbons from the surface; √ Plasma treatment lasts longer than corona discharge treatment; √ Viable for a large array of substrates and for thicker substrates; √ Cheaper than vacuum plasma treatments; √ Low-temperature procedure.	× System may have variability (same conditions may result in different degrees of surface modification); × High initial investment in equipment; × Thinner substrates might end up being damaged; × Size limited to the plasma chamber.
		Low pressure gas plasma	√ Removes hydrocarbons from surfaces without the need for previous solvent cleaning (unless the contaminants are poly-aromatic hydrocarbons); √ Low-temperature procedure;	× Needs an enclosed evacuated chamber; × Does not remove poly-aromatic hydrocarbons.
		CVD	√ Viable for a large array of substrates and for thicker substrates; √ Prepares substrates for extreme temperature variations.	× Demands high temperature; × Needs an enclosed evacuated chamber; × Size limited to CVD chamber; × Nonselective coating.
		Flame treatment	√ Breaks molecular bonds on surface and excites free radicals increasing surface energy and ink receptivity;	× Equipment of large dimensions that occupies an entire room; × Requires gas supply; × Can only treat flat surfaces.
		Corona discharge	√ Energy from high-charged electrical corona breaks the molecular bonds on the surface of a nonpolar substrate resulting in higher surface energy and better wettability; √ Usually used in flat surfaces but special probes exist to treat 3D parts. √ Cheaper than most of the atmospheric plasma systems.	× Some substrates (e.g., fluoropolymer-based materials) do not respond to this treatment; × Requires high electrical voltage.
		Fluoroxidation	√ Fluorine gas is used for surface modification at ambient conditions; √ When neutralized fluorine gas can be used as a safe and ecofriendly treatment; √ It promotes high-strength adhesion bonding between inks and substrates; √ Oxygen-containing functional groups, such as hydroxyl, carbonyl, and carboxyl are created making the surface hydrophilic and very polar; √ It can be used over either large or small substrates or even over nonflat surfaces.	× Safety concerns arise from the use of fluorine gas.
		UV-Ozone	√ Enables dry and precision cleaning. Uses UV-rays and strong oxidation caused by the formation and decomposition of ozone to convert contaminants into volatile substances; √ Lowers surface energy and promotes wettability.	× Thick contamination may not be effectively removed; × Only removes contaminants if they are organic; × UV light can damage natural or synthetic elastomers and polymers at a molecular level.

Table 13. Continued.

Type	Function	Technique	Advantages	Disadvantages
		Laser	√ Selective; √ Laser intensity can be tuned taking into account the characteristics of the substrate; √ Cleans and prepares surface;	× Expensive.
	3. Homogenization of ink or paste prior to printing/ deposition	Mixing	√ Cheap and accessible way to homogenize an ink solution or dispersion; √ Can be done resorting to a magnetic stirrer and magnet, a homogenizer, a shaker, or, in the case of higher quantities of material, a higher-grade mechanical agitator.	× If the stirring is too vigorous the nanoparticles may be damaged and alter their diameter causing the ink solution to become poly-disperse; × Material from the magnet and its handling can contaminate the solution.
		Sonication	√ More efficient and faster homogenization;	× Temperature must be controlled; × In the case of NP inks, if the applied energy is too high the nanoparticles can become deformed; × If the temperature is too high, the materials can start degrading.
		Heating	√ Helps homogenization of the ink/paste; √ Decreases ink/paste viscosity; √ Prevents thermal shock if the printing/deposition procedure demands high temperatures.	× If the temperature is too high, the materials can start degrading.
		Filtering	√ Removes higher dimension nanoparticles and homogenizes the ink dispersion; √ Helps prevent clogging of nozzles.	× Can be time-consuming; × The added steps and materials used can increase the chance of contamination
Post-treatment	4. Sintering/Curing	Thermal sintering	√ Inexpensive (usually performed in an oven, hot air flow, or on a hotplate);	× Nonselective; × Can damage the substrate; × Can cause uneven melting of particles (metal NP).
		Spark plasma sintering	√ Ultrafast sintering process; √ Uniform sintering; √ No need for binders; √ Sinters the material by pulsed electric current sintering (PECS)	× Nonselective and can only be applied to simple symmetrical shapes; × Requires an expensive pulsed direct current (DC) generator.
		Low-temperature sintering (Ostwald ripening)	√ Spontaneous process that happens when smaller particles come into contact and merge with larger ones; √ Does not heat the substrate; √ Causes particle growth by surface energy reduction at room temperature.	× The end result is a porous surface with lower electrical conductivity than bulk material.
		Laser sintering	√ Selective, can be used for patterning; √ Does not damage the substrate; √ Fast procedure; √ Promotes interlayer adhesion.	× The end result might be porous and brittle; × Can cause shrinkage and warping of the substrate; × Expensive material is required.
		Microwave sintering	√ Selective and fast procedure; √ Reduced energy consumption during the procedure and enhanced heat diffusion; √ Lower processing costs than other sintering methods; √ Lower environmental hazards.	× Limited to thinner films;
		Mechanical sintering	√ Selective and simple method; √ Environmental conditions; √ Uses tip to apply pressure and to rupture and coalesce particles.	× Might damage substrate; × Variability in resulting electrical conductivity.
		Argon Ion laser beam	√ Does not heat the substrate; √ Localized input of energy on top of the substrate; √ Selective, can be used for patterning.	× Expensive.

Table 13. Continued.

Type	Function	Technique	Advantages	Disadvantages
		Low-pressure argon plasma	√ Relies on plasma-induced electrochemical reduction of ions in solution to form conductive structures; √ Changing plasma exposure times and power tunes the resistivity of the sintered pathways.	–
		UV curing	√ Suitable to be equipped in a printer; √ Allows for a high selectivity and smooth morphology of printed patterns without distortion	× UV curable materials are not frequently used in printed electronics.
		Photonic curing	√ Irradiates the sample with multiple high-intensity short flashes of light; √ By tuning the intensity of the lamp, the pulse length, and the number of flashes the integrity of the substrate can be preserved; √ Advantageous for R2R processes since it offers rapid processing.	× Without proper study of the light characteristics the energy of the flashes can damage the substrate (heat dissipates to the substrate foil); × High-cost set-up.
	5. Annealing	Thermal	√ Enhances electrical conductivity of coatings; √ Normally used to produce FET and solar cells.	× High-temperature process might damage the final product; × Limited by the temperature gradient developed through the surface
		Solvent vapor	√ Room-temperature process; √ Samples positioned in environment saturated with solvent vapors, resulting in the rearrangement of the molecules into higher degree order structures; √ Improvement of the performance of organic electronic devices.	× Low precision; × Reliability problems; × No standardized methods.
		Excimer Laser Annealing	√ Used to create high performance TFT; √ Cold, ultrafast and robust process; √ In the long-term this process can reduce consumer expenses.	× Large and expensive equipment.

are starting to be tested.[400–404] Pressure sensor arrays can also be used to avoid pressure ulcers and assess postural imbalance.[405–407] Another useful application in this field respects the detection of VOC. For this purpose, carbon allotropes and other 2D materials, combined with polymeric materials are frequently employed.[116,408] Moreover, with the increasing need to both prevent and closely monitor Covid-19 infections the development of related sensor devices increased as a response. As an example, companies such as Henkel AG & Co., Byteflies, Melexis N. V., Quad Industries SA., Nitto Denko Corporation and Televic N. K., which are already known to produce printed electronics devices and establish IoT communication protocols, worked together to developed an on-skin adhesive capable of wirelessly monitor the respiration and heart-rate, as well as the temperature of symptomatic patients.[409]

Along with the innovations in the healthcare area, the automotive industries are also experiencing a shift toward the manufacturing of flexible, slimmer, customizable, and lightweight parts that will contribute to the development of the "car of the future." This field, in particular, is very supported by innovations in the area of in-mold electronics (IME) and in-mold decoration (IMD) that combine the use of FHE thin foils with injection molding of lightweight polymers.[410] In this field, the areas of actuation range from the exterior design, to the "smartification" of the interiors. Adding to this, all the heavy and bulky electrical connections inside vehicles, that range several meters, are expected to become almost seamless and lightweight. Some companies, such as TactoTek, are already fully dedicated to the production of these structural devices. With the employment of the Injection Molded Structural Electronics (IMSE), developed by TactoTek, and aided by their partnership with prominent ink manufacturers, such as Dupont Inc., Henkel AG, and Sun Chemical, it is already possible to decrease the thickness and weight of products such as on-board control-panels and displays in 90% and 70%, respectively.[411] Another already implemented innovation are the kinetic touch buttons, which give sensorial feedback to drivers.[412] A company named Aito produces its own chips and integrates them with printed piezo sensors and actuators, which serve as a solution for automotive controls.[413,414] Canatu Oy is another successful example of a growing company that specializes not only in the development of 3D touch surfaces but also smart heater solutions for the interiors of automobiles.[414] They patented a material called Carbon NanoBud and baptized their technology CNB.[415] Their solutions encompass transparent conductive and semiconductive thin films, based on carbon materials, which are used in the production of automotive parts, stretchable displays, and even electrochemical sensors for medical diagnosis devices.[416]

Other markets expected to withstand a great deal of innovation and continue to grow steadily are the ones related to energetic sources and harvesting devices. In this case, OLAE technologies are also very advantageous, since they allow for

large-scale and sustainable development. In what concerns energy sources, OLAE is already expected to be used in the development of "greener" and printable batteries and supercapacitors, that can be directly integrated into the devices during their manufacturing.[417–419] Although the preferred materials for these applications are still inorganic, an effort has been done in the development of more sustainable counterparts. Nonetheless carbon, and other 2D materials are currently the most pursued alternatives.[420–424] In the pursue of developing self-sufficient devices, other options have emerged, such as thermoelectric, piezoelectric, and triboelectric generators, which harvest energy from heat, pressure, and movement respectively. Some frequently used materials include PEDOT:PSS and PVdF:TrFE.[425,426] Another recurring alternative is the use of radiofrequency harvesters, such as RFID chips and NFC tags, that are easy to print and to integrate while simultaneously assuring long term autonomous function of devices.[427–429] In the area of energetic harvesting, another market that cannot be overlooked are photovoltaic panels and solar cells. Even though the majority is still made from silicon-based materials, since they assure the highest PCE, many alternatives have been advanced by the scientific community. Such alternatives encompass perovskite solar cells, organic solar cells, and quantum dot cells.[23,430–432] Perovskite solar cells in particular are a very promising technology and are already produced by inkjet printing and commercialized by a company named Saule Technologies.[433] Smart packaging is another area that has been benefiting from these materials and technologies.[434] MOD inks along with flexography, gravure, and screen-printing are often employed to create RFID and NFC tags that add tracking and other informative details to the products.[435]

Finally, the use of seamless and ubiquitous sensors is already being applied in the 4.0 Industry to endow industrial robots and other types of machinery with sensorial and controlled actuating features.[436] When connected to an IoT system, such devices help to control the functioning of the plant-floor, while simultaneously optimizing the industrial processes, assuring the safety of factory workers.[436] For this purpose, the on-line recovery of data from proximity, temperature, environmental, and pressure sensors is crucial.[392,437] This paradigm also benefits from the development of human–machine interfaces (HMI), that help in the remote control of processes that demand human interference but the surrounding environment is too hostile.[395,438,439]

5. Sustainability and Environmental Safety

Even though there is a growing concern regarding the use of sustainable, recyclable, and nontoxic materials, in reality, the production of devices containing toxicants or capable of producing hazardous by-products during fabrication steps is still increasing.[394] The dangers and difficulties associated with the processing of traditional electronics are already well-known and platforms dedicated to improving the operating efficiency between the production and end-of-life (EoL) stages of devices have been advanced.[311] Some emerging materials in flexible electronics, however, might still present risks to users and the environment. For instance, the use of certain nanoparticles (including QD) and even some carbon allotropes is associated with some degree of environmental pollution or health concerns.[394,440] Graphene and related materials are prone to aggregation and may cause oxidative stress and toxic effects in organisms.[394] Similarly, adverse human and environmental effects have been reported in association with QD, especially related to QD with core metals (Cd, Pb, Se), which are known to be toxic to vertebrate systems, even at low concentrations.[440] Moreover, ink formulations often require the use of chemical precursors, organic solvents, or even VOC that are recognized as carcinogens and environmental pollutants.

As a way of promoting the use of environmentally friendly manufacturing alternatives, researchers are focused on developing "greener" processing techniques, such as water-soluble inks or inks stabilized with innocuous surfactants or low energy consumption processes.[54,64] The use of natural and biodegradable substrates is also a route to follow to decrease the environmental footprint of electronics manufacture. Maximizing the operating life of PE devices is also a desirable goal from the environmental perspective. Maintainability and reparability issues are also to be considered. Improving recyclability must be a concern during the design of PE components. As a result, ecodesign strategies should be developed and implemented from theory to concept. In light of these concerns, OLAE is expected to combine the use of safe, renewably sourced, and/or biodegradable materials with low-cost and energetically efficient manufacturing processes, while simultaneously applying them to the sustainable growth of IoT and its respective sensor/actuator applications.

6. Future Challenges

This paper presented an overview of the OLAE enabling materials, formulations, and main manufacturing technologies. Several organic and inorganic functional materials have been detailed, as well as their core applications in flexible electronics manufacturing. Flexible, stretchable, and compliant substrates were also discussed with a focus on polymeric and natural/biodegradable ones.

Emerging and traditional manufacturing techniques were compared as a way of highlighting the importance of printing technologies in the field of OLAE. Printing technologies, available for large scale and low-cost production were then described in detail. Current limitations and challenges associated with these technologies have also been advanced throughout this paper.

Finally, some concerns regarding the environmental sustainability of the materials were presented, as well as some green and safe manufacturing alternatives. For sustainable growth of IoT and CPS applications, further research and investment in these alternative technologies should be assured.

OLAE stands for a fast-growing technology with enormous potential, capable of bringing value to almost every economical sector. We are currently sitting on the verge of a digital transition that prioritizes fast and ubiquitous inter-connections of data between systems. Applications in the areas of smart-healthcare, smart-homes, smart-transportation, smart-agriculture, smart-cities, and smart-factories are emerging or being reinvented to

comply with a new digital reality. In this sense, the need for low-cost, on-demand, tailorable, adaptable, and in some cases, disposable sensors, displays, and actuators are on the rise. Currently, OLAE is still a recent technology that needs maturing. Hence, improvements regarding the manufacturing technologies and overall performance of the devices are still needed, as well as adequate quality control and manufacturing guidelines. Notwithstanding, this innovative way of creating electronic platforms holds promise to revolutionize the way new products are designed and developed.

Acknowledgements

This work was supported by NORTE-06-3559-FSE-000018, integrated in the invitation NORTE-59-2018-41, aiming the Hiring of Highly Qualified Human Resources, co-financed by the Regional Operational Programme of the North 2020, thematic area of Competitiveness and Employment, through the European Social Fund (ESF), and by the scope of projects with references UIDB/05256/2020 and UIDP/05256/2020, financed by FCT – Fundação para a Ciência e Tecnologia, Portugal. The authors also thank Prof. Luís A. Rocha for his support and guidance during the writing of this review work.

Conflict of Interest

The authors declare no conflict of interest.

Keywords

additive manufacturing technologies, organic large-area electronics, organic materials, printed electronics, sustainable development

Received: October 12, 2020
Revised: December 26, 2020
Published online: March 29, 2021

[1] A. Hanson, *Br. Pat. 4* **1903**, 681.
[2] K. Gilleo, J. Murray, in *Next Century Print. Circuit*, PC FAB, USA **2000**, pp. 20–23.
[3] D. A. Luke, *Trans. IMF* **1969**, *47*, 36.
[4] P. Eisler, M. E. W. Williams, *My Life with the Printed Circuit*, Lehigh University Press, Pennsylvania **1989**.
[5] C. Ducas, *US1563731A*, **1925**.
[6] G. Smith, *US 3723635A*, **1973**.
[7] M. Prudenziati, J. Hormadaly, *Printed Films: Materials Science and Applications in Sensors, Electronics and Photonics*, Woodhead Publishing, Cambridge **2012**.
[8] The Nobel Prize in Chemistry 2000, https://www.nobelprize.org/prizes/chemistry/2000/summary/ (accessed: November 2020).
[9] J. L. Brédas, S. R. Marder, W. R. Salaneck, *Macromolecules* **2002**, *35*, 1137.
[10] S. H. Kim, T. H. Zyung, J. H. Lee, *US20060124922A1*, **2005**.
[11] M. Hamzah, E. Saion, A. Kassim, N. Yahya, H. N. M. Mahmud, *UCSI Acad. J. J. Adv. Sci. Arts* **2007**, *2*, 63.
[12] S. M. F. Cruz, L. A. Rocha, J. C. Viana, *Flexible Electronics*, IntechOpen, Rijeka, Croatia **2018**.
[13] V. Correia, J. Oliveira, N. Perinka, P. Costa, E. Sowade, K. Y. Mitra, R. R. Baumann, S. Lanceros-Mendez, *ACS Appl. Electron. Mater.* **2020**, *2*, 1470.
[14] X. Fan, W. Nie, H. Tsai, N. Wang, H. Huang, Y. Cheng, R. Wen, L. Ma, F. Yan, Y. Xia, *Adv. Sci.* **2019**, *6*, 1900813.
[15] E. Bihar, D. Corzo, T. C. Hidalgo, D. Rosas-Villalva, K. N. Salama, S. Inal, D. Baran, *Adv. Mater. Technol.* **2020**, *5*, 2000226.
[16] T. Sekitani, T. Someya, *Adv. Mater.* **2010**, *22*, 2228.
[17] W. Shi, Y. Guo, Y. Liu, *Adv. Mater.* **2020**, *32*, 1901493.
[18] H. Matsui, Y. Takeda, S. Tokito, *Org. Electron.* **2019**, *75*, 105432.
[19] Q. Shi, B. Dong, T. He, Z. Sun, J. Zhu, Z. Zhang, C. Lee, *InfoMat* **2020**, *2*, 1131.
[20] H. Chen, *J. Ind. Integr. Manag.* **2017**, *02*, 1750012.
[21] M. Thibaud, H. Chi, W. Zhou, S. Piramuthu, *Decis. Support Syst.* **2018**, *108*, 79.
[22] H. Zhu, E. S. Shin, A. Liu, D. Ji, Y. Xu, Y. Y. Noh, *Adv. Funct. Mater.* **2020**, 30, 1904588.
[23] G. Wang, M. A. Adil, J. Zhang, Z. Wei, *Adv. Mater.* **2019**, *31*, 1805089.
[24] V. Kumar, L. E. Aygun, N. Verma, J. C. Sturm, B. Glisic, in *Sensors Smart Struct. Technol. Civil, Mech. Aerosp. Syst. 2019* (Eds: J. P. Lynch, H. Huang, H. Sohn, K.-W. Wang), SPIE, Denver, Colorado, USA **2019**, pp. 723–730.
[25] W. J. Hyun, E. B. Secor, C. Kim, M. C. Hersam, L. F. Francis, C. D. Frisbie, *Adv. Energy Mater.* **2017**, *7*, 1700285.
[26] C. M. Homenick, R. James, G. P. Lopinski, J. Dunford, J. Sun, H. Park, Y. Jung, G. Cho, P. R. L. Malenfant, *ACS Appl. Mater. Interfaces* **2016**, *8*, 27900.
[27] S. Jung, S. D. Hoath, G. D. Martin, I. M. Hutchings, *Large Area and FlexIble Electronics*, John Wiley & Sons, Ltd, New Jersey **2015**, pp. 315–344.
[28] J. S. Chang, A. F. Facchetti, R. Reuss, *IEEE J. Emerg. Sel. Top. Circuits Syst.* **2017**, *7*, 7.
[29] G. Tong, Z. Jia, J. Chang, in *2018 IEEE Int. Symp. on Circuits Systems*, IEEE, New York City **2018**, pp. 1–5.
[30] Y. Khan, A. Thielens, S. Muin, J. Ting, C. Baumbauer, A. C. Arias, *Adv. Mater.* **2020**, *32*, 1905279.
[31] V. R. Marinov, *Int. Symp. Microelectron.* **2017**, 103.
[32] J. N. Burghartz, G. Alavi, B. Albrecht, T. Deuble, M. Elsobky, S. Ferwana, C. Harendt, Y. Mahsereci, H. Richter, Z. Yu, *IEEE J. Electron Devices Soc.* **2019**, *7*, 776.
[33] S. Qiu, C. Zhou, *PrintEd Electronics*, John Wiley & Sons Singapore Pte. Ltd, Singapore **2016**, p. 21.
[34] F. Bossuyt, T. Vervust, J. Vanfleteren, *IEEE Trans. Components, Packag. Manuf. Technol.* **2013**, *3*, 229.
[35] Y. Cao, Y. J. Tan, S. Li, W. W. Lee, H. Guo, Y. Cai, C. Wang, B. C.-K. Tee, *Nat. Electron.* **2019**, *2*, 75.
[36] M. Amjadi, K.-U. Kyung, I. Park, M. Sitti, *Adv. Funct. Mater.* **2016**, *26*, 1678.
[37] J. Ge, X. Wang, M. Drack, O. Volkov, M. Liang, G. S. Cañón Bermúdez, R. Illing, C. Wang, S. Zhou, J. Fassbender, M. Kaltenbrunner, D. Makarov, *Nat. Commun.* **2019**, *10*, 4405.
[38] J. Byun, B. Lee, E. Oh, H. Kim, S. Kim, S. Lee, Y. Hong, *Sci. Rep.* **2017**, *7*, 45328.
[39] J. Kim, R. Kumar, A. J. Bandodkar, J. Wang, *Adv. Electron. Mater.* **2017**, *3*, 1600260.
[40] Y. Qian, X. Zhang, L. Xie, D. Qi, B. K. Chandran, X. Chen, W. Huang, *Adv. Mater.* **2016**, *28*, 9243.
[41] T. Löher, M. Seckel, J. Haberland, J. Marques, M. von Krshiwobl ozki, C. Kallmayer, A. Ostmann, in *2019 IEEE CPMT Symp. Japan*, IEEE, Piscataway, NJ **2019**, pp. 113–117.
[42] M. Ozatay, L. Aygun, H. Jia, P. Kumar, Y. Mehlman, C. Wu, S. Wagner, J. C. Sturm, N. Verma, in *2018 IEEE CustOm Integrated Circuits Conf. (CICC)*, IEEE, Piscataway, NJ **2018**, p. 1.
[43] F. Li, A. Nathan, Y. Wu, B. S. Ong, *Organic Thin Film Transistor Integration*, Wiley, New York **2011**.
[44] R. R. Søndergaard, M. Hösel, F. C. Krebs, *J. Polym. Sci., Part B: Polym. Phys.* **2013**, *51*, 16.
[45] R. Abbel, Y. Galagan, P. Groen, *Adv. Eng. Mater.* **2018**, *20*, 1701190.

[46] J. Kettunen, I. Kaisto, E. Kieboom, R. Rikkola, R. Korhonen, *VTT Tied. - Valt. Tek. Tutkimusk.* **2011**, *2590*, 1.
[47] S. Khan, L. Lorenzelli, R. S. Dahiya, *IEEE Sens. J.* **2015**, *15*, 3164.
[48] G. Zhan, A. Mukherjee, *Rev. Adv. Mater. Sci* **2005**, *10*, 185.
[49] Q. Huang, Y. Zhu, *Adv. Mater. Technol.* **2019**, *4*, 1.
[50] B. Vedhanarayanan, V. K. Praveen, G. Das, A. Ajayaghosh, *NPG Asia Mater.* **2018**, *10*, 107.
[51] S. Nambiar, J. Yeow, *Biosens. Bioelectron.* **2010**, *26*, 1825.
[52] Y. Wang, L. Sun, C. Wang, F. Yang, X. Ren, X. Zhang, H. Dong, W. Hu, *Chem. Soc. Rev.* **2019**, *48*, 1492.
[53] T. Kim, D. M. Kim, B. J. Lee, J. Lee, *Sensors* **2019**, *19*, 4250.
[54] A. V. Novikov, L. I. Kuznetsova, N. N. Dremova, A. A. Parfenov, P. A. Troshin, *J. Mater. Chem. C* **2020**, *8*, 495.
[55] J. A. Cardenas, J. B. Andrews, S. G. Noyce, A. D. Franklin, *Nano Futur.* **2020**, *4*, 12001.
[56] X. Sun, C. A. Di, Y. Liu, *J. Mater. Chem.* **2010**, *20*, 2599.
[57] J. Li, W. Tang, Q. Wang, W. Sun, Q. Zhang, X. Guo, X. Wang, F. Yan, *Mater. Sci. Eng., R: Rep.* **2018**, *127*, 1.
[58] M. S. Saveleva, K. Eftekhari, A. Abalymov, T. E. L. Douglas, D. Volodkin, B. V Parakhonskiy, A. G. Skirtach, *Front. Chem.* **2019**, *7*, 179.
[59] I. Warad, H. Omar Abd-Elkader, S. Al-Resayes, A. Husein, M. Al-Nuri, A. Boshaala, N. Al-Zaqri, T. Ben Hadda, *Int. J. Mol. Sci.* **2012**, *13*, 6279.
[60] D. D. L. Chung, *Composite Materials*, Springer Science & Business Media, New York, NY, USA **2010**, p. 371.
[61] J. N. Tiwari, R. N. Tiwari, K. S. Kim, *Prog. Mater. Sci.* **2012**, *57*, 724.
[62] NanoWerk,https://www.nanowerk.com/nanotechnology/introduction/introduction_to_nanotechnology_2.php (accessed: June 2020).
[63] F. C. Krebs, *Sol. Energy Mater. Sol. Cells* **2009**, *93*, 394.
[64] Y. Li, M. Misra, S. Gregori, *IEEE Trans. Components, Packag. Manuf. Technol.* **2018**, *8*, 1307.
[65] J. M. Chem, *J. Mater. Chem. C* **2019**, *7*, 14035.
[66] J. C. Costa, F. Spina, P. Lugoda, L. Garcia-Garcia, D. Roggen, N. Münzenrieder, *Technologies* **2019**, *7*, 35.
[67] H. Wang, *IOP Conf. Ser. Mater. Sci. Eng.* **2017**, *207*, 012040.
[68] P. Lee, J. Ham, J. Lee, S. Hong, S. Han, Y. D. Suh, S. E. Lee, J. Yeo, S. S. Lee, D. Lee, S. H. Ko, *Adv. Funct. Mater.* **2014**, *24*, 5671.
[69] S. Agarwala, G. L. Goh, T. S. Dinh Le, J. An, Z. K. Peh, W. Y. Yeong, Y. J. Kim, *ACS Sens.* **2019**, *4*, 218.
[70] I. J. Fernandes, A. F. Aroche, A. Schuck, P. Lamberty, C. R. Peter, W. Hasenkamp, T. L. A. C. Rocha, *Sci. Rep.* **2020**, *10*, 8878.
[71] S. A. Odom, S. Chayanupatkul, B. J. Blaiszik, O. Zhao, A. C. Jackson, P. V Braun, N. R. Sottos, S. R. White, J. S. Moore, *Adv. Mater.* **2012**, *24*, 2578.
[72] X. Yu, T. J. Marks, A. Facchetti, *Nat. Mater.* **2016**, *15*, 383.
[73] J. Leppäniemi, Presentation for BET-EU.5/11, **2018**.
[74] Materion Tecnhical Paper, *Transparent Conductive Oxide Thin Films*, Buffalo, NY, **2012**.
[75] T. S. Kim, Y. Lee, W. Xu, Y. H. Kim, M. Kim, S. Y. Min, T. H. Kim, H. W. Jang, T. W. Lee, *Nano Energy* **2019**, *58*, 437.
[76] Y. Wang, J. Zhou, H. Li, T. Zhang, M. Gao, Z. Cheng, C. Yu, S. Patel, Y. Shi, in *Proc. of the ACM on Interactive, Mobile, Wearable and Ubiquitous Technologies*, Vol. *3*, ACM, New York, NY **2019**, p. 1.
[77] F. Merdj, A. Mekki, D. Guettiche, B. Mettai, Z. B. D. Sayah, Z. Safidine, A. Abdi, R. Mahmoud, M. M. Chehimi, *Macromol. Res.* **2018**, *26*, 511.
[78] P. Woias, *Micro Nano Lett.* **2018**, *13*, 1525.
[79] P. Shi, W. Wang, D. Liu, J. Zhang, W. Ren, B. Tian, J. Zhang, *ACS Appl. Electron. Mater.* **2019**, *1*, 1105.
[80] H. Zhou, J. Xie, M. Mai, J. Wang, X. Shen, S. Wang, L. Zhang, K. Kisslinger, H.-Q. Wang, J. Zhang, Y. Li, J. Deng, S. Ke, X. Zeng, *ACS Appl. Mater. Interfaces* **2018**, *10*, 16160.
[81] E. Fortunato, P. Barquinha, R. Martins, *Adv. Mater.* **2012**, *24*, 2945.
[82] H. B. Lee, W. Y. Jin, M. M. Ovhal, N. Kumar, J. W. Kang, *J. Mater. Chem. C* **2019**, *7*, 1087.
[83] Y. Choi, K. Seong, Y. Piao, *Adv. Mater. Interfaces* **2019**, *6*, 1901002.
[84] K. Teng, R. Vest, *IEEE Trans. Components, Hybrids, Manuf. Technol.* **1987**, *10*, 545.
[85] Y. Dong, Z. Lin, X. Li, Q. Zhu, J.-G. Li, X. Sun, *J. Mater. Chem. C* **2018**, *6*, 6406.
[86] D.-H. Shin, S. Woo, H. Yem, M. Cha, S. Cho, M. Kang, S. Jeong, Y. Kim, K. Kang, Y. Piao, *ACS Appl. Mater. Interfaces* **2014**, *6*, 3312.
[87] Y. Dong, X. Li, S. Liu, Q. Zhu, J.-G. Li, X. Sun, *Thin Solid Films* **2015**, *589*, 381.
[88] S. F. Jahn, T. Blaudeck, R. R. Baumann, A. Jakob, P. Ecorchard, T. Rüffer, H. Lang, P. Schmidt, *Chem. Mater.* **2010**, *22*, 3067.
[89] G. M. Vest, V. P. Cone, C. J. Herzfeld, A. K. Bhansali, *MRS Proc.* **1986**, *72*, 47.
[90] C. Cano-Raya, Z. Z. Denchev, S. F. Cruz, J. C. Viana, *Appl. Mater. Today* **2019**, *15*, 416.
[91] L. Wang, J. Liu, *Front. Mater.* **2019**, 6.
[92] M. D. Dickey, R. C. Chiechi, R. J. Larsen, E. A. Weiss, D. A. Weitz, G. M. Whitesides, *Adv. Funct. Mater.* **2008**, *18*, 1097.
[93] S. Yu, M. Kaviany, *J. Chem. Phys.* **2014**, *140*, 64303.
[94] S. Liu, M. C. Yuen, E. L. White, J. W. Boley, B. Deng, G. J. Cheng, R. Kramer-Bottiglio, *ACS Appl. Mater. Interfaces* **2018**, *10*, 28232.
[95] P. Reineck, Y. Lin, B. C. Gibson, M. D. Dickey, A. D. Greentree, I. S. Maksymov, *Sci. Rep.* **2019**, *9*, 5345.
[96] P. Jiang, C. Yan, Y. Guo, X. Zhang, M. Cai, X. Jia, X. Wang, F. Zhou, *Biomater. Sci.* **2019**, *7*, 1805.
[97] M. Varga, C. Ladd, S. Ma, J. Holbery, G. Tröster, *Lab Chip* **2017**, *17*, 3272.
[98] M. G. Mohammed, R. Kramer, *Adv. Mater.* **2017**, *29*, 1604965.
[99] E. J. Markvicka, M. D. Bartlett, X. Huang, C. Majidi, *Nat. Mater.* **2018**, *17*, 618.
[100] C. H. Kim, I. Kymissis, *J. Mater. Chem. C* **2017**, *5*, 4598.
[101] D. M. Sun, C. Liu, W.-C. Ren, H. M. Cheng, *Small* **2013**, *9*, 1188.
[102] K. S. Novoselov, A. K. Geim, S. V Morozov, D. Jiang, Y. Zhang, S. V Dubonos, I. V Grigorieva, A. A. Firsov, *Science* **2004**, *306*, 666.
[103] T. S. Tran, N. K. Dutta, N. R. Choudhury, *Adv. Colloid Interface Sci.* **2018**, *261*, 41.
[104] W. Yang, C. Wang, *J. Mater. Chem. C* **2016**, *4*, 7193.
[105] M. H. Overgaard, M. Kühnel, R. Hvidsten, S. V. Petersen, T. Vosch, K. Nørgaard, B. W. Laursen, *Adv. Mater. Technol.* **2017**, *2*, 1700011.
[106] Y. Wang, L. Wang, T. Yang, X. Li, X. Zang, M. Zhu, K. Wang, D. Wu, H. Zhu, *Adv. Funct. Mater.* **2014**, *24*, 4666.
[107] C. Casiraghi, M. Macucci, K. Parvez, R. Worsley, Y. Shin, F. Bronte, C. Borri, M. Paggi, G. Fiori, *Carbon N. Y.* **2018**, *129*, 462.
[108] D. McManus, S. Vranic, F. Withers, V. Sanchez-Romaguera, M. Macucci, H. Yang, R. Sorrentino, K. Parvez, S.-K. Son, G. Iannaccone, K. Kostarelos, G. Fiori, C. Casiraghi, *Nat. Nanotechnol.* **2017**, *12*, 343.
[109] M. Franco, R. Alves, N. Perinka, C. Tubio, P. Costa, S. Lanceros-Mendéz, *ACS Appl. Electron. Mater.* **2020**, *2*, 2857.
[110] L. Wang, S. Chen, T. Shu, X. Hu, *ChemSusChem* **2020**, *13*, 1330.
[111] F. Liu, X. Qiu, J. Xu, J. Huang, D. Chen, G. Chen, *Prog. Org. Coatings* **2019**, *133*, 125.
[112] W. Yang, C. Wang, *J. Mater. Chem. C* **2016**, *4*, 7193.
[113] R. Tortorich, J.-W. Choi, *Nanomaterials* **2013**, *3*, 453.
[114] C. S. Boland, U. Khan, G. Ryan, S. Barwich, R. Charifou, A. Harvey, C. Backes, Z. Li, M. S. Ferreira, M. E. Möbius, R. J. Young, J. N. Coleman, *Science* **2016**, *354*, 1257.
[115] C. S. Boland, U. Khan, C. Backes, A. O'Neill, J. McCauley, S. Duane, R. Shanker, Y. Liu, I. Jurewicz, A. B. Dalton, J. N. Coleman, *ACS Nano* **2014**, *8*, 8819.
[116] Y. Seekaew, S. Lokavee, D. Phokharatkul, A. Wisitsoraat, T. Kerdcharoen, C. Wongchoosuk, *Org. Electron.* **2014**, *15*, 2971.

[117] T. Vuorinen, J. Niittynen, T. Kankkunen, T. M. Kraft, M. Mäntysalo, *Sci. Rep.* **2016**, *6*, 35289.
[118] Z. He, W. Chen, B. Liang, C. Liu, L. Yang, D. Lu, Z. Mo, H. Zhu, Z. Tang, X. Gui, *ACS Appl. Mater. Interfaces* **2018**, *10*, 12816.
[119] S. Chen, Y. Wei, X. Yuan, Y. Lin, L. Liu, *J. Mater. Chem. C* **2016**, *4*, 4304.
[120] M. Ghahremanpour, E. Baumgartner, M. Bogner, N. Boufercha, J. Sägebarth, H. Sandmaier, in *2011 IEEE Sensors Proc.*, IEEE, Piscataway, NJ **2011**, pp. 1032–1035.
[121] A. Benchirouf, S. Palaniyappan, R. Ramalingame, P. Raghunandan, T. Jagemann, C. Müller, M. Hietschold, O. Kanoun, *Sens. Actuators, B* **2016**, *224*, 344.
[122] M. Tonga, L. Wei, P. M. Lahti, *Int. J. Energy Res.* **2020**, *44*, 9149.
[123] N. A. Cooling, E. F. Barnes, F. Almyahi, K. Feron, M. F. Al-Mudhaffer, A. Al-Ahmad, B. Vaughan, T. R. Andersen, M. J. Griffith, A. S. Hart, A. G. Lyons, W. J. Belcher, P. C. Dastoor, *J. Mater. Chem. A* **2016**, *4*, 10274.
[124] J. L. Hart, K. Hantanasirisakul, A. C. Lang, B. Anasori, D. Pinto, Y. Pivak, J. T. van Omme, S. J. May, Y. Gogotsi, M. L. Taheri, *Nat. Commun.* **2019**, *10*, 522.
[125] G. Hu, J. Kang, L. W. T. Ng, X. Zhu, R. C. T. Howe, C. G. Jones, M. C. Hersam, T. Hasan, *Chem. Soc. Rev.* **2018**, *47*, 3265.
[126] Y. Yi-Na, W. Ran-Ran, S. U. N. Jing, *J. Inorg. Mater.* **2019**, 282.
[127] L. Zhao, K. Wang, W. Wei, L. Wang, W. Han, *InfoMat* **2019**, *1*, 407.
[128] C. (John) Zhang, M. P. Kremer, A. Seral-Ascaso, S.-H. Park, N. McEvoy, B. Anasori, Y. Gogotsi, V. Nicolosi, *Adv. Funct. Mater.* **2018**, *28*, 1705506.
[129] L. Mariucci, Organic Large Area Electronics, https://www.imm.cnr.it/articles/organic-large-area-electronics (accessed: March 2020).
[130] M. C. Petty, T. Nagase, H. Suzuki, H. Naito, E. C. Organic, *Springer Handbook of Electronic and Photonic Materials*, Springer, Berlin **2017**, p. 1257.
[131] W. J. Feast, J. Tsibouklis, K. L. Pouwer, L. Groenendaal, E. W. Meijer, *Polymer* **1996**, *37*, 5017.
[132] B. Winther-Jensen, N. Clark, P. Subramanian, R. Helmer, S. Ashraf, G. Wallace, L. Spiccia, D. MacFarlane, *J. Appl. Polym. Sci.* **2007**, *104*, 3938.
[133] Y. Guo, M. T. Otley, M. Li, X. Zhang, S. K. Sinha, G. M. Treich, G. A. Sotzing, *ACS Appl. Mater. Interfaces* **2016**, *8*, 26998.
[134] L. V Kayser, D. J. Lipomi, *Adv. Mater.* **2019**, *31*, 1806133.
[135] G. B. Tseghai, B. Malengier, K. A. Fante, A. B. Nigusse, L. Van Langenhove, *Sensors* **2020**, *20*, 1742.
[136] Y.-F. Wang, T. Sekine, Y. Takeda, K. Yokosawa, H. Matsui, D. Kumaki, T. Shiba, T. Nishikawa, S. Tokito, *Sci. Rep.* **2020**, *10*, 2467.
[137] J. Kawahara, P. A. Ersman, I. Engquist, M. Berggren, *Org. Electron.* **2012**, *13*, 469.
[138] T. Kololuoma, C. Pinheiro, I. Kaisto, A. Colley, K. Ronka, M. Keranen, T. Kurkela, T. Happonen, M. Korkalainen, M. Kehusmaa, L. Gomes, A. Branco, S. Ihme, *IEEE J. Electron Devices Soc.* **2019**, *7*, 761.
[139] D. Levasseur, I. Mjejri, T. Rolland, A. Rougier, *Polymers* **2019**, *11*, 179.
[140] S. K. Nemani, D. Chen, M. H. Mohamed, H. Sojoudi, *J. Nanomater.* **2018**, *2018*, 3230293.
[141] F. Michelis, L. Bodelot, Y. Bonnassieux, B. Lebental, *Carbon N. Y.* **2015**, *95*, 1020.
[142] Y. He, Y. Ming, W. Li, Y. Li, M. Wu, J. Song, X. Li, H. Liu, *Sensors* **2018**, *18*, 1338.
[143] A. Denneulin, J. Bras, F. Carcone, C. Neuman, A. Blayo, *Carbon N. Y.* **2011**, *49*, 2603.
[144] P. Angelo, R. Farnood, *J. Adhes. Sci. Technol. – J. Adhes. Sci. Technol.* **2010**, *24*, 643.
[145] G. Rodrigues, *Master Degree Thesis*, Universidade Nova de Lisboa, **2014**.
[146] W. Lee, Y. H. Kang, J. Y. Lee, K.-S. Jang, S. Y. Cho, *RSC Adv.* **2016**, *6*, 53339.
[147] U. Kraft, F. Molina-Lopez, D. Son, Z. Bao, B. Murmann, *Adv. Electron. Mater.* **2020**, *6*, 1900681.
[148] C. O. Baker, X. Huang, W. Nelson, R. B. Kaner, *Chem. Soc. Rev.* **2017**, *46*, 1510.
[149] C. U. Seo, Y. Yoon, D. H. Kim, S. Y. Choi, W. K. Park, J. S. Yoo, B. Baek, S. Bin Kwon, C.-M. Yang, Y. H. Song, D. H. Yoon, W. S. Yang, S. Kim, *J. Ind. Eng. Chem.* **2018**, *64*, 97.
[150] S. Cho, J. S. Lee, J. Jun, S. G. Kim, J. Jang, *Nanoscale* **2014**, *6*, 15181.
[151] H. Jamalabadi, A. Mani-Varnosfaderani, N. Alizadeh, *Sens. Actuators, A* **2018**, *280*, 228.
[152] S. K. Garlapati, M. Divya, B. Breitung, R. Kruk, H. Hahn, S. Dasgupta, *Adv. Mater.* **2018**, *30*, 1707600.
[153] J. Troughton, D. Atkinson, *J. Mater. Chem. C* **2019**, *7*, 12388.
[154] M. G. Kim, M. G. Kanatzidis, A. Facchetti, T. J. Marks, *Nat. Mater.* **2011**, *10*, 382.
[155] J. W. Hennek, Y. Xia, K. Everaerts, M. C. Hersam, A. Facchetti, T. J. Marks, *ACS Appl. Mater. Interfaces* **2012**, *4*, 1614.
[156] S. Lim, J. Oh, J. Koo, C. Park, S.-W. Jung, B. Na, H. Chu, *J. Nanosci. Nanotechnol.* **2014**, *14*, 8665.
[157] S. Park, S. W. Heo, W. Lee, D. Inoue, Z. Jiang, K. Yu, H. Jinno, D. Hashizume, M. Sekino, T. Yokota, K. Fukuda, K. Tajima, T. Someya, *Nature* **2018**, *561*, 516.
[158] A. Pierre, S. E. Doris, R. Lujan, R. A. Street, *Adv. Mater. Technol.* **2019**, *4*, 1.
[159] N. Münzenrieder, D. Karnaushenko, L. Petti, G. Cantarella, C. Vogt, L. Büthe, D. D. Karnaushenko, O. G. Schmidt, D. Makarov, G. Tröster, *Adv. Electron. Mater.* **2016**, *2*, 1600188.
[160] X. Wu, J. Huang, S. Yu, P. Ruan, R. Sun, C. P. Wong, *Macromol. Res.* **2020**, *28*, 373.
[161] F. Hetsch, N. Zhao, S. V. Kershaw, A. L. Rogach, *Mater. Today* **2013**, *16*, 312.
[162] A. Kojima, K. Teshima, Y. Shirai, T. Miyasaka, *J. Am. Chem. Soc.* **2009**, *131*, 6050.
[163] Y. Chen, W. Xing, Y. Liu, X. Zhang, Y. Xie, C. Shen, J. G. Liu, C. Geng, S. Xu, *Nanomaterials* **2020**, *10*, 317.
[164] M. Que, W. Guo, X. Zhang, X. Li, Q. Hua, L. Dong, C. Pan, *J. Mater. Chem. A* **2014**, *2*, 13661.
[165] Z. Luo, G. Qi, K. Chen, M. Zou, L. Yuwen, X. Zhang, W. Huang, L. Wang, *Adv. Funct. Mater.* **2016**, *26*, 2739.
[166] H. Chen, T. H. Yeh, J. He, C. Zhang, R. Abbel, M. R. Hamblin, Y. Huang, R. J. Lanzafame, I. Stadler, J. Celli, S. W. Liu, S. T. Wu, Y. Dong, *J. Soc. Inf. Disp.* **2018**, *26*, 296.
[167] L. Shi, L. Meng, F. Jiang, Y. Ge, F. Li, X. Wu, H. Zhong, *Adv. Funct. Mater.* **2019**, *29*, 1903648.
[168] C.-W. Chen, T.-C. Chang, P.-T. Liu, H.-Y. Lu, K.-C. Wang, C.-S. Huang, C.-C. Ling, T.-Y. Tseng, *IEEE Electron Device Lett.* **2005**, *26*, 731.
[169] H. Gleskova, S. Wagner, Z. Suo, *Appl. Phys. Lett.* **1999**, *75*, 3011.
[170] T. C. Chang, Y. C. Tsao, P. H. Chen, M. C. Tai, S. P. Huang, W. C. Su, G. F. Chen, *Mater. Today Adv.* **2020**, *5*, 100040.
[171] A. Pecora, L. Maiolo, M. Cuscunà, D. Simeone, A. Minotti, L. Mariucci, G. Fortunato, *Solid. State. Electron.* **2008**, *52*, 348.
[172] X. Gao, L. Lin, Y. Liu, X. Huang, *IEEE/OSA J. Disp. Technol.* **2015**, *11*, 666.
[173] M. Trifunovic, T. Shimoda, R. Ishihara, *Appl. Phys. Lett.* **2015**, *106*, 163502.
[174] C. Jiang, X. Cheng, A. Nathan, *Proc. IEEE* **2019**, *107*, 2084.
[175] J. A. Lim, W. H. Lee, H. S. Lee, J. H. Lee, Y. D. Park, K. Cho, *Adv. Funct. Mater.* **2008**, *18*, 229.
[176] H. S. Kim, J. H. Park, W. H. Lee, H. H. Kim, Y. D. Park, *Soft Matter* **2019**, *15*, 7369.
[177] K. S. Park, J. Baek, Y. Park, L. Lee, Y.-E. K. Lee, Y. Kang, M. M. Sung, *Adv. Mater.* **2016**, *28*, 2874.

[178] A. L. Briseno, R. J. Tseng, M. M. Ling, E. H. L. Falcao, Y. Yang, F. Wudl, Z. Bao, *Adv. Mater.* **2006**, *18*, 2320.
[179] J. Liu, H. Zhang, H. Dong, L. Meng, L. Jiang, L. Jiang, Y. Wang, J. Yu, Y. Sun, W. Hu, A. J. Heeger, *Nat. Commun.* **2015**, *6*, 10032.
[180] L. S. Panwar, S. Kala, V. Panwar, S. S. Panwar, S. Sharma, in *2017 3rd Int. Conf. on Advances in Computing, Communication and Automation*, IEEE, Piscataway, NJ **2017**, pp. 1–7.
[181] Y. L. Huang, Y. J. Zheng, Z. Song, D. Chi, A. T. S. Wee, S. Y. Quek, *Chem. Soc. Rev.* **2018**, *47*, 3241.
[182] S. Boandoh, S. H. Choi, J. H. Park, S. Y. Park, S. Bang, M. S. Jeong, J. S. Lee, H. J. Kim, W. Yang, J. Y. Choi, S. M. Kim, K. K. Kim, *Small* **2017**, *13*, 1701306.
[183] J. M. Ball, M. M. Lee, A. Hey, H. J. Snaith, *Energy Environ. Sci.* **2013**, *6*, 1739.
[184] J. Burschka, N. Pellet, S.-J. Moon, R. Humphry-Baker, P. Gao, M. K. Nazeeruddin, M. Grätzel, *Nature* **2013**, *499*, 316.
[185] H. Zhou, C. Qi, L. Gang, L. Song, S. Tze-bing, D. Hsin-Sheng, H. Ziruo, J. You, L. Yongsheng, Y. Yan, *Science* **2014**, *345*, 542.
[186] W. S. Yang, J. H. Noh, N. J. Jeon, Y. C. Kim, S. Ryu, J. Seo, S. Il Seok, *Science* **2015**, *348*, 1234.
[187] Y. Hu, S. Si, A. Mei, Y. Rong, H. Liu, X. Li, H. Han, *Sol. RRL* **2017**, *1*, 1600019.
[188] Q. Hu, H. Wu, J. Sun, D. Yan, Y. Gao, J. Yang, *Nanoscale* **2016**, *8*, 5350.
[189] M. Singh, A. Ng, Z. Ren, H. Hu, H.-C. Lin, C.-W. Chu, G. Li, *Nano Energy* **2019**, *60*, 275.
[190] X. Li, D. Yu, J. Chen, Y. Wang, F. Cao, Y. Wei, Y. Wu, L. Wang, Y. Zhu, Z. Sun, J. Ji, Y. Shen, H. Sun, H. Zeng, *ACS Nano* **2017**, *11*, 2015.
[191] Q. Xue, Z. Hu, C. Sun, Z. Chen, F. Huang, H.-L. Yip, Y. Cao, *RSC Adv.* **2015**, *5*, 775.
[192] C. Xie, P. You, Z. Liu, L. Li, F. Yan, *Light Sci. Appl.* **2017**, *6*, e17023.
[193] N. Choudhary, M. A. Islam, J. H. Kim, T. J. Ko, A. Schropp, L. Hurtado, D. Weitzman, L. Zhai, Y. Jung, *Nano Today* **2018**, *19*, 16.
[194] B. Radisavljevic, A. Radenovic, J. Brivio, V. Giacometti, A. Kis, *Nat. Nanotechnol.* **2011**, *6*, 147.
[195] Y. Yao, L. Tolentino, Z. Yang, X. Song, W. Zhang, Y. Chen, C. Wong, *Adv. Funct. Mater.* **2013**, *23*, 3577.
[196] M. Amani, R. Burke, R. Proie, M. Dubey, *Nanotechnology* **2015**, *26*, 115202.
[197] T.-Y. Kim, J. Ha, K. Cho, J. Pak, J. Seo, J. Park, J.-K. Kim, S. Chung, Y. Hong, T. Lee, *ACS Nano* **2017**, *11*, 10273.
[198] F. M. Li, Y. Wu, B. Ong, Y. Vygranenko, A. Nathan, *Mater. Res. Soc. Symp. Proc.* **2007**, *1003*, 124.
[199] G. McKerricher, R. Maller, V. Mohammad, M. A. McLachlan, A. Shamim, *Ceram. Int.* **2017**, *43*, 9846.
[200] C. Mendes-Felipe, J. Oliveira, I. Etxebarria, J. L. Vilas-Vilela, S. Lanceros-Mendez, *Adv. Mater. Technol.* **2019**, *4*, 1800618.
[201] S. Ansari, M. N. Muralidharan, in *Flex. Stretchable Electron. Compos.* (Eds: D. Ponnamma, K. Sadasivuni, C. Wan, S. Thomas, M. Al-Ali AlMa'adeed), Springer International Publishing, New York, USA **2015**, pp. 87–134.
[202] Y. Jang, D. Kim, Y. Park, J. Cho, M. Hwang, K. Cho, *Appl. Phys. Lett.* **2006**, *88*, 72101.
[203] G.-W. Kang, K.-M. Park, J.-H. Song, C. H. Lee, D. H. Hwang, *Curr. Appl. Phys.* **2005**, *5*, 297.
[204] T.-S. Huang, Y.-K. Su, P.-C. Wang, *Appl. Phys. Lett.* **2007**, *91*, 92116.
[205] A. Mohapatra, K. S. Tuli, K. Liu, T. Fujiwara, W. R. Hewitt, F. Andrasik, I. B. Morshed, in *2018 40th Annual Int. Conf. of the IEEE Engineering in Medicine and Biology Society*, IEEE, Piscataway, NJ **2018**, pp. 4277–4280.
[206] J. Jeon, B. Murmann, Z. Bao, *Electron Device Lett. IEEE* **2011**, *31*, 1488.
[207] S. Li, L. Feng, J. Zhao, X. Guo, Q. Zhang, *Polym. Chem.* **2015**, *6*, 5884.
[208] W. Tang, L. Feng, P. Yu, J. Zhao, X. Guo, *Adv. Electron. Mater.* **2016**, *2*, 1500454.
[209] M. Zea, A. Moya, I. Abrao-Nemeir, J. Gallardo-Gonzalez, N. Zine, A. Errachid, R. Villa, G. Gabriel, in *2019 20th Int. Conf. Solid-State Sensors, Actuators Microsystems Eurosensors XXXIII*, IEEE, Piscataway, NJ **2019**, pp. 2472–2475.
[210] M. Sangermano, A. Chiolerio, P. Martino, *Macromol. Mater. Eng.* **2013**, 298.
[211] E. Saleh, P. Woolliams, B. Clarke, A. Gregory, S. Greedy, C. Smartt, R. Wildman, I. Ashcroft, R. Hague, P. Dickens, C. Tuck, *Addit. Manuf.* **2017**, *13*, 143.
[212] H. Najafi-Ashtiani, *J. Mater. Sci. Mater. Electron.* **2019**, *30*, 7087.
[213] X. Wu, F. Fei, Z. Chen, W. Su, Z. Cui, *Compos. Sci. Technol.* **2014**, *94*, 117.
[214] F.-Y. Yang, K.-J. Chang, M.-Y. Hsu, C.-C. Liu, *Org. Electron.* **2008**, *9*, 925.
[215] Q. Ke, Q. Wu, L. Liang, Y. Pei, X. Lu, M. Li, K. Huang, X. Liu, C. Liu, *Semicond. Sci. Technol.* **2017**, *32*, 104007.
[216] Y. Lu, W. H. Lee, H. S. Lee, Y. Jang, K. Cho, *Appl. Phys. Lett.* **2009**, *94*, 113303.
[217] C. Wang, J. C. Chien, K. Takei, T. Takahashi, J. Nah, A. M. Niknejad, A. Javey, *Nano Lett.* **2012**, *12*, 1527.
[218] E. R. € Garcia, *Doctoral Dissertation*, Universitat Autònoma de Barcelona, **2014**.
[219] D. K. Hwang, J. H. Park, J. Lee, J.-M. Choi, J. H. Kim, E. Kim, S. Im, *Electrochem. Solid-State Lett.* **2005**, *8*, G140.
[220] K. Y. Mitra, S. Kapadia, M. Hartwig, E. Sowade, Z. Xu, R. R. Baumann, R. Zichner, *Int. Conf. Digit. Print. Technol.* **2018**, *62*, 040407.
[221] H. F. Castro, V. Correia, E. Sowade, K. Y. Mitra, J. G. Rocha, R. R. Baumann, S. Lanceros-Méndez, *Org. Electron.* **2016**, *38*, 205.
[222] E. Sowade, E. Ramon, K. Y. Mitra, C. Martínez-Domingo, M. Pedró, J. Pallarès, F. Loffredo, F. Villani, H. L. Gomes, L. Terés, R. R. Baumann, *Sci. Rep.* **2016**, *6*, 33490.
[223] E. Sowade, K. Y. Mitra, E. Ramon, C. Martinez-Domingo, F. Villani, F. Loffredo, H. L. Gomes, R. R. Baumann, *Org. Electron.* **2016**, *30*, 237.
[224] Z. Xing, J. Zhao, L. Shao, H. Xiao, T. Liu, Z. Cui, *Carbon N. Y.* **2018**, *133*, 390.
[225] D. Roy, *AIP Conf. Proc.* **2018**, *1953*, 50051.
[226] Z. Yin, B. Tian, Q. Zhu, C. Duan, *Polymers* **2019**, *11*, 2033.
[227] B. Kheradmand-Boroujeni, G. C. Schmidt, D. Höft, M. Bellmann, K. Haase, K. Ishida, R. Shabanpour, T. Meister, C. Carta, P. Ghesquiere, A. C. Hübler, F. Ellinger, *IEEE Trans. Circuits Syst. I Regul. Pap.* **2016**, *63*, 785.
[228] X. Hu, Z. Ding, L. Fei, Y. Xiang, Y. lin, *J. Mater. Sci.* **2019**, *54*, 6401.
[229] B. Stadlober, M. Zirkl, M. Irimia-Vladu, *Chem. Soc. Rev.* **2019**, *48*, 1787.
[230] S.-W. Jung, K.-J. Baeg, S.-M. Yoon, I.-K. You, J.-K. Lee, Y.-S. Kim, Y.-Y. Noh, *J. Appl. Phys.* **2010**, *108*, 102810.
[231] Y. Oh, S. Pyo, M. H. Yi, S.-K. Kwon, *Org. Electron.* **2006**, *7*, 77.
[232] J. Gao, K. Asadi, J. Bin Xu, J. An, *Appl. Phys. Lett.* **2009**, *94*, 93302.
[233] C. Wang, W.-Y. Lee, R. Nakajima, J. Mei, D. H. Kim, Z. Bao, *Chem. Mater.* **2013**, *25*, 4806.
[234] T. Lee, J. H. Shin, I.-N. Kang, S. Lee, *Adv. Mater.* **2007**, *19*, 2702.
[235] W. A. Macdonald, *Large Area and Flexible Electronics*, Wiley-VCH, Weinheim **2015**, p. 291.
[236] J. Zhou, A. V. Ellis, N. H. Voelcker, *Electrophoresis* **2010**, *31*, 2.
[237] G. Ryu, J. You, V. Kostianovskii, E. Lee, Y. Kim, C. Park, Y. Noh, *IEEE Trans. Electron Devices* **2018**, *65*, 2997.
[238] W. Wu, *Sci. Technol. Adv. Mater.* **2019**, *20*, 187.
[239] C. Yang, E. J. Yoo, S. W. Lee, T. K. An, S. H. Kim, *Chinese J. Phys.* **2016**, *54*, 471.
[240] N. Saba, M. Jawaid, *J. Ind. Eng. Chem.* **2018**, *67*, 1.
[241] A. Matavž, V. Bobnar, B. Malič, *Langmuir* **2017**, *33*, 11893.

[242] C. X. Liu, J. W. Choi, *J. Micromechanics Microengineering* **2009**, *19*, 085019.
[243] A. A. S. Bhagat, P. Jothimuthu, I. Papautsky, *Lab Chip* **2007**, *7*, 1192.
[244] S. Bhattacharya, A. Datta, J. M. Berg, S. Gangopadhyay, *J. Microelectromech. Syst.* **2005**, *14*, 590.
[245] J. A. Jofre-Reche, J. Pulpytel, F. Arefi-Khonsari, J. M. Martín-Martínez, *J. Phys. D: Appl. Phys.* **2016**, *49*, 334001.
[246] A. Chiolerio, P. Rivolo, S. Porro, S. Stassi, S. Ricciardi, P. Mandracci, G. Canavese, K. Bejtka, C. F. Pirri, *RSC Adv.* **2014**, *4*, 51477.
[247] P. Lee, J. Lee, H. Lee, J. Yeo, S. Hong, K. H. Nam, D. Lee, S. S. Lee, S. H. Ko, *Adv. Mater.* **2012**, *24*, 3326.
[248] Q. Fan, Z. Qin, S. Gao, Y. Wu, J. Pionteck, E. Mäder, M. Zhu, *Carbon N. Y.* **2012**, *50*, 4085.
[249] L. Tian, B. Zimmerman, A. Akhtar, K. J. Yu, M. Moore, J. Wu, R. J. Larsen, J. W. Lee, J. Li, Y. Liu, B. Metzger, S. Qu, X. Guo, K. E. Mathewson, J. A. Fan, J. Cornman, M. Fatina, Z. Xie, Y. Ma, J. Zhang, Y. Zhang, F. Dolcos, M. Fabiani, G. Gratton, T. Bretl, L. J. Hargrove, P. V Braun, Y. Huang, J. A. Rogers, *Nat. Biomed. Eng.* **2019**, *3*, 194.
[250] X. Huang, Y. Liu, G. W. Kong, J. H. Seo, Y. Ma, K.-I. Jang, J. A. Fan, S. Mao, Q. Chen, D. Li, H. Liu, C. Wang, D. Patnaik, L. Tian, G. A. Salvatore, X. Feng, Z. Ma, Y. Huang, J. A. Rogers, *Microsyst. Nanoeng.* **2016**, *2*, 16052.
[251] M. Rizwan, M. W. A. Khan, L. Sydanheimo, J. Virkki, L. Ukkonen, *IEEE Antennas Wirel. Propag. Lett.* **2017**, *16*, 3108.
[252] S. Moscato, R. Bahr, T. Le, M. Pasian, M. Bozzi, L. Perregrini, M. M. Tentzeris, *IEEE Antennas Wirel. Propag. Lett.* **2016**, *15*, 1506.
[253] M. Rizwan, M. W. A. Khan, H. He, J. Virkki, L. Sydänheimo, L. Ukkonen, *Electron. Lett.* **2017**, *53*, 1054.
[254] J. Vaithilingam, E. Saleh, C. Tuck, R. Wildman, R. Hague, I. Ashcroft, P. Dickens, in *Annual Solid Freeform Fabrication (SFF) Symp.*, University of Texas, Austin **2015**.
[255] R. I. Haque, O. Chandran, S. Lani, D. Briand, *Nano Energy* **2018**, *52*, 54.
[256] F. Pece, J. J. Zarate, V. Vechev, N. Besse, O. Gudozhnik, H. Shea, O. Hilliges, in *UIST 2017— Proc. 30th Annual ACM Symp. on User Interface Software and Technology*, ACM, NY **2017**, p. 143.
[257] A. E. Tonelli, *Polymer* **2002**, *43*, 637.
[258] M. Ohsawa, N. Hashimoto, N. Takeda, S. Tsuneyasu, T. Satoh, *Microelectron. Reliab.* **2020**, *109*, 113673.
[259] S. Sim, Y. Lee, H. Kang, K.-Y. Shin, S.-H. Lee, J.-M. Kim, *Micro Nano Syst. Lett.* **2016**, *4*, 7.
[260] G. Xiao, P. Aflaki, S. Lang, Z. Zhang, Y. Tao, C. Py, P. Lu, C. Martin, S. Change, *IEEE J. Radio Freq. Identif.* **2018**, *2*, 31.
[261] X. Zeng, L. Ye, K. Guo, R. Sun, J. Xu, C.-P. Wong, *Adv. Electron. Mater.* **2016**, *2*, 1500485.
[262] H. H. Hsu, C. Y. Chang, C. H. Cheng, S. H. Yu, C. Y. Su, C. Y. Su, *Solid. State Electron.* **2013**, *89*, 194.
[263] J. Chang, X. Zhang, T. Ge, J. Zhou, *Org. Electron.* **2014**, *15*, 701.
[264] M. Hasegawa, Y. Hoshino, N. Katsura, J. Ishii, *Polymer* **2017**, *111*, 91.
[265] S.-Y. Yang, H.-X. Yang, A.-J. Hu, in *Adv. Polyim. Mater.* (Ed: S.-Y. Yang), Elsevier, Amsterdam **2018**, pp. 137–193.
[266] H. Ni, J. Liu, Z. Wang, S. Yang, *J. Ind. Eng. Chem.* **2015**, *28*, 16.
[267] A. S. Mathews, I. Kim, C.-S. Ha, *J. Appl. Polym. Sci.* **2006**, *102*, 3316.
[268] A. S. Mathews, I. Kim, C.-S. Ha, *Macromol. Res.* **2007**, *15*, 114.
[269] A. S. Mathews, I. Kim, C.-S. Ha, *Macromol. Symp.* **2007**, *249–250*, 344.
[270] J. Oishi, S. Hiramatsu, S. Kihara, H. Sotaro, H. Kihara, *US8357322*, **2013**.
[271] J. Corea, P. Ye, D. Seo, K. Butts-Pauly, A. C. Arias, M. Lustig, *Sci. Rep.* **2018**, *8*, 3392.
[272] N. T. Vo, D. Kim, *Korean J. Chem. Eng.* **2017**, *34*, 2536.
[273] R. Luise, *Applications of High Temperature Polymers*, CRC Press, Boca Raton **1997**.
[274] D. Liu, D. J. Broer, *Langmuir* **2014**, *30*, 13499.
[275] H. K. Bisoyi, Q. Li, *Chem. Rev.* **2016**, *116*, 15089.
[276] J. Jeong, B. So Hyun, J.-M. Seo, H. Chung, S. Kim, *J. Neural Eng.* **2016**, *13*, 25004.
[277] J. Maeng, R. T. Rihani, M. Javed, J. S. Rajput, H. Kim, I. G. Bouton, T. A. Criss, J. J. Pancrazio, B. J. Black, T. H. Ware, *J. Mater. Chem. B* **2020**, *8*, 6286.
[278] H. Kim, J. Gibson, J. Maeng, M. O. Saed, K. Pimentel, R. T. Rihani, J. J. Pancrazio, S. V Georgakopoulos, T. H. Ware, *ACS Appl. Mater. Interfaces* **2019**, *11*, 19506.
[279] T. A. Kent, M. J. Ford, E. J. Markvicka, C. Majidi, *Multifunct. Mater.* **2020**, *3*, 025003.
[280] T. S. Radhakrishnan, *J. Appl. Polym. Sci.* **2006**, *99*, 2679.
[281] F. Analysis, *Characterization and Failure Analysis of Plastics*, ASM International, Cleveland, OH **2004**.
[282] J. Quagliano, in *Thermosoftening Plast.* (Ed: G. A. Evingür), IntechOpen, London, UK **2019**, pp. 66–84.
[283] P. Patel, T. R. Hull, R. W. McCabe, D. Flath, J. Grasmeder, M. Percy, *Polym. Degrad. Stab.* **2010**, *95*, 709.
[284] E. N. Peters, in *Applied Plastics Engineering Handbook*, (Ed: M. Kutz), William Andrew Publishing, Norwich, NY **2017**, pp. 3–26.
[285] S. Homaeigohar, N. Botcha, E. Zarie, M. Elbahri, *Nanomaterials* **2019**, *9*, 250.
[286] M. Bin Ahmad, Y. Gharayebi, M. S. Salit, M. Z. Hussein, S. Ebrahimiasl, A. Dehzangi, *Int. J. Mol. Sci.* **2012**, *13*, 4860.
[287] Y. Lin, D. Gritsenko, Q. Liu, X. Lu, J. Xu, *ACS Appl. Mater. Interfaces* **2016**, *8*, 20501.
[288] E. Fortunato, N. Correia, P. Barquinha, L. Pereira, G. Goncalves, R. Martins, *IEEE Electron Device Lett.* **2008**, *29*, 988.
[289] G. V. Martins, A. P. M. Tavares, E. Fortunato, M. G. F. Sales, *Sci. Rep.* **2017**, *7*, 14558.
[290] M. L. Matias, D. Nunes, A. Pimentel, S. H. Ferreira, R. Borda D'Agua, M. P. Duarte, E. Fortunato, R. Martins, *J. Nanomater.* **2019**, *2019*, 1.
[291] L. Huang, P. Jiang, D. Wang, Y. Luo, M. Li, H. Lee, R. A. Gerhardt, *Sens. Actuators, B* **2014**, *197*, 308.
[292] D. Barmpakos, A. Segkos, C. Tsamis, G. Kaltsas, *J. Phys. Conf. Ser.* **2017**, *931*, 012003.
[293] J. M. Nassar, K. Mishra, K. Lau, A. A. Aguirre-Pablo, M. M. Hussain, *Adv. Mater. Technol.* **2017**, *2*, 1600228.
[294] M. Gama, F. Dourado, C. Freire, A. Silvestre, F. Hong, Y. Wan, D. Klemm, S. Bielecki, M. F. Rosa, J. D. Fontana, I. Saxena, in *4th Int. Symp. on Bacterial Nanocellulose*, Almeida Garrett Library Auditorium, Porto-Portugal **2019**.
[295] E. Vasileva, H. Chen, Y. Li, I. Sychugov, M. Yan, L. Berglund, S. Popov, *Adv. Opt. Mater.* **2018**, *6*, 1800999.
[296] Q. Fu, Y. Chen, M. Sorieul, *ACS Appl. Mater. Interfaces* **2020**, *14*, 3528.
[297] R. Sabo, A. Yermakov, C. T. Law, R. Elhajjar, *J. Renew. Mater.* **2016**, *4*, 297.
[298] A. N. Subba Rao, G. B. Nagarajappa, S. Nair, A. M. Chathoth, K. K. Pandey, *Compos. Sci. Technol.* **2019**, *182*, 107719.
[299] E. Sipilä, J. Virkki, J. Wang, L. Sydänheimo, L. Ukkonen, *Int. J. Antennas Propag.* **2016**, *2016*, 3694198.
[300] P. Rawat, M. Sharma, B. Kaur, D. Mittal, D. Singh, E. Sidhu, in *2017 Int. Conf. Smart Technologies for Smart Nation*, IEEE, Piscataway, NJ **2017**, pp. 153–157.
[301] R. Gonçalves, S. Rima, R. Magueta, A. Collado, P. Pinho, N. B. Carvalho, A. Georgiadis, in *2014 IEEE MTT-S Int. Microwave Symp.*, IEEE, Piscataway, NJ **2014**, pp. 1–4.
[302] D. S. Esteves, *Master Degree Thesis*, Universidade Nova de Lisboa, **2017**.
[303] J. Figueira, C. Gaspar, J. T. Carvalho, J. Loureiro, E. Fortunato, R. Martins, L. Pereira, *Micromachines* **2019**, *10*, 601.

[304] M. Tessarolo, L. Possanzini, E. G. Campari, R. Bonfiglioli, F. S. Violante, A. Bonfiglio, B. Fraboni, *Flex. Print. Electron.* **2018**, *3*, 34001.
[305] IMM Institute, Wearable band equipped with nanostructured strain gauge sensors for biomedical applications, https://www.imm.cnr.it/articles/wearable-band-equipped-nanostructured-strain-gauge-sensors-biomedical-applications (accessed: April 2020).
[306] E. Bihar, T. Roberts, Y. Zhang, E. Ismailova, T. Hervé, G. Malliaras, J. Graaf, S. Inal, M. Saadaoui, *Flex. Print. Electron.* **2018**, *3*, 034004.
[307] A. Nathan, A. Kumar, K. Sakariya, P. Servati, K. S. Karim, D. Striakhilev, A. Sazono, *IEEE J. Sel. Top. Quantum Electron.* **2004**, *10*, 58.
[308] I. Sayago, E. Hontañón, M. Aleixandre, in *Tin Oxide Materials* (Ed.: M. O. Orlandi), Elsevier, Amsterdam **2020**, pp. 247–280.
[309] M. Pavan, S. Rühle, A. Ginsburg, D. A. Keller, H.-N. Barad, P. M. Sberna, D. Nunes, R. Martins, A. Y. Anderson, A. Zaban, E. Fortunato, *Sol. Energy Mater. Sol. Cells* **2015**, *132*, 549.
[310] J. Aranovich, A. Ortiz, R. H. Bube, *J. Vac. Sci. Technol.* **1979**, *16*, 994.
[311] M. Marconi, C. Favi, M. Germani, M. Mandolini, M. Mengarelli, *Procedia CIRP* **2017**, *61*, 166.
[312] R. Turunen, M. Nakayama, D. Numakura, **2007**, *24*, 44.
[313] C. W. P. Shi, X. Shan, G. Tarapata, R. Jachowicz, J. Weremczuk, H. T. Hui, *Microsyst. Technol.* **2011**, *17*, 661.
[314] W. Chang, T. Fang, H. Lin, Y. Shen, Y. Lin, *J. Disp. Technol.* **2009**, *5*, 178.
[315] S. Khan, L. Lorenzelli, R. S. Dahiya, in *Proc. of the 10th Conf. on Ph.D. Research in Microelectronics and Electronics (PRIME 2014)*, IEEE, Piscataway, NJ **2014**, p. 4.
[316] F. C. Krebs, M. Jørgensen, K. Norrman, O. Hagemann, J. Alstrup, T. D. Nielsen, J. Fyenbo, K. Larsen, J. Kristensen, *Sol. Energy Mater. Sol. Cells* **2009**, *93*, 422.
[317] T. Julin, *Master of Science Thesis*, Tampere University of Technology, **2011**.
[318] H. Kempa, M. Hambsch, K. Reuter, M. Stanel, G. C. Schmidt, B. Meier, A. C. Hübler, *IEEE Trans. Electron Devices* **2011**, *58*, 2765.
[319] Z. W. Zhong, J. H. Ee, S. H. Chen, X. C. Shan, *Mater. Manuf. Process.* **2020**, *35*, 1.
[320] F. C. Krebs, *Sol. Energy Mater. Sol. Cells* **2009**, *93*, 394.
[321] D. Vak, H. Weerasinghe, J. Ramamurthy, J. Subbiah, M. Brown, D. J. Jones, *Sol. Energy Mater. Sol. Cells* **2016**, *149*, 154.
[322] C.-H. Kim, B.-O. Choi, B.-S. Ryu, D.-S. Kim, *J. Korean Soc. Precis. Eng.* **2008**, *25*, 96.
[323] T.-M. Lee, J.-H. Noh, C. H. Kim, J. Jo, D.-S. Kim, *Thin Solid Films* **2010**, *518*, 3355.
[324] D. Shiokawa, K. Izumi, R. Sugano, T. Sekine, T. Minami, D. Kumaki, S. Tokito, *Jpn. J. Appl. Phys.* **2017**, *56*, 05EA04.
[325] Y. Kusaka, N. Fukuda, H. Ushijima, *Jpn. J. Appl. Phys.* **2020**, *59*, SG0802.
[326] J. Hagberg, M. Pudas, S. Leppävuori, K. Elsey, A. Logan, *Microelectron. Int.* **2001**, *18*, 32.
[327] T. Masaki, T. Nishimoto, K. Miyajima, Japanese Patent S60-29358, **1980**.
[328] K. Fukuda, Y. Yoshimura, T. Okamoto, Y. Takeda, D. Kumaki, Y. Katayama, S. Tokito, *Adv. Electron. Mater.* **2015**, *1*, 1500145.
[329] B. Michel, E. Delamarche, D. Juncker, *Ibm J. Res. Dev.* **2001**, *45*, 697.
[330] S. Jinyou, C. Xiaoliang, L. I. Xiangming, T. Hongmiao, W. Chunhui, L. U. Bingheng, *Sci. China Techol. Sci.* **2019**, *62*, 175.
[331] C. M. Boutry, A. Nguyen, Q. O. Lawal, A. Chortos, **2015**, 1.
[332] S. C. B. Mannsfeld, B. C.-K. Tee, R. M. Stoltenberg, C. V. H.-H. Chen, S. Barman, B. V. O. Muir, A. N. Sokolov, C. Reese, Z. Bao, *Nat. Mater.* **2010**, *9*, 859.
[333] A. Tabatabai, A. Fassler, C. Usiak, C. Majidi, *Langmuir* **2013**, *29*, 6194.
[334] P. Ma, Z. Xu, M. Wang, L. Lu, M. Yin, X. Chen, D. Li, W. Ren, *Mater. Res. Bull.* **2017**, *90*, 253.
[335] J. H. M. Maurer, L. González-García, B. Reiser, I. Kanelidis, T. Kraus, *Nano Lett.* **2016**, *16*, 2921.
[336] C. Linghu, S. Zhang, C. Wang, J. Song, *npj Flex. Electron.* **2018**, *2*, 26.
[337] H. Zhou, W. Qin, Q. Yu, H. Cheng, X. Yu, H. Wu, *Nanomater.* **2019**, *9*, 283.
[338] Z. Huang, Y. Hao, Y. Li, H. Hu, C. Wang, A. Nomoto, T. Pan, Y. Gu, Y. Chen, T. Zhang, W. Li, Y. Lei, N. Kim, C. Wang, L. Zhang, J. W. Ward, A. Maralani, X. Li, M. F. Durstock, A. Pisano, Y. Lin, S. Xu, *Nat. Electron.* **2018**, *1*, 473.
[339] R. Zhao, R. Guo, X. Xu, J. Liu, *ACS Appl. Mater. Interfaces* **2020**, *12*, 36723.
[340] M. Melzer, D. Karnaushenko, G. Lin, S. Baunack, D. Makarov, O. G. Schmidt, *Adv. Mater.* **2015**, *27*, 1333.
[341] S. L. Merilampi, T. Björninen, L. Ukkonen, P. Ruuskanen, L. Sydänheimo, *Int. J. Adv. Manuf. Technol.* **2011**, *53*, 577.
[342] A. Russo, B. Y. Ahn, J. J. Adams, E. B. Duoss, J. T. Bernhard, J. A. Lewis, *Adv. Mater.* **2011**, *23*, 3426.
[343] A. Rivadeneyra, F. C. Loghin, A. Falco, in *Flexible Electronics*, (Ed.: S. Rackauskas), IntechOpen, Rijeka **2018**.
[344] K. D. Sattler, *21st Century Nanoscience—A Handbook: Design Strategies for Synthesis and Fabrication*, Vol. *2*, CRC Press, Boca Raton, FL **2019**.
[345] E. B. Secor, P. L. Prabhumirashi, K. Puntambekar, M. L. Geier, M. C. Hersam, *J. Phys. Chem. Lett.* **2013**, *4*, 1347.
[346] D. Green Marques, P. Alhais Lopes, A. de Almeida, C. Majidi, M. Tavakoli, *Lab Chip* **2019**, *19*, 897.
[347] S. Seipel, J. Yu, A. P. Periyasamy, M. Viková, M. Vik, V. Nierstrasz, *Narrow Smart Textiles*, MDPI, AG **2018**, pp. 251–257.
[348] L. Guo, Y. Duan, Y. Huang, Z. Yin, *Micromachines* **2018**, *9*, 522.
[349] A. K. Ball, R. Das, S. S. Roy, D. R. Kisku, N. C. Murmu, *Sadhana—Acad. Proc. Eng. Sci.* **2019**, *44*, 1.
[350] C. Liu, N. Huang, F. Xu, J. Tong, Z. Chen, X. Gui, Y. Fu, C. Lao, *Polymers* **2018**, *10*, 1.
[351] M. Abas, Q. Salman, A. M. Khan, K. Rahman, *J. Brazilian Soc. Mech. Sci. Eng.* **2019**, *41*, 1.
[352] D.-Y. Shin, S.-S. Yoo, H.-E. Song, H. Tak, D. Byun, *Sci. Rep.* **2015**, *5*, 16704.
[353] S. Gong, W. Schwalb, Y. Wang, Y. Chen, Y. Tang, J. Si, B. Shirinzadeh, W. Cheng, *Nat. Commun.* **2014**, *5*, 1.
[354] Z. Yang, D.-Y. Wang, Y. Pang, Y.-X. Li, Q. Wang, T.-Y. Zhang, J.-B. Wang, X. Liu, Y.-Y. Yang, J.-M. Jian, M.-Q. Jian, Y.-Y. Zhang, Y. Yang, T.-L. Ren, *ACS Appl. Mater. Interfaces* **2018**, *10*, 3948.
[355] L. Pan, A. Chortos, G. Yu, Y. Wang, S. Isaacson, R. Allen, Y. Shi, R. Dauskardt, Z. Bao, *Nat. Commun.* **2014**, *5*, 3002.
[356] J. Shi, X. Li, H. Cheng, Z. Liu, L. Zhao, T. Yang, Z. Dai, Z. Cheng, E. Shi, L. Yang, Z. Zhang, A. Cao, H. Zhu, Y. Fang, *Adv. Funct. Mater.* **2016**, *26*, 2078.
[357] S. Mousavi, D. Howard, F. Zhang, J. Leng, C. H. Wang, *ACS Appl. Mater. Interfaces* **2020**, *12*, 15631.
[358] Z. Chen, Z. Wang, X. Li, Y. Lin, N. Luo, M. Long, N. Zhao, J.-B. Xu, *ACS Nano* **2017**, *11*, 4507.
[359] S. Chen, N. Wu, L. Ma, S. Lin, F. Yuan, Z. Xu, W. Li, B. Wang, J. Zhou, *ACS Appl. Mater. Interfaces* **2018**, *10*, 3660.
[360] D. J. Lipomi, M. Vosgueritchian, B. C.-K. Tee, S. L. Hellstrom, J. A. Lee, C. H. Fox, Z. Bao, *Nat. Nanotechnol.* **2011**, *6*, 788.
[361] H. Zeng, M. Feng, J. Zhuang, R. Cai, Y. Xie, J. Li, in *2019 IEEE Int. Conf. on Robotics and Biomimetics*, IEEE, Piscataway, NJ **2019**, pp. 2641–2646.
[362] V. Bhavar, P. Kattire, V. Patil, S. Khot, K. Gujar, R. Singh, presented at 4th Int. Conf. and Exhibition on Additive Manufacturing Technology, September **2014**.

[363] M. M. Hussain, N. El-Atab, *Handbook of Flexible and Stretchable Electronics*, CRC Press, Boca Raton **2020**.
[364] M. Smith, Y. S. Choi, C. Boughey, S. Kar-Narayan, *Flex. Print. Electron.* **2017**, *2*, 015004.
[365] E. Jabari, E. Toyserkani, *Mater. Lett.* **2016**, *174*, 40.
[366] S. Khan, S. Ali, A. Bermak, in *Hybrid Nanomater. - Flex. Electron. Mater.* (Ed: R. V. Bernal), IntechOpen, London, UK **2019**, p. 18.
[367] G. Grau, J. Cen, H. Kang, R. Kitsomboonloha, W. Scheideler, V. Subramanian, *Flex. Print. Electron.* **2016**, *1*, 23002.
[368] G. Grau, R. Kitsomboonloha, V. Subramanian, *Proc. SPIE* **2015**, *9568*, 95680M.
[369] L. Gonzalez-Macia, A. J. Killard, in *Medical Biosensors for Point of Care Applications*, (Ed.: R. J. Narayan), Woodhead Publishing, New Delhi **2017**, pp. 69–98.
[370] B. Horváth, E. Al Jassin-Al-Hashemi, H. Schift, *Flex. Print. Electron.* **2019**, *4*, 35002.
[371] J. Leppäniemi, A. Sneck, Y. Kusaka, N. Fukuda, A. Alastalo, *Adv. Electron. Mater.* **2019**, *5*, 1900272.
[372] M. J. Uddin, M. K. Hossain, W. Qarony, M. I. Hossain, M. N. H. Mia, S. Hossen, *J. Sci. Adv. Mater. Devices* **2017**, *2*, 385.
[373] B. Zhang, B. Seong, V. Nguyen, D. Byun, *J. Micromech. Microeng.* **2016**, *26*, 25015.
[374] H. Khaliq, R. Gomes, C. Fernandes, J. M. Nobrega, O. Carneiro, L. Ferrás, *Rapid Prototyp.* **2017**, *23*, 727.
[375] V. G. Rocha, E. Saiz, I. S. Tirichenko, E. García-Tuñón, *J. Mater. Chem. A* **2020**, *8*, 15646.
[376] K. Suganuma, *Introduction to Printed Electronics*, Springer, New York, **2014**.
[377] J.-U. Park, M. Hardy, S. Kang, K. Barton, K. Adair, D. Mukhopadhyay, C. Lee, M. Strano, A. G. Alleyne, J. Georgiadis, P. Ferreira, J. Rogers, *Nat. Mater.* **2007**, *6*, 782.
[378] W. Zou, H. Yu, P. Zhou, L. Liu, *Mater. Des.* **2019**, *166*, 107609.
[379] F. Cai, Y.-H. Chang, K. Wang, W. Khan, S. Pavlidis, J. Papapolymerou, in *IEEE MTT-S Int. Microwave Symposium Digest*, IEEE, Piscataway, NJ **2014**, pp. 1–3.
[380] J. Lin, in *Printed Electronics*, John Wiley & Sons, Ltd, New Jersey **2016**, pp. 106–144.
[381] Y. Sui, A. Hess-Dunning, P. Wei, E. Pentzer, R. M. Sankaran, C. A. Zorman, *Adv. Mater. Technol.* **2019**, *4*, 1900834.
[382] J. Izdebska-Podsiadły, in *Non-Thermal Plasma Technol. Polym. Mater.,* Elsevier, New York **2019**, pp. 159–191.
[383] N. S. Shabanov, A. K. Akhmedov, A. B. Isaev, A. S. Asvarov, K. S. Rabadanov, K. Kaviyarasu, *Mater. Today Proc.* **2020**, *5*, 2971.
[384] A. A. Aly, *Int. J. Mater. Chem. Phys.* **2015**, *1*, 132.
[385] A.-M. Reinecke, P. Regenfuß, M. Nieher, S. Klötzer, R. Ebert, *J. Ceram. Process. Res.* **2002**, *3*, 8.
[386] C. J. Miller, *Master Degree Thesis*, Case Western Reserve University School of Graduate Studies, **2017**.
[387] M. K. Banerjee, in *Mater. Sci. Mater. Eng.* (Eds: M. S. J. Hashmi), Elsevier, Oxford **2017**, pp. 1–49.
[388] G. De Luca, E. Treossi, A. Liscio, J. M. Mativetsky, L. M. Scolaro, V. Palermo, P. Samorì, *J. Mater. Chem.* **2010**, *20*, 2493.
[389] T.-P. Huynh, H. Haick, *Adv. Mater.* **2018**, *30*, 1802337.
[390] P. Braeuer, T. Kuhn, M. Mueller, J. Franke, in *2019 42nd Int. Spring Seminar on Electronics Technology*, IEEE, Piscataway, NJ **2019**, pp. 1–6.
[391] P. S. Taylor, R. J. Horne, J. C. Batchelor, *2019 IEEE Int. Symp. on Antennas and Propagation and USNC-URSI Radio Science Meeting (APSURSI 2019)*, Vol. *1*, IEEE, Piscataway, NJ **2019**, p. 1787.
[392] L. M. Faller, C. Stetco, H. Zangl, in *IEEE Int. Conf. Intell. Robot. Syst.*, IEEE, NY City **2019**, pp. 5620–5627.
[393] D. Gregor-Svetec, in *Nanomaterials for Food Packaging* (Eds: M. Â. P. R. Cerqueira, J. M. Lagaron, L. M. Pastrana Castro, A. O. Vicente), Elsevier, Amsterdam **2018**, pp. 203–247.
[394] B. I. Kharisov, O. V. Kharissova, B. I. Kharisov, O. V. Kharissova, in *Carbon Allotropes Met. Chem. Prop. Appl.*, Springer Nature, Switzerland **2019**, pp. 639–652.
[395] M. Wessely, T. Tsandilas, W. E. Mackay, in *Proc. 29th Annu. Symp. on User Interface Software and Technology*, Association For Computing Machinery, New York, NY, USA, **2016**, pp. 697–704.
[396] M. Zhu, Z. Sun, Z. Zhang, Q. Shi, T. He, H. Liu, T. Chen, C. Lee, *Sci. Adv.* **2020**, *6*, 1.
[397] J. Bennett, O. Rokas, L. Chen, *Sustainability* **2017**, *9*, 840.
[398] H. U. Chung, B. H. Kim, J. Y. Lee, J. Lee, Z. Xie, E. Ibler, K. Lee, A. Banks, J. Jeong, J. Kim, C. Ogle, D. Grande, Y. Yu, H. Jang, P. Assem, D. Ryu, J. Kwak, M. Namkoong, J. Park, J. Rogers, *Science* **2019**, 363.
[399] Z. Wang, Z. Yang, T. Dong, *Sensors* **2017**, *17*, 341.
[400] M. Zulqarnain, S. Stanzione, J. L. P. J. Van Der Steen, G. H. Gelinck, K. Myny, E. Cantatore, in *Proc. of the 2019 8th Int. Workshop on AdvAnces in Sensors Interfaces (IWASI)*, IEEE, Piscataway, NJ **2019**, p. 205.
[401] R. Gupta, *Smart Sensors, Meas. Instrum.* **2017**, *25*, 219.
[402] Y. Kim, M. Mahmood, S. Kwon, K. Maher, J. W. Kang, W. Yeo, *IEEE Trans. Biomed. Eng.* **2020**, *67*, 2159.
[403] T. Wu, J.-M. Redoute, M. Yuce, **2019**, pp. 165–173.
[404] S. Niu, N. Matsuhisa, L. Beker, J. Li, S. Wang, J. Wang, Y. Jiang, X. Yan, Y. Yun, W. Burnett, A. S. Y. Poon, J. B. H. Tok, X. Chen, Z. Bao, *Nat. Electron.* **2019**, *2*, 361.
[405] L. W. Lo, H. Shi, H. Wan, Z. Xu, X. Tan, C. Wang, *Adv. Mater. Technol.* **2020**, *5*, 1.
[406] S. Han, J. Kim, S. M. Won, Y. Ma, D. Kang, Z. Xie, K. T. Lee, H. U. Chung, A. Banks, S. Min, S. Y. Heo, C. R. Davies, J. W. Lee, C. H. Lee, B. H. Kim, K. Li, Y. Zhou, C. Wei, X. Feng, Y. Huang, J. A. Rogers, *Sci. Transl. Med.* **2018**, *10*, eaan4950.
[407] S. Cruz, J. Viana, L. Rocha, *Instrum. Meas. IEEE Trans.* **2015**, *64*, 2813.
[408] S. Khan, S. Ali, A. Bermak, *IEEE Access* **2019**, *7*, 134047.
[409] Innovative patch may soon be used to monitor coronavirus patients remotely 24/7, https://www.nitto.com/eu/en/press/2020/0423.jsp (accessed: December 2020).
[410] Y. Huang, H. Wu, L. Xiao, Y. Duan, H. Zhu, J. Bian, D. Ye, Z. Yin, *Mater. Horiz.* **2019**, *6*, 642.
[411] O. Rusanen, T. Simula, P. Niskala, V. Lindholm, M. Heikkinen, in *2019 22nd Eur. Microelectronics and Packaging Conf. and Exhibition*, IEEE, Piscataway, NJ **2019**, pp. 1–7.
[412] S. H. Yoon, S. Ma, W. S. Lee, S. Thakurdesai, D. Sun, F. P. Ribeiro, J. D. Holbery, in *Proc. 32nd Annual ACM Symp. on User Interface Software and Technology*, Association For Computing Machinery, New York, NY, USA, **2019**, pp. 949–961.
[413] P. Stol, Master Degree Thesis in Industrial Design Engineering, Delft University of Technology, **2019**.
[414] Global Frontrunner in Touch and Haptics, https://aito-touch.com/technology (accessed: December 2020).
[415] E. I. Kauppinen, H. Jiang, D. P. Brown, A. G. Nasibulin, *US20090226704A1*, **2009**.
[416] Our solutions—Shaping surfaces into experiences, https://canatu.com/solutions/ (accessed: December 2020).
[417] R. Kumar, K. M. Johnson, N. X. Williams, V. Subramanian, *Adv. Energy Mater.* **2019**, *9*, 1803645.
[418] C. (John) Zhang, L. McKeon, M. P. Kremer, S.-H. Park, O. Ronan, A. Seral-Ascaso, S. Barwich, C. Ó. Coileáin, N. McEvoy, H. C. Nerl, B. Anasori, J. N. Coleman, Y. Gogotsi, V. Nicolosi, *Nat. Commun.* **2019**, *10*, 1795.
[419] Y. Lu, K. Jiang, D. Chen, G. Shen, *Nano Energy* **2019**, *58*, 624.
[420] K. Khan, A. K. Tareen, M. Aslam, A. Mahmood, Q. khan, Y. Zhang, Z. Ouyang, Z. Guo, H. Zhang, *Prog. Solid State Chem.* **2020**, *58*, 100254.

[421] K. Mensah-Darkwa, C. Zequine, P. Kahol, R. Gupta, *Sustainability* **2019**, *11*, 414.
[422] Q. Li, M. Horn, Y. Wang, J. Macleod, N. Motta, J. Liu, *Materials* **2019**, *12*, 703.
[423] Y.-Z. Zhang, Y. Wang, T. Cheng, L.-Q. Yao, X. Li, W.-Y. Lai, W. Huang, *Chem. Soc. Rev.* **2019**, *48*, 3229.
[424] M. Yu, X. Feng, *Joule* **2019**, *3*, 338.
[425] J.-Y. Kim, W. Lee, Y. Kang, S. Y. Cho, K.-S. Jang, *Carbon N. Y.* **2018**, *133*, 293.
[426] S. Kim, J. Mo, J.-Y. Kim, K.-S. Jang, *e-Polymers* **2017**, *17*, 501.
[427] T. Le, Z. Lin, R. Vyas, V. Lakafosis, L. Yang, A. Traille, M. Tentzeris, C. P. Wong, *J. Electron. Packag.* **2013**, *135*, 11007.
[428] S. Kumar, J. Buckley, J. Barton, B. O'Flynn, in *Smart Syst. Integr. 2018 - Int. Conf. Exhib. Integr. Issues Miniaturized Syst.* (Ed: T. Otto), Curran Associates, Inc., Dresden, Germany **2018**, pp. 432–435.
[429] C. Herrojo, F. Paredes, R. Escudé, E. Ramon, F. Martin, in *2019 IEEE Asia-Pacific Microwave Conf.*, IEEE, Piscataway, NJ **2019**, pp. 108–110.
[430] J. Zhang, L. Zhu, Z. Wei, *Small Methods* **2017**, *1*, 1700258.
[431] Y. Wei, M. Xing, D. Wang, R. Wang, *Energy Rep.* **2020**, *6*, 2370.
[432] Y. Rong, Y. Hu, A. Mei, H. Tan, M. I. Saidaminov, S. Il Seok, M. D. McGehee, E. H. Sargent, H. Han, *Science* **2018**, *361*, eaat8235.
[433] Solar Cells Reimagined, https://sauletech.com/ (accessed: December 2020).
[434] M. Mraović, T. Muck, M. Pivar, J. Trontelj, A. Pleteršek, *Sensors* **2014**, *14*, 13628.
[435] K. B. Connolly, Johnnie Walker 'smart bottle' performs for consumers and supply chain, https://www.packagingdigest.com/beverage-packaging/johnnie-walker-smart-bottle-performs-for-consumers-and-supply-chain150306 (accessed: December 2020).
[436] A. Chowdhury, S. A. Raut, *Int. J. Comput. Intell. IoT* **2019**, *2*, 822.
[437] G. Pasetti Monizza, R. A. Rojas, E. Rauch, M. A. R. Garcia, D. T. Matt, in *IFIP Int. Conf. Prod. Lifecycle Manag.* (Eds: P. Chiabert, A. Bouras, F. Noël, J. Ríos), Springer International Publishing, Cham, Switzerland **2018**, pp. 227–237.
[438] K. C. Welch, A. S. Kulkarni, A. M. Jimenez, B. Douglas, in *2018 United States Natl. CommIttee of URSI Natl. Radio Science Meeting (USNC-URSI NRSM)*, IEEE, Piscataway, NJ **2018**, pp. 1–2.
[439] A. Dementyev, J. Qi, J. Ou, J. Paradiso, in *2018 IEEE/RSJ Int. on Intelligent Robots and Systems*, IEEE, Piscataway, NJ **2018**, pp. 6099–6104.
[440] R. Hardman, *Environ. Health Perspect.* **2006**, *114*, 165.

Cláudia S. Buga is currently pursuing a Ph.D. degree in Materials Engineering and is a junior research technician for the DTx – Digital Transformation CoLAB association. She received her Master's degree in Biomedical Engineering, in the area of Biomaterials and Instrumentation, from the University of Coimbra in 2018. For her master thesis she studied the optimization of formulations for photodynamic therapy. She has also conducted previous research work in the area of materials' functionalization and sustainable materials for 4D printing.

Júlio C. Viana received its Ph.D. in Science and Engineering of Polymers and Composites from University of Minho in 2000, a M.Sc. in Computer Aided Engineering-Mechanical Design from Queen's University of Belfast, UK, in 1993, and Graduated in Industrial Engineering - Plastics Branch, University of Minho in 1991. He joined University of Minho as professor in 1991, being currently associate professor, at the Department of Polymer Engineering, University of Minho. He is currently the director of IPC – Institute for Polymers and Composites, a research unit from University of Minho.